Integrated Geophysical Analysis for reservoir characterization of Lumshiwal, Hangu and Lockhart Formations in Manzalai Area, Upper Indus Basin, Pakistan.

BY

Farman Ullah

M. Phil (Geophysics)

(2021-2023)

DEPARTMENT OF EARTH SCIENCES

QUAID-I-AZAM UNIVERSITY, ISLAMABAD

PAKISTAN

2023

“In the Name of ALLAH, the Most Merciful & Mighty”

“PAY THANKS TO ALLAH EVERY MOMENT AND GO TOEXPLORE THE HIDDEN TREASURES ITS ALL FOR YOUR BENEFIT”

(AL-QURAN)

CERTIFICATE

This dissertation is submitted by **Farman Ullah** S/O **Ikram Ullah Khan** is accepted in its present by the Department of Earth Sciences, Quaid-I-Azam University, Islamabad as satisfying the requirement for the award of Master of Philosophy in Geophysics.

RECOMMENDED BY

Dr. Shazia Naseem _____
(Supervisor)

Prof. Dr. Mumtaz Muhammad Shah _____
(Chairman Department of Earth Sciences)

External Examiner_____

DEPARTMENT OF EARTH SCIENCES

QUAID-I-AZAM UNIVERSITY, ISLAMABAD

DEDICATION

“This dissertation is dedicated to ALLAH, the almighty”“His prophet HAZRAT MUHAMMAD (P.B.U.H)”.

&

To My Parents, Family, and Respected Teachers, as I could not have achieved this level of achievement without their prayers, support, and belief in me. I pray that Allah would always keep your shadow over me and bless you.

&

To My Department of Earth Sciences, (QAU)

ACKNOWLEDGEMENT

"In the name of Allah, The Most Gracious and the most Merciful, Beneficent." Praise be to God. I affirm that the Holy Prophet Muhammad (PBUH) is the final messenger, whose life serves as an exemplary model for all of humanity until the Day of Judgement. I express gratitude to Allah for the fortitude and divine favor that facilitated the successful completion of this endeavor.

I would like to express my sincere gratitude to Dr. Shazia Naseem, my supervisor, for her priceless advice and unwavering backing during the duration of this project. The researcher's success in this study may be due to the valuable contributions of her favorable criticism, encouragement, inspiration, and recommendations provided throughout the experimental and thesis work. I would like to extend my utmost gratitude to Mr. Yawar Amin for his invaluable help throughout the process of preparing this thesis and his unwavering support in addressing any inquiries I may have had.

I would like to extend my gratitude to my entire family, particularly my parents, for their unwavering support and assistance, without which I would not have been able to attain my current level of achievement. I would like to express my gratitude to the entire faculty of my department for furnishing me with a solid academic foundation, which has facilitated my pursuit of this course of study.

I express my sincere gratitude to all my acquaintances, with a special mention to Mr. Umer Ghaffar, Mr. Aftab Shabbir, Mr. Nasrullah, Mr. Javid Iqbal, Mr. Aqib Mirza, Mr. Ahmed Rafeh, Mr. Junaid Shah and Mr. Ihtesham Gardezi for their unwavering affection, concern, and ethical encouragement during my academic journey.

I express profound gratitude to all of my teachers for their unwavering support, benevolence, and motivation. Additionally, I extend my acknowledgment to those individuals who have indirectly aided in the progression of our research endeavor.

Farman Ullah

M.Phil.
(Geophysics)
2021-2023

ABSTRACT

Hydrocarbons play a crucial role in contemporary industrialized societies due to their capacity to supply energy. In order to accurately delineate and characterize a hydrocarbon reservoir, it is important to acquire more comprehensive subsurface data. The task at hand necessitates the examination and evaluation of geological formations pertaining to petroleum reservoirs and other geological features. The Upper Indus Basin exhibits proven potential for hydrocarbon reservoirs in the Paleocene and Cretaceous periods. Extensive investigation is necessary for the Manzalai Gas Field, which contains structural traps that hold hydrocarbon reserves. In order to evaluate the potential for hydrocarbon deposits and determine the structural favorability of the area, an analysis of seismic data was conducted. This analysis resulted in the mapping of five horizons, namely Lockhart, Hangu, Kawagarh, Lumshiwal, and Chichali and their time contour maps are generated which shows that horizons are dipping from North-West to South-East. The petrophysical investigation reveals the existence of a gas-bearing zone in the Hangu and Lumshiwal formations in wells Mnazalai-01, Manzalai-05, and Manzalai-06. However, the Lockhart formation only exhibits a possible gas-bearing zone in well Manzalai-05. The hydrocarbon-bearing zones demonstrate a high degree of hydrocarbon saturation; yet, the effective porosity is significantly low, resulting in a reservoir characterized as tight. The procedure of facies classification reveals the presence of five unique facies, which are gas sands, shale, shaly sand, limestone-wackstone, and limestone-packstone. The utilization of Rock physics modelling enhances the accuracy of logs by mitigating the adverse effects of undesirable logging phenomena, hence leading to improved outcomes in petrophysical analysis. The inversion analysis has been performed which gives the spatial distribution of low impedance zones characterized by the hydrocarbon bearing zones.

Table of Contents

LIST OF FIGURES

LIST OF TABLES

Chapter 01

Introduction

1.1 Introduction

Pakistan has an abundance of mineral resources, but many enterprises and daily life are fueled by hydrocarbons, a commodity that the country still lacks. The industry uses conventional approaches to explore for hydrocarbons; nevertheless, the utilization of reservoirs can only be improved by accurately defining the reservoirs. Reservoir characterization includes the assessment of critical physical parameters such as porosity, permeability, lower and upper reservoir limits, lateral and vertical extension, heterogeneous nature, and the volume and type of subsurface fluids (Bacon et al., 2007; Avseth et al., 2005). Seismic and well log data are commonly used to estimate reservoir parameters; however, Drill Stem Test (DST) and core cuttings of wells aid in restricting the data and limiting uncertainties in the study. These data sets can be used to investigate and estimate reservoir parameters at various scales (Hearts et al., 2002; Chen and Sidney, 1997; Chopra and Marfurt, 2007; King, 1990; Lindseth, 1979). Different interpolation or other geostatistical approaches are used to augment the data to observations made in the field and make a tie with the local geology to efficiently link the data sets (Bosch et al., 2010).

There is a recognition that even the most calibrated data set can have erroneous recordings, impacting the real outcomes of the parameters estimated for reservoir characterization. A quality check understanding is thus maintained on the data sets, particularly the well log data set, in which particular templates can be used to further validate the well log data sets in the absence of core cuttings. This reduces the degree of ambiguity when describing reservoir rock.

Although qualitative analysis makes use of the interpretation of tracking horizons in connection to geologic features in the subsurface, following the stratigraphic normal sequence, the true objective for every geoscientist working in the upstream sector is the mapping of zones of hydrocarbon accumulation. Although seismic reflectors can be spatially traced using trip time, the quantitative properties of the reservoir remain somewhat uncertain.

The combination of seismic and well log data, along with the utilization of seismic inversion techniques, plays a pivotal role in deriving reservoir parameters (Landa et al., 2000; Simm & Bacon, 2014). The detailed well log information can be effectively integrated into seismic inversion methods to extract acoustic impedance from seismic data. This information offers valuable insights into distinctive reservoir parameters, the spatial distribution of depositions, and local petrophysical properties (Bosch et al., 2009; Angeleri and Capri, 1982; Walls et al., 2004; Yao and Gan, 2000; Grana and Dvorkin, 2011). Notably, seismic inversion significantly enhances vertical resolution, leading to improved interpretations. This is particularly important as layer-oriented impedance displays assist in refining reservoir models (Ashcroft, 2011). The dataset employed in this study consists of post-stack 3D seismic data and well log data from Tajjal-02,03. The inversion methodologies encompass model-based inversion (for acoustic and shear impedance) and the lambda rho-mu rho (LMR) attribute, each employing distinct algorithmic approaches (Veeken 2007; Silva et al., 2004; Veeken and Silva et al., 2004; Ashcroft, 2011; Veeken and Rauch-Davies, 2006; Wang, 2017).

1.2 Objectives

- Conduct an in-depth analysis of the 3D seismic data to thoroughly examine the underlying geological composition, with the ultimate aim of gaining insights into the lithological diversity and spatial extent within the study area.
- The application of petrophysical analysis, rock physics analysis, and facies assessment of well log data is employed to accurately identify zones exhibiting potential for hydrocarbon accumulation, hence enhancing comprehension of reservoir characteristics.
- Apply stochastic inversion approaches to the seismic data to produce an inverted impedance volume for increased vertical resolution and upgraded reservoir characterization.
- Establish a Rock Physics Modeling (RPM) technique to explore the consequences of elastic properties on the reservoir, incorporating multimineral composition, porosity, fluid characteristics, and an extensive examination of shale minerals, matrix pores, and fluids.

1.3 Introduction to Study area

The Manzalai field is located at a distance of around 278 kilometers from Islamabad, which serves as the capital city of Pakistan. The geographical location of the site is situated at coordinates 33° 17' 15.39" N 70° 42' 36.03" E, namely in the southwestern region of the Kohat Basin, adjacent to Gurguri village. The identification of oil and gas reserves in the Manzalai region can be traced back to the year 2002, signifying a noteworthy achievement in the pursuit of exploring these valuable resources within the area. In January 2007, the Development and Production Lease for the Manzalai area was granted by the Government of Pakistan. In the Manzalai region, there exists a collective count of 11 wells, including of one appraisal well (referred to as Manzalai well-03), one exploratory well, and nine development wells. The average daily production output from these wells is 21.54 million standard cubic feet per day (MMSCF) of gas, 300.8 barrels of condensate, and 3.38 tons of LPG (liquefied petroleum gas). The Manzalai field is situated inside the Upper Indus Basin, notably on the Kohat Plateau, as depicted in the accompanying figure 1.1

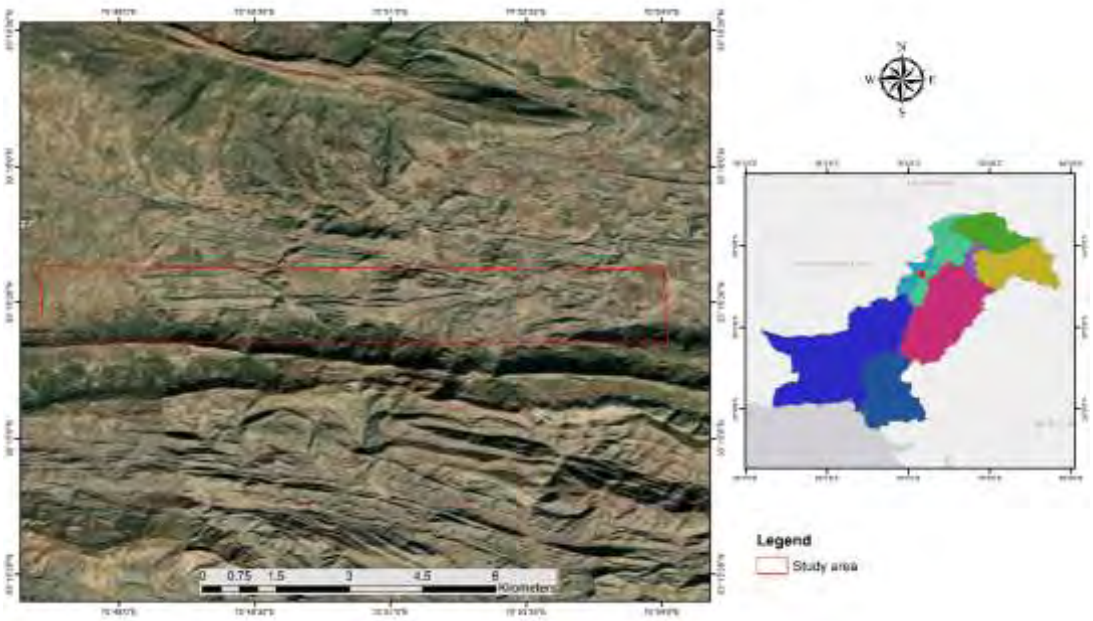

Figure 1.1 Location of Study Area indicated by red rectangle on satellite map.

1.4 Data Description

The database plays a crucial part in guaranteeing the successful outcome of the project. The data is employed within the confines of this research to estimate the intended goals, encompassing several techniques such as 3D seismic interpretation, petrophysical analysis, stochastic inversion, electrofacies, and rock physics modelling.

The data was obtained from the LMKR with the full approval of the supervisor, after authorization from the Director General of Petroleum Concessions (DGPC). Table 1.1 displays the visual representation of seismic data, whereas Table 1.2 showcases the graphical depiction of well data. The seismic data displays an in-line range that ranges from 411 to 516, and a cross-line range that spans from 358 to 420.

The data acquired from wells is commonly reported in the Log ASCII Standard (LAS) format. The dataset comprises three wells, specifically identified as Manzalai-01, Manzalai-05, and Manzalai-06. The Kingdom Software, developed by IHS, is employed to input three-dimensional seismic data, resulting in the creation of a fundamental map. The base map depicted in Figure 1.3 showcases various elements, such as the spatial distribution of wells, borders of concern, orientation of seismic survey lines, and the specific positions of survey shots. The cartographic representations of cultural data pertaining to roads and buildings rely on base maps that integrate geographic references, such as latitude and longitude, or Universal Transverse Mercator (UTM) grid information. The provided map visually represents the arrangement of in-line, cross-line, and well positions in space. The placement of in-line lines can vary along the x-axis, whereas the placement of cross-line lines can vary along the y-axis. According to Sroor (2010), the geophysical base map illustrates the spatial distribution of seismic lines and the precise locations where seismic data was collected.

1.4 Data Sets

- Seismic data in SEG-Y format
- Well Log Data (LAS File)
- Base map

1.4.1 Seismic Data

The seismic dataset utilized for this investigation is presented in Table 1.1. The research endeavor incorporates a 3D seismic cube spanning an area of 12 km^2. This research used a cube consisting of 415 in-lines, commencing at 642 and extending up to 1064, in addition to 128 cross-lines spanning from 358 to 420.

.

Table 1.1 Displays the seismic data utilized in the course of this investigation

Lines	Strat	End	Total no of lines
In-lines	642	1064	415
Cross-line	358	420	63

1.4.2 Base Map

The incorporation of a base map is an essential element in the interpretation process, since it provides a visual depiction of the spatial arrangement of individual seismic pickets. Geophysicists employ a base map that exhibits the spatial configuration of seismic lines, denoting the precise positions where seismic data was gathered. Alternatively, it could comprise the quantitative measurement of In-lines and Crosslines that were utilized during the execution of a seismic survey. A standard base map often includes the spatial depiction of lease and license boundaries, wells, seismic survey sites, and diverse cultural features such as buildings and roads. Furthermore, it encompasses geographic coordinates, namely latitude and longitude. As illustrated in Figure 1.2, the map commonly presents the spatial locations of wells and seismic survey sites.

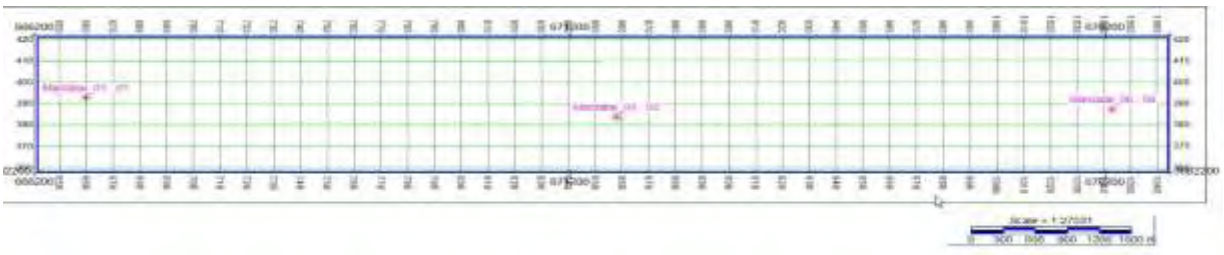

Figure 1.2 Base Map of Study Area

The data pertaining to the Manzalai-01, Manzalai-05, and Manzalai-06 wells, which were utilized in this study, have been shown in Table 1.2, Table 1.3, and Table 1.4, respectively.

Table 1.2 Well Data used for the research

Sr. No	In-line	X-line	Wells
1	657	391	Manzalai-01
2	858	383	Manzalai-05
3	1041	388	Manzalai-06

1.4.3 Technical well data of Manzalai Wells

The available well data has been shown in below tables for all three wells.

Table 1.3 Technical well data of Manzalai-01

Operator	MOL	Province	KPK
Type	Exploratory	Status	Gas and Condensates
Well bore name	Manzalai-01	Source	Vibroseis/Dynamite
Longitude	70°47′20.07"	Latitude	33°16′27.43"
Elevation (m)	976		
Depth reference	KB		
Well tops			
Formation	**Age**	**Top (m)**	**Thickness (m)**
Murree	Miocene	16.00	1335.00
Kohat	Eocene	1351.00	186.00
Kuldana	Eocene	1537.00	1991.00
Lockhart	Paleocene	3528.00	159.00
Hangu	Paloecene	3687.00	15.00
Kawagarh	Late Cretaceous	3702.00	195.00
Lumshiwal	Cretaceous	3897.00	63.00
Chichali	Cretaceous	3960.00	184.00
Samanasuk	Jurrasic	4144.00	191.00
Shinwari	Jurrasic	4335.00	176.00
Datta	Jurrasic	4511.00	---------

Table 1.4 Technical Well Data and Formation Tops of Manzalai-05

Operator	MOL	Province	KPK
Type	Development	Status	Gas/Condensates
Well bore name	Manzalai-05	Source	Vibroseis/Dynamite
Longitude	70°50′34.275"	Latitude	33°16′15.914"
Elevation (m)	919		
Depth reference	KB		
Well tops			
Formation	**Age**	**Top (m)**	**Thickness (m)**
Kamlial	Miocene	0.00	1218.00
Kohat	Eocene	1218.00	162.00
Kuldana-Mamikhel	Eocene	1380.00	34.00
Panoba	Eocene	1414.00	968.00
Jatta	Eocene	2382.00	135.00
Panoba	Eocene	2517.00	729.00
Patala	Paleocene	3246.00	505.00
Lockhart	Paleocene	3751.00	183.00
Hangu	Paleocene	3934.00	13.00
Kawagarh	Cretaceous	3947.00	104.00
Lumshiwal	Cretaceous	4051.00	88.00
Chichali	Cretaceous	4139.00	--------

Table 1.5 Technical Well Data and Formation Tops of Manzalai-06

Operator	MOL	Province	KPK
Type	Development	Status	Gas/Condensates
Well bore name	Manzalai-06	Source	Vibroseis/Dynamite
Longitude	70°53′33.47"	Latitude	33°16′16.04"
Elevation (m)	876.00		
Depth reference	KB		
Formation	**Age**	**Top (m)**	**Thickness (m)**
Chinji	Miocene	0.00	467.00
Kamlial	Miocene	467.00	553.00
Kohat	Eocene	1020.00	66.00
Kuldana-Mamikhel	Eocene	1086.00	85.00
Panoba	Eocene	1171.00	394.00
Kamlial	Eocene	1565.00	29.00
Kohat	Eocene	1594.00	21.00
Kuldana-Mamikhel	Eocene	1615.00	294.00
Kohat	Eocene	1909.00	78.00
Kuldana-Mamikhel	Eocene	1987.00	42.00
Panoba	Eocene	2029.00	1117.00
Patala	Eocene	3146.00	585.00
Lockhart	Paleocene	3731.00	287.00
Hangu	Paleocene	3968.00	38.00
Kawagarh	Cretaceous	4006.00	103.00
Lumshiwal	Cretaceous	4109.00	72.00
Chichali	Cretaceous	4181.00	---------

1.5 Methodology

As part of the current investigation, seismic data (SEG-Y) and well data (LAS File) from the Manzalai gas field (Manzalai-01, Manzalai-05, and Manzalai-06) were integrated.

Review of the Literature: Examine the literature that has already been written in order to fully comprehend the geology, stratigraphy, and geological/tectonic setting of the research area.

Seismic Interpretation: In preparation for interpretation, the 3D seismic volume and well data were methodically fed into the workstation. The 3D volume was then processed using the structural smooth and trace AGC volume attribute methods before being realized. These were carried out to amplify weak events for better interpretability and lengthen the seismic reflectors.

Geostatistical Inversion: To identify these thin deposits, the seismic inversion method is applied. Before executing the inversion, we predict the wavelet and low frequency models before performing the seismic to well tie.

The reservoir X time window was located, selected, and interpreted after seismic data and well data were linked. On each tenth in-line, horizon tracking was done. The full seismic volume was used for this mapping and digitization.

The petrophysical parameters (shale volume, porosity, water saturation, and hydrocarbon saturation) of hydrocarbon-bearing zones were estimated using well data using petrophysical analysis. The placement of the Gamma Ray and Caliper curves was observed in Track 1, followed by the placement of the Resistivity curves (both shallow and deep) in Track 2. Lastly, the Density and Neutron curves were positioned in Track 3.

The present study conducted an electrofacies analysis to estimate the distribution of facies within the designated zone of interest. Stochastic inversion was employed to assess the lateral continuity of Zone of interests. The utilization of impedance measurements has been employed in the construction of inverted sections, facilitating the examination of vertical resolution inside the reservoir.

1.6 Organization of the Dissertation

The structure of the thesis is as follows: Chapter 1: Introduction This chapter provides a general overview of the topic under investigation. It aims to introduce the reader to the subject matter and provide a foundation for the subsequent chapters. This chapter provides a comprehensive overview of the topic matter. The text encompasses the investigation objectives, introduces the topic field, analyzes the data sets employed in the investigation, and outlines the overarching technique and workflow of the dissertation. Chapter 2: Geological context and Stratigraphy: This chapter provides an analysis of the geological context of the region, encompassing both the geological and structural perspectives. The sedimentary basins of Pakistan exhibit a well-established stratigraphic framework. Furthermore, this study examines the various constituents of petroleum reservoirs and identifies the potential petroleum reserves present in the region.

Chapter 4 of this study centers on the examination and procedural framework pertaining to petrophysical analysis. The analysis encompasses the determination of shale volume, as well as the verification of porosity, encompassing effective porosity and total porosity. In addition, the process involves conducting calculations to determine the saturation levels of water and hydrocarbons, followed by a subsequent petrophysical examination. Chapter 3: Seismic Interpretation: This chapter provides an in-depth exploration of seismic interpretation techniques employed in the research of geological structures. The methodology involves the production of synthetic seismograms and the delineation of horizons. Time and depth form maps are utilized for the visualization of seismic data.

Chapter 5 of the dissertation delves into the comprehensive analysis of electrofacies, outlining the systematic approach employed for the exploration of electrofacies. This paper addresses the categorization of electrofacies and provides a comprehensive explanation of the fuzzy classification approach employed. Additionally, this study investigates the methodologies employed in the interpretation of facies. Chapter 6: Geostochastic Inversion for Seismic to Well Tie and Wavelet Extraction The primary emphasis of this chapter is on the geostatistics inversion of seismic data in order to establish a connection with well data and extract wavelets. This statement elucidates the procedure for correlating seismic data with well information, as well as the process of extracting wavelets. The presentation includes the exposition of the low-

frequency exhibit and the earlier demonstration, specifically the SI Model. Additionally, the discussion encompasses variograms and facies classification. Furthermore, probability density functions are employed in the analysis, namely in the generation of inverted impedance segments, modified facies sections, and inverted facies slices. Chapter 5: Modelling of Rock Physics.

1.7 Workflow of the Dissertation

The generation of a base map is facilitated by the importation of seismic data in the SEG-Y format. In the seismic section, faults are identified and delineated for the purpose of constructing fault polygons and grids of specified horizons. The utilization of well log data enables the execution of petrophysical analysis and facilitates the estimation of electrofacies analysis pertaining to the reservoir. The integration of seismic data and well log data is employed in seismic inversion, as depicted in Figure 1.3.

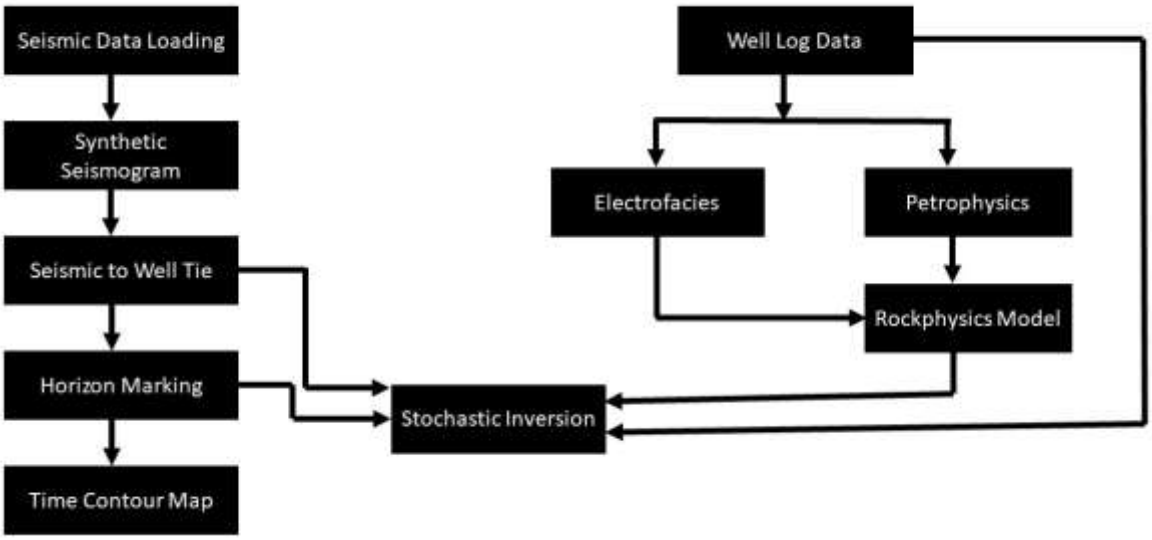

Figure 1.3 Complete Workflow of the Dissertation

Chapter 02

Geology and Stratigraphy

2.1 Introduction

The discipline that encompasses the examination of the Earth's solid structure, the composition of its rocks, and the dynamic processes occurring within its interior is commonly known as "geology."Geology encompasses the examination of Earth's past, encompassing several aspects such as the development of life forms, changes in climatic conditions throughout history, as well as the study of plate tectonics and the evolutionary progression of organisms. Geology plays a crucial role in contemporary society by facilitating the exploration and analysis of minerals and hydrocarbons, while also contributing to the prediction and understanding of natural catastrophes.

The existing knowledge we possess regarding the specific domain, encompassing its geological characteristics and velocity fluctuations, aids us in conducting a precise evaluation of the lithological composition and other relevant variables. The analysis of variations in the velocity of the area can yield valuable insights for the identification of distinct reflectors. Geologic information can also provide valuable insights into the detection of defects and the extent of their damage. Map showing the tectonics of Pakistan has been presented in figure 2.1

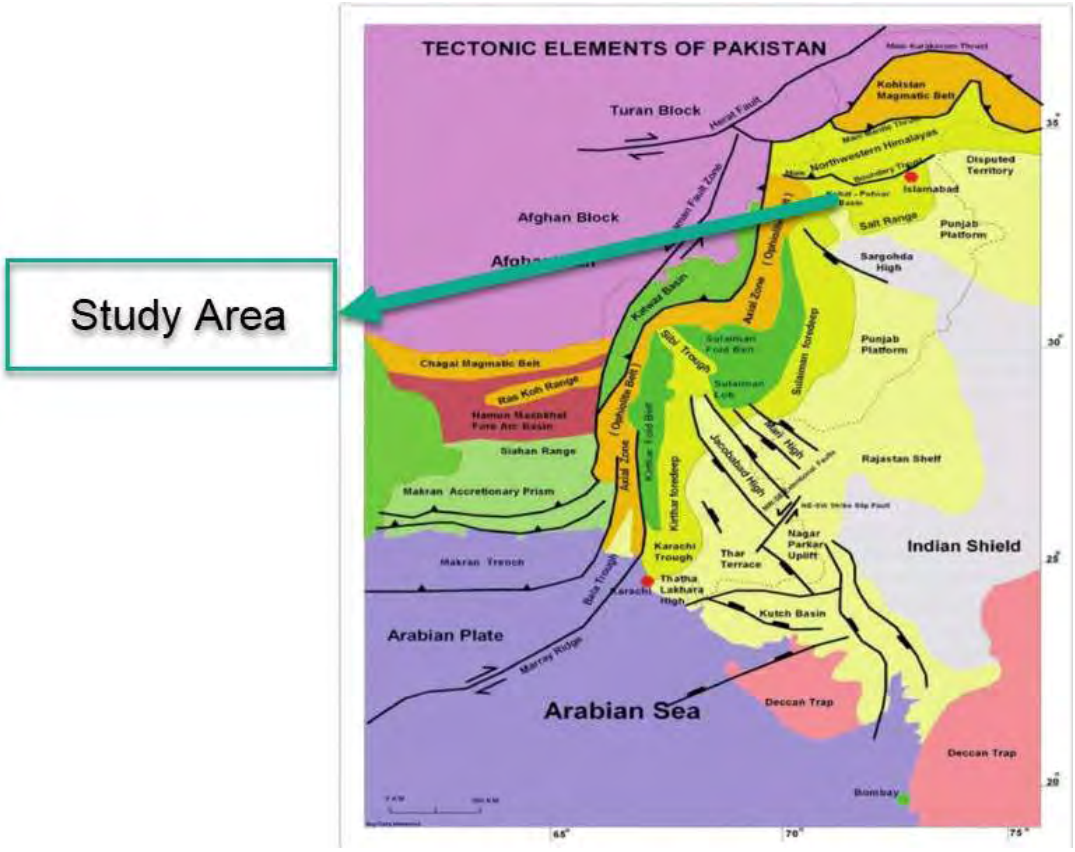

Figure 2.1 Tectonic Framework of Pakistan (Kazmi and Snee, 1989)

2.2 Geological Settings

Pakistan possesses a distinctiveness due to its geographical location at the confluence of two disparate areas. The Indian subcontinental crustal plate provides support to the southern region of Pakistan, which is considered a continuation of the Gondwanian Domain. The Tethyan Domain, encompassing the western and northern regions of Pakistan, exhibits a significant degree of geological intricacy.

According to Kazmi and Jan (1997), Pakistan encompasses three primary geological divisions, namely the Laurasian, Tethyan, and Gondwanaland domains. The origins of this phenomenon can be traced back to the Late Paleozoic era. The supercontinent that emerged from the amalgamation of the continents was referred to as Pangea. The fragmentation of Pangea occurred due to the northward movement of Laurasia and the southward movement of Gondwanaland in the late Triassic epoch. The final division of these two landmasses occurred as a result of the formation of the Tethys seaway. Pakistan is located at the intersection of the Gondwanian and Tethyan domains. As previously mentioned, the research site is located in the Upper Indus Basin of Pakistan.

Anticlines and thrusts are common in this region contrast to horst and graben structures in the southern region of Pakistan. The Sargodha High is a prominent geological feature that clearly distinguishes the northern region of Pakistan's geological basin from the lower Indus basin. The captivating convergence observed along the northern and eastern boundaries highlights the remarkable presence of the Main Boundary Thrust (MBT), a geological phenomenon that represents the eastern segment of the principal Himalayan thrusts. The Main Boundary Thrust, also known as the MBT, adeptly traverses a wide array of geological landscapes, including the Margalla Hills, the Kohat Range, and the Kala Chitta Range. The delineation of the western limit of the basin is predominantly reliant on the examination of Pre-Eocene sedimentary deposits and the existence of a thrust fault oriented towards the east, situated westward of Bannu. The Potwar basin is situated in the eastern sector of the geological formation, while the Kohat basin can be found in the western sector of the same formation. The two basins under examination are situated on diametrically opposite sides of the Indus River, as duly observed by Kadri in 1995.

The research area has an approximate area of 12 square kilometers and is situated in the western region of KFB (Kohat Foreland Basin). The Main Boundary Thrust (MBT) is a geological fault that plays a significant role in the tectonic activity of a region. The northern boundary of the Kirthar Fold Belt (KFB) is demarcated by the Sulaiman Range and the Kohat Range (KR). The study conducted by Khan et al. (1986) examined the uplift of the Mesozoic-Paleocene period. The sediments in question are in opposition to the Tertiary sediments found in the KFB. user's text is already academic. The phenomenon of north-south trending is seen. The Kurram Fault demarcates the western region. The KFB is demarcated by its western boundary, while its eastern extent is delimited by the course of the Indus River. Furthermore, it distinguishes it from its eastern counterpart, namely Potwar. The foreland basin is a geological feature that forms in response to the tectonic processes associated with the collision of two tectonic plates. The southern boundary of the KFB is delineated by the Bannu Basin, as shown by previous studies conducted by McDougall and Khan (1990), Pivnik and Khan (1996), and Ghaffari et al. (2015).

2.3 Sedimentary Basins of Pakistan

Pakistan consists of two main sedimentary basins, each exhibiting unique origins and geological histories. The following flow chart (figure 2.2) depicts the distribution of basins in Pakistan.

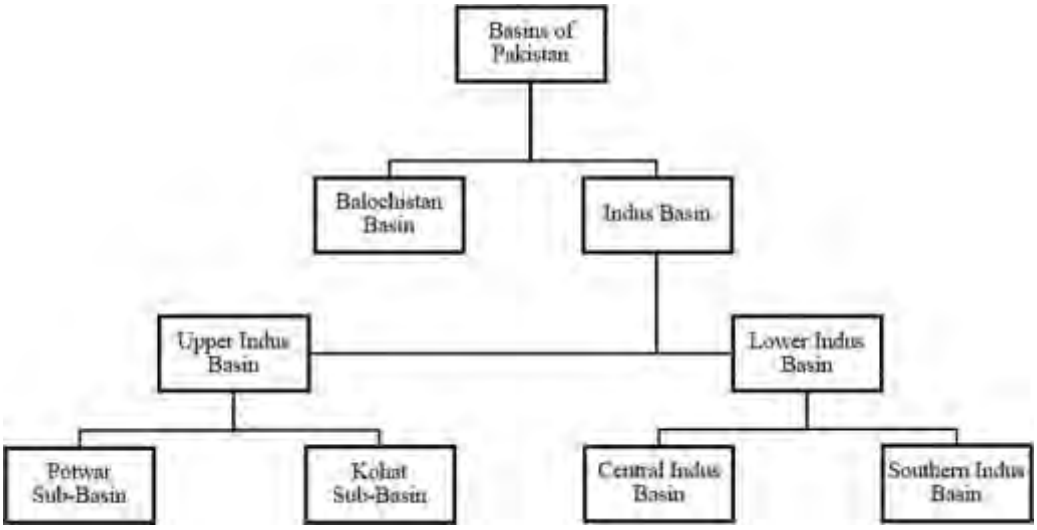

Figure 2.2 Sedimentary Basins of Pakistan (Kadri, 1995)

The amalgamation and organization of these geological depressions took place in the Cretaceous and Paleocene periods, aided by the Ornach Nal/Chaman Strike slip faults. To date, the identification of a smaller basin known as the Kakar-Khorasan Basin has been made. The basin has a discernible geological history that exerted a notable influence on its genesis. The formation of the Median Basin, often known as a result of the convergence between the Indian Plate and the Eurasian Plate, was documented by Kadri in 1995.

2.3.1 Balochistan Basin

The Makran accretionary wedge and the Makran offshore trench are fundamental constituents of the Balochistan Basin, constituting an important aspect of its geological constitution. The extent of geological investigation conducted in the specified region has been comparatively restricted in relation to other regions encompassed by the territorial boundaries of Pakistan. Within this vast basin, just six wells have been excavated, resulting in a rather restricted comprehension of its geological structure. Moreover, it is worth noting that the level of seismic surveying conducted in this particular area has been significantly limited. It is noteworthy to

mention that many gas reserves have been identified in the region of the Makran Coast. Nevertheless, it is crucial to emphasize that as of now, no economically viable hydrocarbon deposits have been discovered in this specific region (Kazmi and Jan, 1997). The geological basin encompasses the Dalbandin andKharan troughs.

2.3.2 Indus Basin

The basin under scrutiny exhibits remarkable geological magnitude and has been the subject of comprehensive research within the geographical boundaries of Pakistan. The sedimentary formations discovered within the Indus Basin showcase a remarkable chronology, encompassing a vast expanse of time ranging from the ancient Precambrian era to more recent periods. Remarkably, the Ordovician, Silurian, Devonian, and Carboniferous periods are noticeably lacking in these geological formations. In terms of their geographical distribution, these formations exhibit a remarkable northeast-southwest orientation, spanning an impressive distance of more than 1600 kilometers along their axis. The width of the basin, conversely, exhibits notable variation, with an average of approximately 300 kilometers. The aforementioned discoveries were meticulously recorded by Shah in the year 2009. The Indus Basin experiences a geological phenomenon knownas partitioning, resulting in the fragmentation of the basin into distinct basins. These separate basins encompass:

- The Upper Indus Basin comprises the Potwar and Kohat sub basins.
- Lower, Central, and Southern Indus Basins.

2.3.3 Lower Indus Basin

The Lower Indus basin, which is the part of the Indus basin that is located the furthest south, includes the Badin Block and its surroundings. Petroleum prospecting in the Lower Indus basin started in the 1950s. The bounds of the region are generally south of Khairpur High and extend into the Arabian Sea. The first significant oil and gas resources were found early in the 1980s close to Khaskheli, close to Badin. The first natural gas discovery was made at Sari-Hundi in the Dadu district, which is situated inside the Kirthar Range. After afterwards, other major as well as minor oil and gas discoveries were discovered in this region. The Lower Indus basin has a split and contains rocks from the Neogene to Cretaceous eras. There are parts of the Kirthar Range, which encircles the basin's western side, where it is difficult to make out the surface geology. In these regions, geological formations from the Neogene to the

Pleistocene epochs can occasionally be discovered. The Badin Block and its environs are devoid of both subsurface and surface geologicalcharacteristics.

2.3.4 Upper Indus Basin

The lower Indus basin and the northern Pakistani basin are distinguished by the Sargodha High. The northern and eastern bounds are overlapped by the Main Boundary Thrust (MBT), which refers to the eastern section of the main Himalayan thrusts. The MBT travels through a number ofplaces, including the Margalla Hills, the Kala Chitta Range, and the Kohat Range. The western boundary of the basin is defined by Pre-Eocene strata and an eastward-directed thrust fault west of Bannu. In the western portion of the basin is the Kohat basin, while in the eastern portion is the Potwar basin. These two basins are situated on the opposing banks of the Indus River (Kadri, 1995).

2.3.4.1 Potwer Sub-Basin

The Potwar Plateau, located to the north of the Salt Range, has a predominantly level topography,particularly in areas where it is traversed by significant river systems. The geographical boundaries of the region under consideration are demarcated by the Kalachitta and Margala Hills in the northern direction, the Indus River and Kohat Plateau in the western direction, and the Jhelum River and Hazara-Kashmir syntaxis in the eastern direction. The primary geological characteristic of the plateau is the Siwalik series. The region may be classified into two distinct zones: The Northern Potwar Deformed Zone (NPDZ), characterized by significant deformation such as thrusts and folds, and the Southern Potwar Platform Zone (SPPZ), which exhibits comparatively lower levels of deformation. The presence of Eocambrian evaporites serves as a constraint on deformation inside the SPPZ. This geographical area holds great importance in comprehending the tectonic forces and geological processes that occur inside its boundaries.

2.3.4.2 Kohat Sub-Basin

The Kohat Foreland Basin (KFB) is located approximately 100 kilometers south of the western Himalayan Foothills. Its genesis may be traced to the convergence of the Indo-Eurasian plates (Najman et al., 2010). The geographical area under consideration served as a significant sedimentary basin throughout the Early Miocene epoch, effectively preserving important evidenceof the Himalayan Orogeny, as described by

Ghani et al. (2018). The KFB, a constituent of the Himalayan Foreland Basin system, exhibits east-west oriented folds and faults due to the ongoing collision of tectonic plates (Wells, 1984). Mollai et al. (2019) suggest that the inclusion of transpressional deformation enhances the complexity of the structural attributes. The study site is situated within the western KFB region. According to Khan et al. (1986), the physical boundaries of the area under question are defined by the Main Boundary Thrust (MBT) and the Kohat Range to the north. The Kurram Fault serves as the demarcation for the western boundary of the region, while the eastern extension is delineated by the Indus River. This natural feature acts as a barrier, effectively isolating the region from the Potwar Foreland Basin. The southern limit is demarcated by the Bannu Basin, as stated by McDougall and Khan (1990).

2.4 Stratigraphy of Kohat Basin

The stratigraphic record of the Kohat Foreland Basin (KFB) has undergone three distinct evolutionary phases. Throughout the Paleozoic to Mesozoic era, a progressive accumulation of sedimentary rocks occurred along the passive northern boundary of the Indian Plate. Following this, a foredeep basin of Paleogene origin was formed, experiencing gradual sedimentation from the Late Cretaceous to the Early Eocene period. After the collision between the Indo-Eurasian plates, the basin saw the development of structures oriented in an east-west direction due to compression occurring in a north-south direction. The formation of an intra-continental foredeep basin occurred, resulting in the slow deposition of sediment over the Miocene-Pliocene era. The aforementioned information is substantiated by research undertaken by Khan et al. (1986), Kazmi and Abbasi (2008), and Shah (2009).

Extensive research has been conducted on the surface geology of the KFB, revealing that it predominantly consists of Eocene platform rocks. The rocks in question are stratigraphically distinct from the underlying Molasse strata of the Miocene to Pliocene epoch, with an unconformable boundary separating the two. The Molasse sediments are composed of two main groups, namely the Rawalpindi and Siwalik groups. This classification has been established by several researchers, including Gee (1945), Fatmi (1973), Sameeni et al. (2009), and Shah (2009). The Panoba Shale, which is of Eocene period origin, is often regarded as the oldest exposed rock unit in the area. Based on a thorough review of well data, it can be determined that the Datta Formation, which is attributed to the Early Jurassic epoch, is the most ancient rock

unit that remains buried and inaccessible. Unfortunately, a dearth of readily available data exists on the stratigraphy of rock formations encompassing the EoCambrian to Triassic epochs within the KFB. This scarcity can be attributed to the absence of exposure or drilling activities conducted on these particular strata. The stratigraphic attributes of rock formations encompassing the Early Eocene to the Early Pliocene epochs have been ascertained using on-site observations and an exhaustive examination of preexisting scholarly works. On the other hand, the knowledge regarding hidden rock formations spanning the Jurassic to the Paleocene epochs is predominantly obtained from publicly available data sources, which encompass the research conducted by Meissner et al. in 1974 and 1975, Shah in 1977, Wells in 1984, Ahmad and Khan in 2012, Ghani et al. in 2018, and Yazdi and Sharifi Teshnizi in 2021.

The seismic data acquired from the western KFB region has enabled the identification of two separate décollement levels. The first décollement, referred to as the basal décollement, is situated at the uppermost limit of the crystalline basement or foundation EoCambrian formations. Furthermore, a secondary décollement has been found as well. During the Early Eocene epoch, the

basin exhibited a shale and evaporite succession with an approximate average thickness of 2000 meters. The geologic map the study area has been shown in figure 2.3

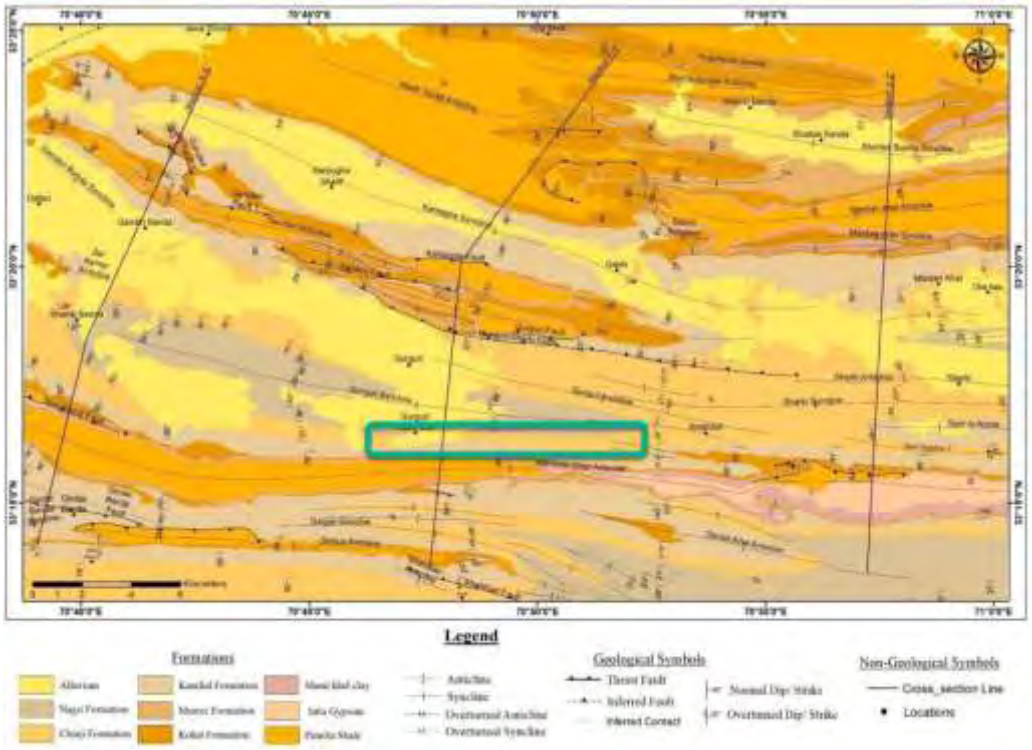

Figure 2.3 Surface Geological map of Kohat Basin showing study area with dark green rectangle (Gardezi et al., 2021)

2.5 Stratigraphy of Study Area

The Stratigraphic formations up to Datta formation of Jurassic have been encountered during drilling in Manzalai field. The overall stratigraphic column has been displayed in below figure 2.4

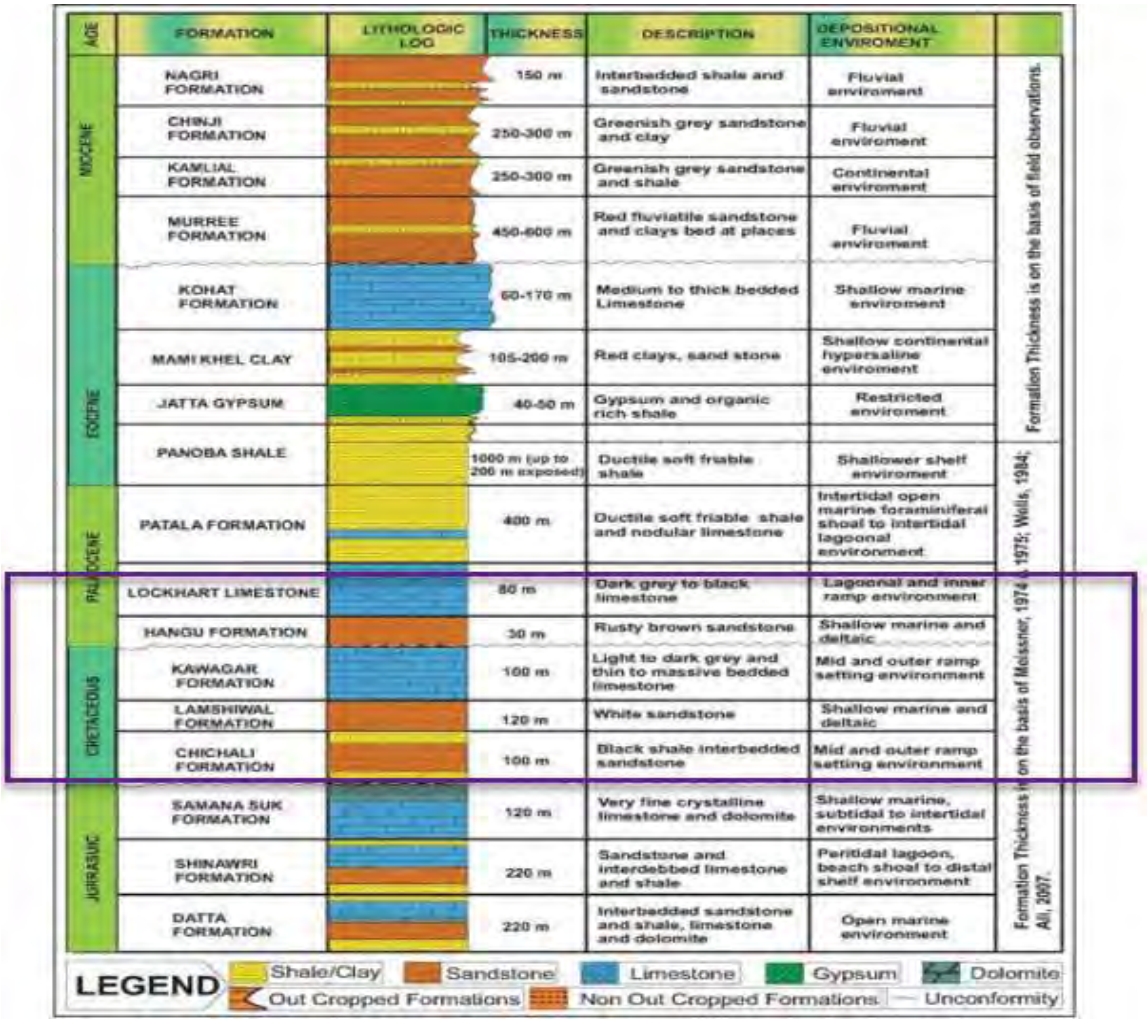

Figure 2.4 Generalized Stratigraphic chart of Kohat Sub-Basin (Gardezi et al. 2021)

2.6 Petroleum System of Kohat Sub-Basin

2.6.1 Source Rock

The Datta formation, which originated during the Jurassic period, and the Chichali formation, which formed during the Cretaceous period, serve as the primary geological sources within the Kohat Basin. The deposition of Datta occurred in an environment characterized by oxic to dyoxic conditions, whereas the deposition of

Chichali took place in an anoxic/reducing marine environment. The formation of Data and Chichali was observed in an environment characterized by high levels of organic production, as shown by Gakkhar et al. (2011).

2.6.2 Reservoir Rock

Saddique et al. (2016) have shown that the Lockhart formation predominantly comprises limestoneand functions as a reservoir within the Kohat basin. Likewise, the Hang formation mostly consists of sandstone and serves as a reservoir inside the corresponding basin. Furthermore, the Lumshiwal Formations within the Kohat basin have a prevailing lithology consisting of sandstone with a range of grain sizes, from fine to coarse. These formations also function as reservoirs.

2.6.3 Cap/Seal Rock

The Panoba/Patala formation, which can be traced back to the Paleocene epoch, serves as a barrier inside the Kohat basin, successfully impeding the movement of fluids. According to Ahmad and Khan (2012), the reservoir is horizontally sealed by a significant Panoba/Patala cap sequence, which demonstrates a widespread distribution and is located inside a structurally culminating zone marked by vigorous tectonic activity.

Chapter 03

Seismic Interpretation

3.1 Introduction

The interpretation process is used to turn seismic data into a model describing the subsurface, which may be divided into two categories: structural and stratigraphic. The major goal of interpretation is to precisely pinpoint the particular coordinates of the abnormal zone by examining the seismic section. This section serves as a graphic representation of the Earth's geological stratum model. Inadequate understanding of geology usually results in a limited ability to determine the validity or falsity of geological conclusions. In the quest for excellence in interpretation, consistency is viewed as the most important requirement, before accuracy. To ensure accurate seismic data analysis, it is critical to have a complete understanding of not just seismic information, but also gravitational and magnetic data, well parameters, surface geology, and a variety of geological and physical concepts.

According to Telford et al. (1999), traditional seismic interpretation requires identifying and monitoring seismic reflectors with lateral continuity. The fundamental goal of this approach is to identify geological formations, stratigraphic layers, and the geometry of the reservoir. The basic goals of this study are to identify, delineate, and quantify hydrocarbon accumulations. The conventional approach for interpreting seismic data is a multidimensional operation that requires a high degree of expertise and considerable practical knowledge in the fields of geology and geophysics. In response to the growing demand to examine more complex objects, significant advances in data technology and seismic processing procedures have occurred during the previous thirty years. As a result of this advancement, the field of seismic analysis has evolved into a science that heavily relies on computer approaches. The use of computer-based processing, which is recognized for its enhanced accuracy, precision, efficiency, and user happiness, enables researchers to devote more time to data analysis.

Many software tools, including Kingdom 2021, are required for the effective implementation of this procedure. The primary goal of our study is to achieve a higher

level of transparency in the reflection process, with the goal of authentically duplicating the underlying structure and stratigraphy. Geologists can determine boundaries by detecting differences in acoustic impedance, as shown by the presence of reflection. The well parameters are examined in combination with the seismic data to differentiate between the corresponding horizons. Data analysis has included the use of well-log data to construct a correlation with seismic data. The analysis of geological structures, as well as the computation of sedimentary layer characteristics, acoustic velocity, seismic succession, and rock attributes, are significantly reliant on high-quality seismic data (Dobrin & Savit, 1988). There are numerous ways to interpret the process.

- Structural Evaluation
- Mechanical feature identification
- Stratigraphic research
- Establishment of stratigraphic boundaries

3.2 Structural Interpretation

Given that a significant proportion of hydrocarbons have previously been depleted from structural traps, this particular study holds particular relevance and applicability in the context of Pakistan. The investigation of reflector geometry necessitates the analysis of reflection times. Seismic structural analysis is mostly employed in the exploration of structural traps associated with hydrocarbon reservoirs. The subsequent are the primary applications for structural analysis.

Most structural interpretations primarily rely on two-way reflection timings instead of time and depth structural maps. These maps are specifically created to visually represent the geometry of a multitude of chosen reflections. There exist several seismic components that can be effectively depicted using comprehensible graphical representations. According to Sheriff (1990), undulating reflections can indicate the presence of folded beds, but discontinuous reflections can facilitate the identification of faults.

3.3 Seismic Interpretation Workflow

Figure 3.1 displays the procedures used in seismic data analysis. The SMT Kingdom application is used to import SEG-Y data during the base map generation procedure.

The process of finding horizons of concern can be accomplished using both human and automatic approaches, particularly when the tracking mode is configured to run automatically.

The method of determining horizons often begins with the use of a synthetic seismogram generated from well data. Horizon contours are created with the goal of determining structural high and low points. Following the conclusion of this approach, contours that indicate both time and depth are seen. The use of well point velocity aids in the creation of depth contours.

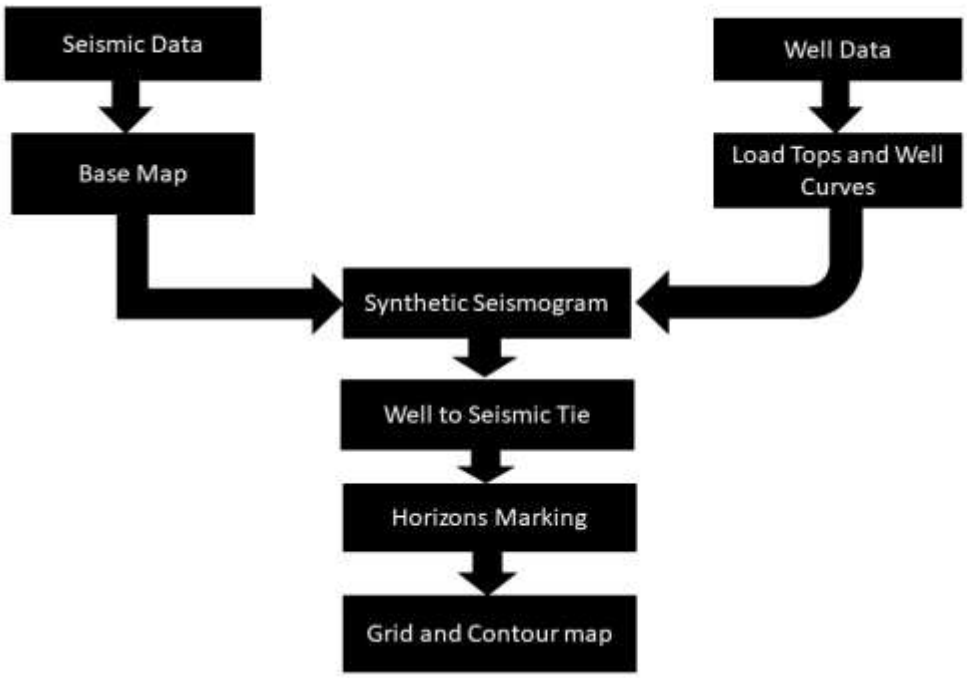

Figure 3.1 Seismic Interpretation workflow

3.3.1 Generation of Synthetic Seismogram

The procedure of creating synthetic seismograms needs the inclusion of two-way travel time for each individual well top. The use of depth, sonic log data, and area replacement velocity facilitates the computation of the two-way time for each well top or reflector. The time-depth chart is created by combining the two-way travel time and the surface depth of each hole. The wavelet, which has been efficiently extracted at a frequency of 25 Hz, is convolved with the well data to generate the synthetic seismogram as the end result. To establish a correlation, investigate the link between

the synthetic seismogram and the seismic data. Figure 3.2 depicts a synthetic seismogram that matches Manzalai-01.

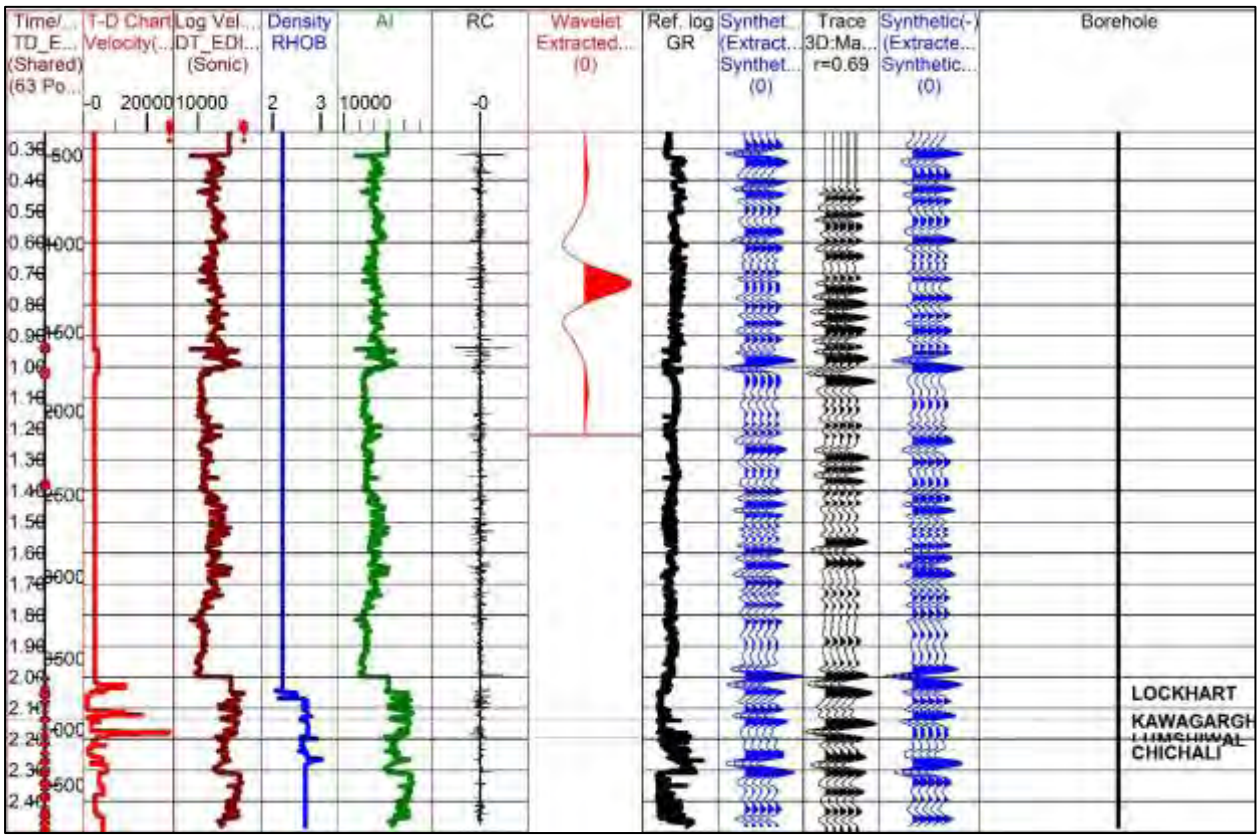

Figure 3.2 Synthetic Seismogram of Manzalai-01 well indicating the horizons of interest.

3.3.2 Horizons Marking

Seismic reflectors of significant magnitude, typically referred to as "horizons" within the discipline of geology, are produced by pronounced seismic amplitudes. In order to boost the accuracy of horizon identification and improve the seismic segment, a pre-existing synthetic seismogram is overlaid onto it. The analysis of the synthetic seismogram and the notable reflection amplitude observed for each horizon led to the recognition and demarcation of five distinct horizons. The disputed boundaries are denoted as Lockhart (cyan), Hangu (yellow), Kawagarh (red), Lumshiwal (light green), and Chichali (pink). The visual representation of all horizons can be seen inside the analyzed region is depicted in Figure 3.3, which can be found on inline 660. The picture notably emphasizes Lockhart, Hangu, and Lumshiwal strata as the primary reservoirs for hydrocarbon accumulation within this unique geological environment.

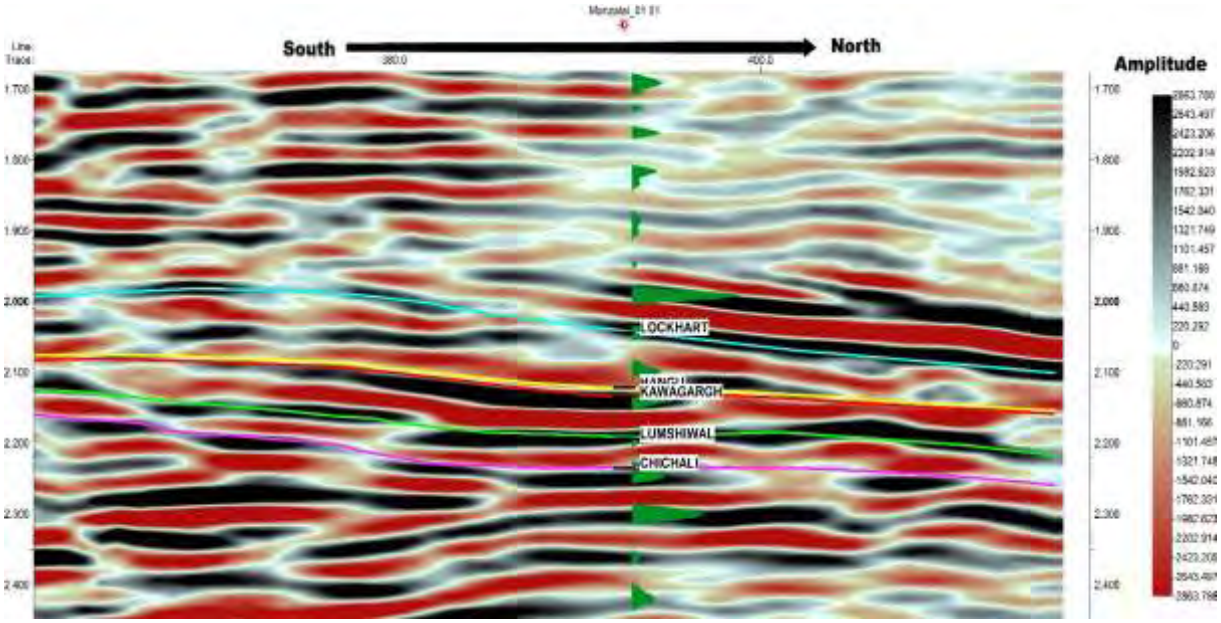

Figure 3.3 Display of Inline 660 showing marked horizons and synthetic seismogram (green)

The cross line 390 has been shown in figure 3.4 with marked horizons.

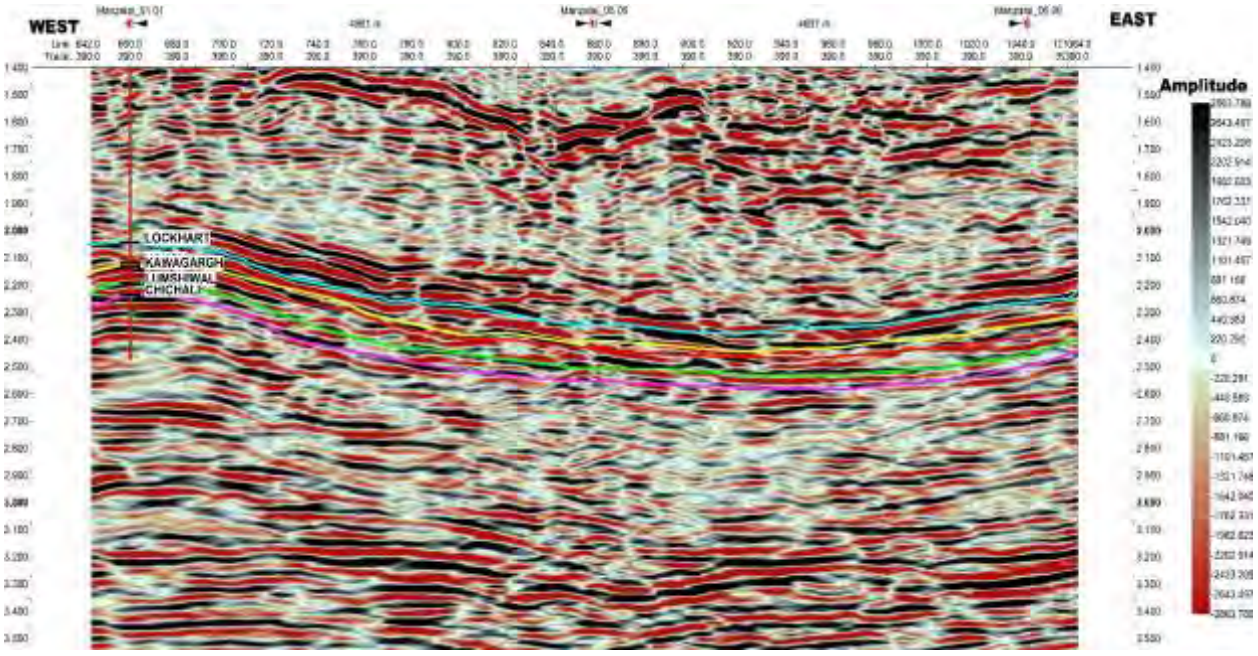

Figure 3.4 Display of Cross Line 390 with marked horizon indicating Formation goes deeper from left to right

3.3.3 Time Contour Map

In order to illustrate the subsurface structure, the maps were created using seismic time travel time for individual seismic lines. The lack of a direct structural depiction is obvious, but it does give us information about the distribution of horizons within

the subsurface and its structural makeup. Because the temporal contour maps are region-specific, they provide a more focused analysis of the area. The goal of this inquiry is to create time contour maps. The travel time of the seismic wave is plotted against the northing and easting coordinates (X and Y), which correspond to the two-way travel time, in order to identify the temporal limits. The generated contour maps are Lockhart, Hangu, Kawagarh, Lumshiwal, Chichali.

3.3.3.1 Time Contour map of Lockhart

Lockhart Formation is the primary reservoir for hydrocarbon exploration in the study area. In order to understand the spatial extent of the reservoir, the time contour map has been generated which is shown in figure 3.5.

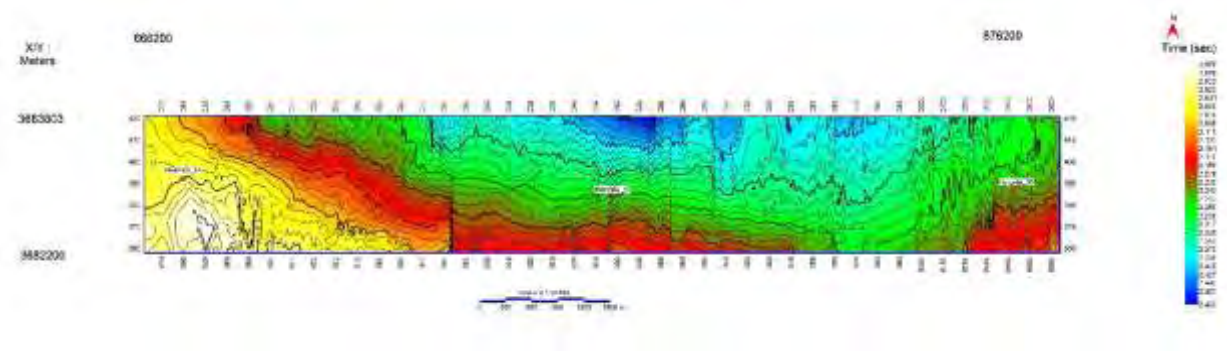

Figure 3.5 Time Contour map of Lockhart Formation indicating shallower region in Northwestern and a deeper region in Southeastern region.

The blue color is for deeper level while yellow color shows a shallow level. The horizon goes deeper as we move from Northwest to Southeast.

3.3.3.2 Time Contour map of Hangu

Hangu Formation is the secondary target for hydrocarbon exploration. In order to understand the spatial extent of the reservoir, the time contour map has been generated which is shown in figure 3.6.

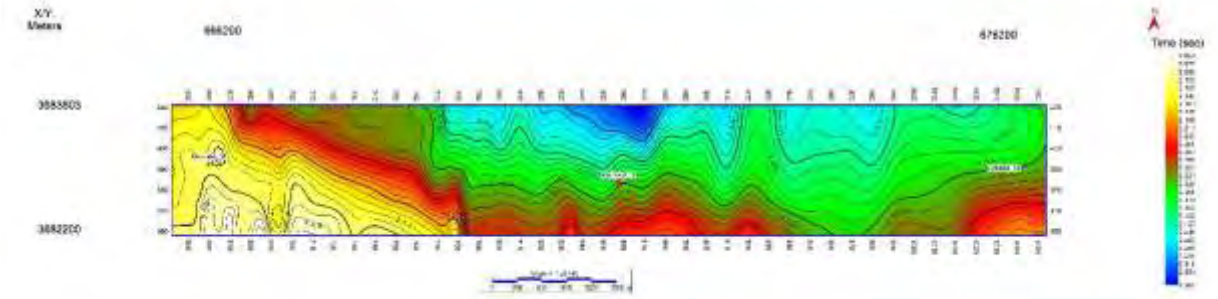

Figure 3.6 Time contour map of Hangu Formation indicating shallower region in Northewestern and a deeper region in Southeastern region..

3.3.3.3 Time Contour map of Kawagarh

Kawagarh has been marked to estimate the bottom of hangu. The time contour map of kawagarh has been shown in figure 3.7.

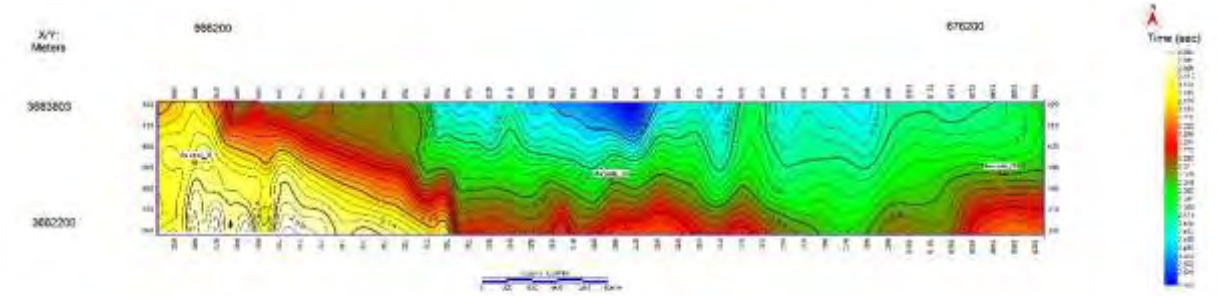

Figure 3.7 Time Contour map of Kawagarh Formation indicating shallower region in Northewestern and a deeper region in Southeastern region.

3.3.3.4 Time Contour map of Lumshiwal

Lumshiwal Formation is the secondary target for hydrocarbon exploration. In order to understand the spatial extent of the reservoir, the time contour map has been generated which is shown in figure 3.8.

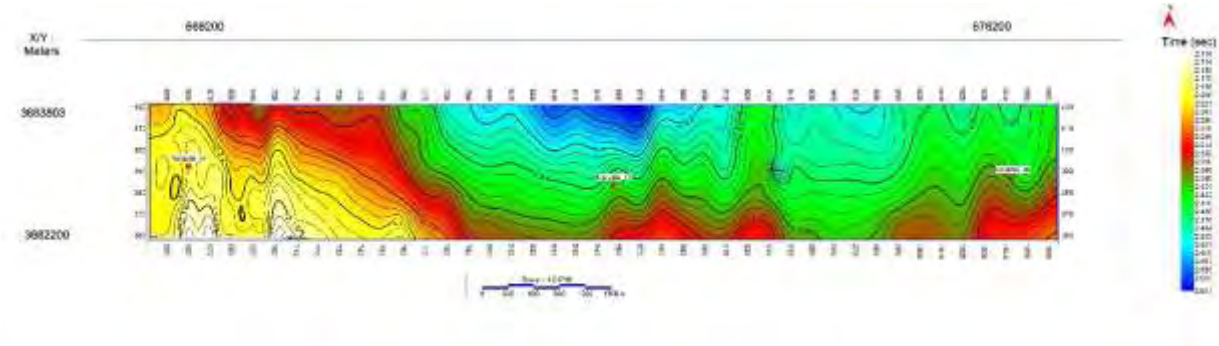

Figure 3.8 Time Contour Map of Lumshiwal Formation indicating shallower region in Northewestern and a deeper region in Southeastern region..

3.3.3.5 Time Contour map of Chichali

Chichali has been marked to estimate the bottom of hangu. The time contour map of kawagarh has been shown in figure 3.9.

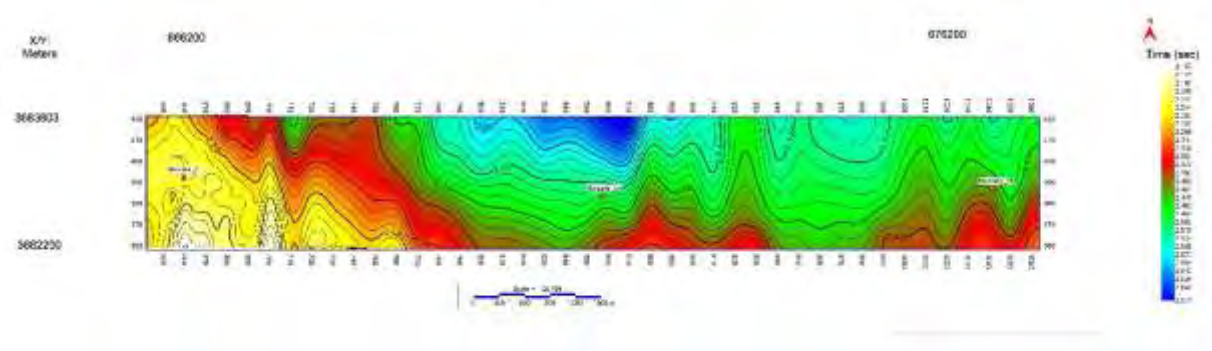

Figure 3.9 Time Contour map of Chichali Formation indicating shallower region in Northewestern and a deeper region in Southeastern region.

Chapter 04

Petrophysical Analysis

4.1 Introduction

The discipline of petrophysics is employed to ascertain the physical characteristics of rocks, with a specific emphasis on rocks found in reservoirs. Reservoir characterisation entails the systematic identification and delineation of subsurface reservoir zones that exhibit the presence of hydrocarbon reserves, hence indicating their potential for future extraction. The process outlined above is of great significance in the oil and gas industry as it assists in the identification of well locations and the evaluation of field opportunities.

Petrophysical analysis is of significant importance in the identification, quantification, and allocation of formations that contain hydrocarbons. The evaluation of petrophysical parameters in porous media involves the analysis of resistivity, permeability, porosity, shale volumes, and fluid characteristics (Kumar et al., 2018). The incorporation of well log data facilitates the establishment of a correlation between seismic and core data, hence playing a crucial role in the thorough characterization of reservoirs (Rider, 1986).

The primary part of doing well log analysis involves the identification and delineation of reservoirs, as well as the determination of zones of interest and transition zones. The attainment of this target can be accomplished through the implementation of a concise analysis of gamma ray attributes, the segregation of resistivity logs, and the integration of crossover between neutron and density logs. Upon completion of log analysis, crucial petrophysical characteristics like shale volume, mean effective porosity, and water saturation are computed (Poupon and Leveaux, 1971). The equation proposed by Archie and Simandoux is utilized to estimate the saturation level of water.

The hydrocarbon reserve was located via a petrophysical examination carried out on the Manzalai Block. The determination of reservoir characteristics requires the exploitation of three unique wells, namely Manzalai-01, Manzalai-05, and Manzalai-

06. The log curves employed in this study included the spontaneous potential log (SP), gamma-ray log (GR), sonic logs (DT), lateral log deep (LLD), lateral log shallow (LLS), neutron log (NPHI), Photoelectric Factor (PEF), Caliper (CALI) and density log (RHOB). Estimations have been performed for the following parameters:

- Volume of Shale
- Total and Effective porosity
- Water and Hydrocarbon Saturation

4.2 Workflow of Petrophysics

The following workflow has been implemented for the petrophysical analysis:

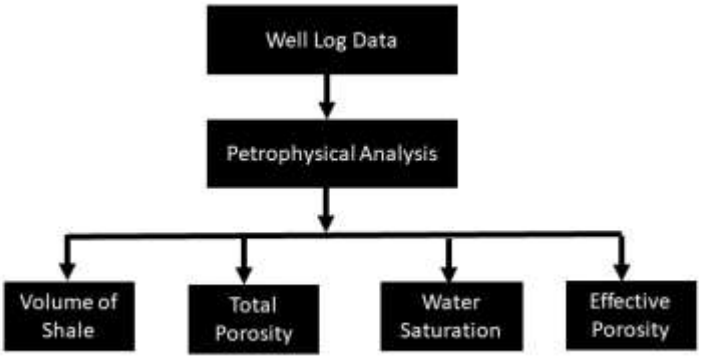

Figure 4.1 Workflow of Petrophysical Analysis

4.3 Computation of Volume of Shale

Shale volume (Vsh), commonly known as shale percentage, denotes the relative amount of mud or shale contained inside a specific geological formation. The occurrence of shale volume (Vsh) is likely to be observed in a variety of reservoir rocks, exhibiting a range of geometrical configurations. Moreover, there existed alternate techniques for the lamination, dispersion, or architectural utilization of the substance. The evaluation of shale within the lithological framework is of great significance in the reservoir characterization process since the volumetric shale content (Vsh) plays a critical role in assessing reservoir porosity.

The Gamma-ray log, which is well recognized as a highly dependable lithology indicator, is utilized for the purpose of quantifying the presence of shale. The fundamental principle that forms the basis of the GR log involves the systematic

observation and measurement of radioactive levels present in geological structures. Certain categories of rocks demonstrate a discernible occurrence of radioactive elements, including thorium, uranium, and potassium, within a defined range (Tiab and Donaldson, 2015).

This study introduces a range of methodologies, including both linear and non-linear approaches, for the quantification of shale volume. The approaches discussed above are dependent on the gamma ray index and can be quantitatively represented as follows:

$$\text{Vsh} = \frac{GR_{log} - GR_{clean}}{GR_{shale} - GR_{clean}} \qquad (4.1)$$

The symbol "Vsh" is used to denote the gamma ray index. The variable GR_log represents the gamma ray value at a specific depth, whereas GR_{shale} and GR_{clean} represent the maximum and minimum values of GR_log, respectively.

4.4 Porosity Computation

Porosity is a fundamental geological property that characterizes the volumetric measurement of the void spaces within a rock. The reservoir exhibits the capability to contain several types of fluids, including hydrocarbons, mobile water, capillary water, or clay-bound water (Cluff and Cluff, 2004, Rider and Kennedy, 2011). The determination of material porosity can be achieved through the utilization of the density log, neutron log, sonic log, or a combination thereof. The utilization of these logs has advantages in precisely determining lithology and conducting comprehensive porosity evaluation, both of which are crucial in efficiently managing fluid saturation levels inside a reservoir.

The determination of porosity was carried out by utilizing the logs described in the subsequent section.

4.4.1 Density Porosity

The density log is an essential instrument utilized in differentiating lithology and assessing porosity and hydrocarbon density. Rider and Kennedy (2011) have shown that the general scale encompasses a measurement range of 1.95 to 2.95, with the units denoted as grams per cubic centimeter (g/cm3). The result of a density log refers to the measurement of the overall density of a rock. The measurement under

consideration encompasses both the fluid and solid components present within the pores of the rock. This is accomplished by employing the subsequent equation, as initially postulated by Wyllie in 1963:

$$\phi_d = \frac{\rho_m - \rho_b}{\rho_m - \rho_f} \qquad (4.2)$$

The symbols $\boldsymbol{\rho_m}$, $\boldsymbol{\rho_f}$ and $\boldsymbol{\rho_b}$ represent the densities of the matrix, fluid, and log response, respectively, measured in grams per cubic centimeter (gm/cm^3).

4.4.2 Neutron Porosity

The neutron log is employed for the purpose of quantifying the porosity that is present within the geological formation. To mitigate the influence of lithologic characteristics, it is recommended to employ the method of averaging porosity values derived from density and neutron logs (Rider and Kennedy, 2011).

The quantification of the hydrogen index in the reservoir, a characteristic that is closely linked to porosity, can be accomplished by utilizing a neutron log to evaluate the count rate of neutrons. The collision between a neutron with the nuclei of a formation results in the generation of energy. The utilization of neutron log measurements improves the efficacy of porosity identification. Tiab and Donaldson (2015) have observed that gas-bearing sands exhibit a drop in neutron porosity as a result of a reduction in hydrogen ion concentration.

4.4.3 Sonic Porosity

The term "sonic porosity" pertains to the utilization of acoustic waves in order to measure the void areas within subterranean rock formations. This technology is utilized in the disciplines of geophysics and reservoir engineering. The primary role of this technology has a substantial impact on the hydrocarbon exploration process and the characterisation of reservoirs. The porosity and fluid content of subsurface reservoirs can be deduced by geoscientists through the analysis of sound wave velocity as it propagates within rock formations. This approach facilitates the assessment of the viability of extracting oil and gas from these sources (Sheriff, 2002). The use of this non-invasive technology has had a notable impact on the oil and gas industry as it possesses the capability to provide crucial insights into the sub surface’s properties. As a result, the utilization of this technology has resulted in

significant improvements in the effectiveness and accuracy of resource evaluation and extraction methodologies (Castagna et al., 1993). The mathematical formulation is given below.

$$\phi_s = \frac{\Delta t_{log} - \Delta t_{ma}}{\Delta t_{fl} - \Delta t_{ma}} \quad (4.3)$$

Where ϕ_s , Δt_{ma} , Δt_{fl} and Δt_{log} represents sonic porosity, matrix interval transit time, fluid interval transit time and interval transit time of the formation using sonic log.

4.4.4 Total Porosity

The entire porosity encompasses all void areas, irrespective of the interconnectivity or isolation of the pores. The determination of total porosity can be achieved through the utilization of neutron and sonic logs, or by applying a combination of density log and neutron log. The existence of hydrocarbons can be deduced from the presented data by the detection of a link between the density log and the neutron log.

The mathematical expression used to calculate the mean porosity is given by the following formula:

$$\phi_T = \frac{\phi_N + \phi_d}{2} \quad (4.4)$$

$$\phi_T = \frac{\phi_N + \phi_s}{2} \quad (4.5)$$

Where ϕ_N represents Neutron porosity.

4.4.5 Effective Porosity

To improve the understanding of reservoir permeability when core data is not available, it is recommended to estimate the effective porosity using Equation 4.4. Additionally, it is important to take into account that the effective porosity provides insight into the level of interconnectivity between pores and the fluid permeability through them. Rider and Kennedy (2011) assert that the productivity of shaly sandstone is relatively diminished in comparison to clean sandstone intervals.

The determination of effective porosity serves a twofold role within the context of reservoir analysis. Firstly, it facilitates the precise determination of water saturation, hence mitigating the degree of ambiguity associated with this parameter. Additionally, it aids in the determination of the specific reservoir interval located inside the parent formation. The term "effective porosity" is widely used to describe the porosity of a rock volume, wherein linked pores enable fluid movement and permeability inside a reservoir. In reality, the overall porosity of a substance is rarely higher than its effective porosity. The determination of porosity entails the deduction of shale volume from the overall rock volume. Formulas are utilized in the computational process.

$$\phi_{eff} = \phi_T\ (1 - Vsh) \qquad (4.6)$$

Where ϕ_{eff} is effective porosity, ϕ_T is the average porosity and Vsh is the volume of shale.

4.5 Water Saturation

Water saturation refers to the fraction of pore volume within a rock that becomes occupied by water throughout the process of formation. In the absence of verified hydrocarbon presence within the pores of the formation, it is postulated that these pores will be occupied by water. The primary objective of well logging is to determine the levels of water and hydrocarbon saturation. The determination of water saturation in the formation is accomplished by the utilization of a mathematical equation referred to as the Archie equation, denoted as equation 4.9.

$$S_w = n\sqrt{\frac{(F*R_w)}{R_t}} \qquad (4.7)$$

The formation factor (F) can be defined as the ratio of a to m, where R_w represents the water resistivity, R_t denotes the true formation resistivity utilized in laterolog deep (LLD) applications, n represents the saturation exponent ranging from 1.8 to 2.5 (assumed as 2), an is a consistent parameter with a value of 1, represents the effective porosity, and m represents the cementation factor, assumed to be 2. The other parameters required for the calculation of R_w can be derived from the data obtained from spontaneous potential logs by following the subsequent procedures.

1. Select SSP from SP log using the equation 4.8 formula (Rider, 1996).

$$SSP = SP_{CLEAN} - SP_{SHALE} \quad (4.8)$$

Where SSP, SP_{CLEAN}, SP_{SHALE} represents Static spontaneous potential, Spontaneous potential for sand and Spontaneous potential for shales.

2. To determine the formation temperature FT against the depth of the reservoir formation, use equation 4.9 (Rider, 1996).

$$\mathrm{FT} = \frac{(\mathrm{BHT}-\mathrm{ST})\mathrm{FD}}{\mathrm{TD}} \quad (4.9)$$

Where FT, BHT, ST, FD and TD represents Formation Temperature, Bottom Hole Temperature, Surface Temperature, Formation Depth and Total Depth, respectively.

3. Equation 4.10 employs the resistivity of the mud filtrate, ascertained at a surface temperature, to ascertain the resistivity of the mud filtrate at the specific zone under consideration.

$$\mathrm{R_{mf2}} = \frac{(\mathrm{ST}+6.77)\mathrm{R_{mf1}}}{(\mathrm{FT}+6.77)} \quad (4.10)$$

Where ST, FT, $\mathrm{R_{mf1}}$, $\mathrm{R_{mf2}}$ represents Surface Temperature, Formation Temperature, Resistivity of mud filtrate at surface and resistivity of mud filtrate at formation depth.

4. The subsequent procedure involves the determination of the resistivity of the mud filtrate. However, this calculation can only be performed if the value of Rmf2 exceeds 0.1 Ωm. In such cases, the resistivity of the mud filtrate (Rmfe) can be obtained by utilizing equation 4.11.

$$\mathrm{R_{mfeq}} = 0.85 \times \mathrm{R_{mf2}} \quad (4.11)$$

If the value of Rmf2 is below 0.1 Ωm, the appropriate method for determining the value of Rmfe at formation temperature is to refer to chart SP-1 (Schlumberger Chart) provided in appendix-2. This process is illustrated in Figure 4.2. The Rwe values are presented in the second bar of the figure. These values are determined by utilizing the SSP, FT, and Rmfe values.

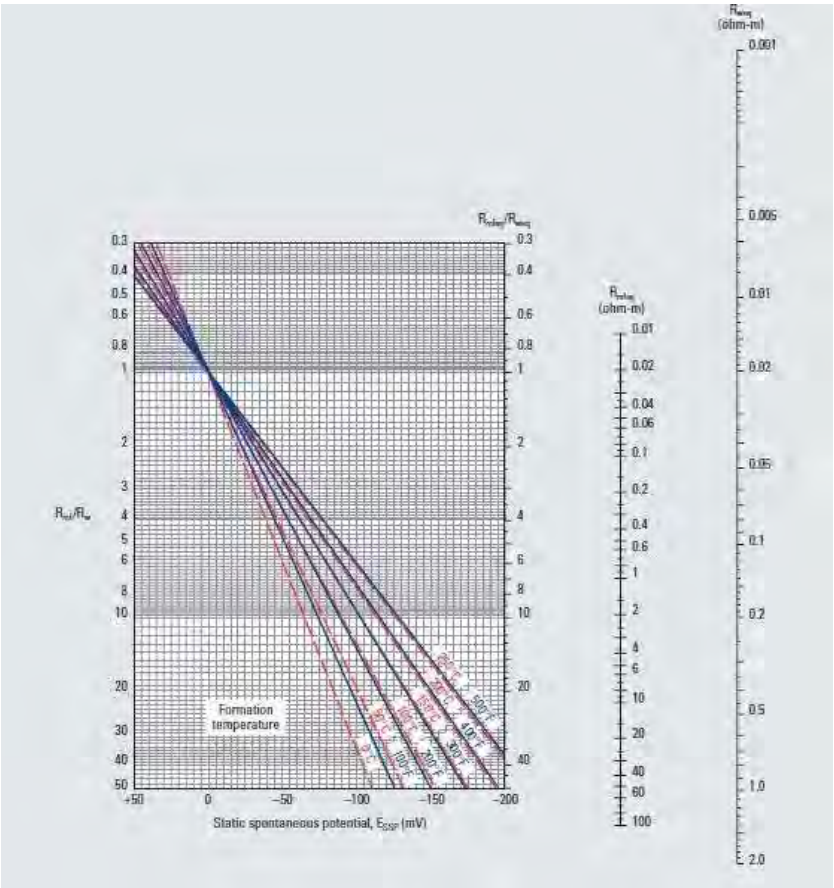

Figure 4.2 The determination of Rweq from the SP-1 chart involves utilizing the well data header file to ascertain the resistivity of water equivalent of water, as described by Schlumberger (1989).

5. The final stage involves determining the value of Rw following the acquisition of the Rwe value from the SP-1 chart. This entails utilizing the FT and Rwe values in conjunction with the SP-3 chart, as seen in Figure 4.3, to compute Rw.

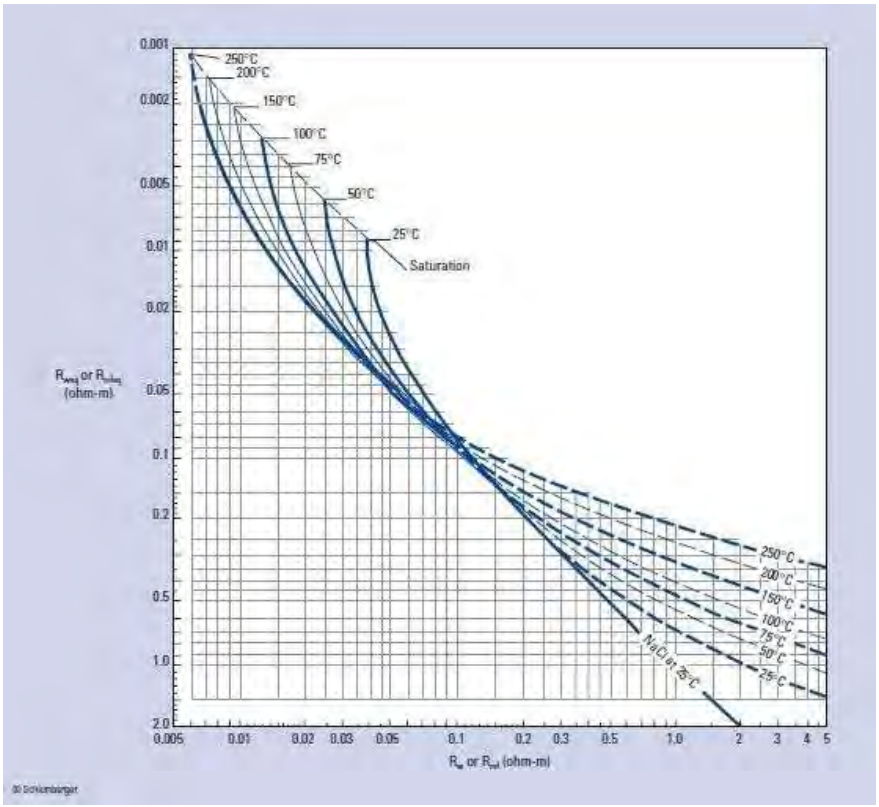

Figure 4.3 The determination of Rw using the SP-3 chart, subsequent to the determination of Rweq and the use of formation temperature curves, can be employed to ascertain the most suitable match for Rw in a given well (Schlumberger, 1989).

Once the value of Rw is obtained, the Archie equation can be used to compute water saturation. But in most cases the reservoir is shaky (having shale volume more than 10%), in those cases Archie Saturation Law overestimates the formation water saturation. In order to overcome those problems certain modified versions of Archie Law are available and one of those is Simandoux equation. The Modified Simandoux Equation is a mathematical formulation that expands upon the original equation designed for shaly rocks, in order to accommodate scenarios when the saturation exponent (n) is not equal to 2. The Simandoux equation, proposed in 1963, stands as an early example of a model that effectively addresses and rectifies the overestimation of conductivity in the matrix caused by the existence of distributed clays. In contrast, the Archie equation of 1942 tends to overestimate the level of water saturation in the presence of clays. The equation, as presented in the conventional version by Bardon and Pied (1969), is:

$$SW_{sim} = \frac{a.R_w}{2.\emptyset_{eff}}\left[\sqrt{\left(\frac{Vsh}{Rsh}\right)^2 + \frac{4.\emptyset^m}{a.R_w.R_t}} - \frac{Vsh}{Rsh}\right] \qquad (4.12)$$

Where SW_{sim}, Rsh, Rt represent Simandoux Saturation, Resistivity of Shales and LLD log, respectively.

4.6 Interpretation of Well logs

The process of formation identification involves the analysis and comprehension of the data present in well logs. In general, the combination of well logs and their respective evaluation results in the formation of a cohesive representation known as a "composite log." The focus of this discussion will revolve around the petrophysical observations obtained from Wells Manzalai-01, Manzalai-05, and Manzalai-06.

4.6.1 Petrophysics of Manzalai-01

The petrophysical analysis of Lockhart, Hangu and Lumshiwal has been carried out. On the basis of petrophysical parameters, the Lockhart formation has lower shale volume on average up to 12 %. The upper portion of the Lockhart formation has a highly disturbing density log and the lower portion of Lockhart is attributed to very tight limestone have no porosity. These all make it a non-reservoir zone in Manzalai-01. The petrophysical analysis of Lockhart Formation in Mnazalai-01 has been shown in figure 4.4.

Hangu Formation is the second to be analyzed in terms of its reservoir potential. On the basis of available log responses, a hydrocarbon bearing zone from depth ranging 3687 m to 3698 m (approximately 12 m) has been identified. The petrophysical parameters are listed in Table 4.1 for Hangu formation

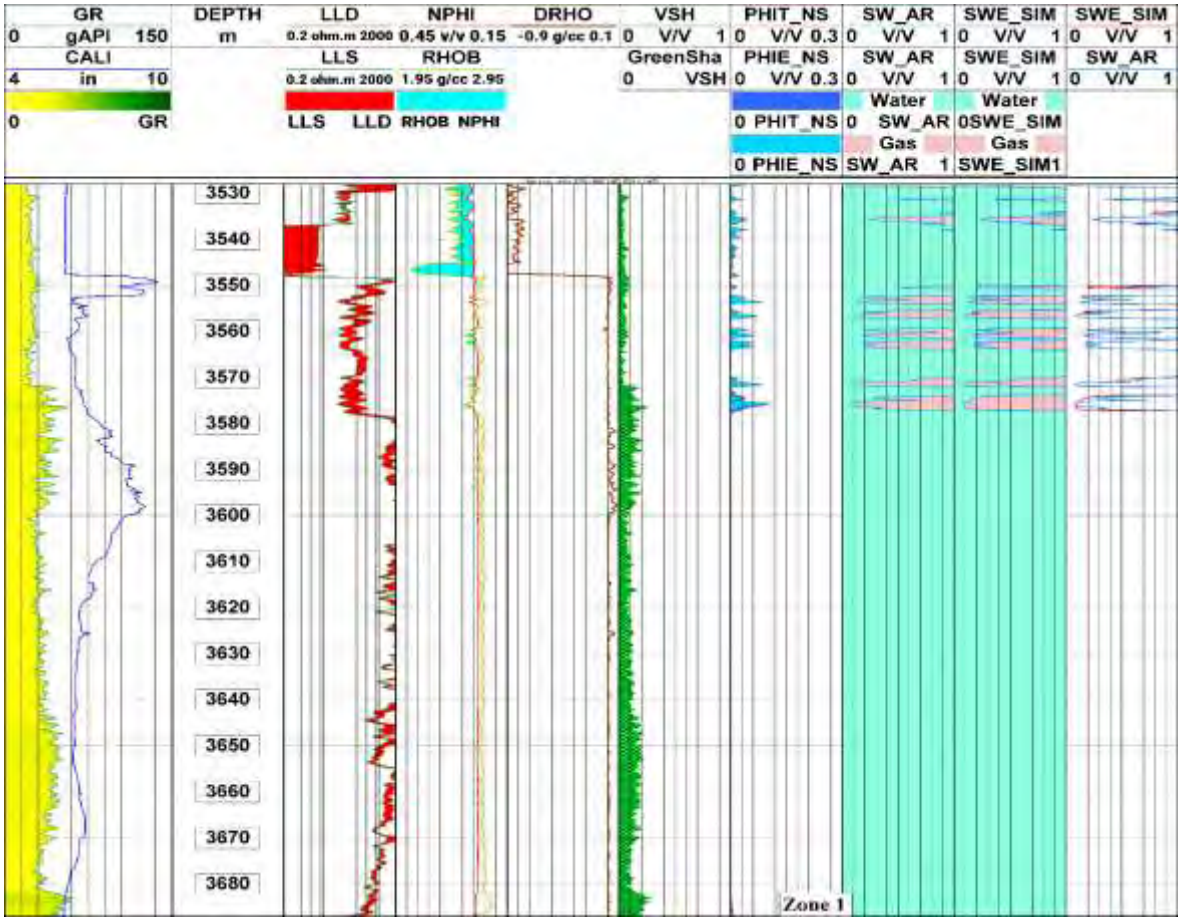

Figure 4.4 Petrophysical Parameters of Lockhart in Manzalai-01

.

Table 4.1 The average values of the petrophysical parameters estimated for Hangu Formation in Manzalai-01.

Serial No	Calculation Parameter	Value (%)
1	Gross Thickness	12 m
2	Volume of Shale	8.77
3	Effective Porosity	4.51
4	Water Saturation	27.07
5	Hydrocarbon Saturation	72.93

The petrophysical analysis of Hangu Formation has been shown in figure 4.5.

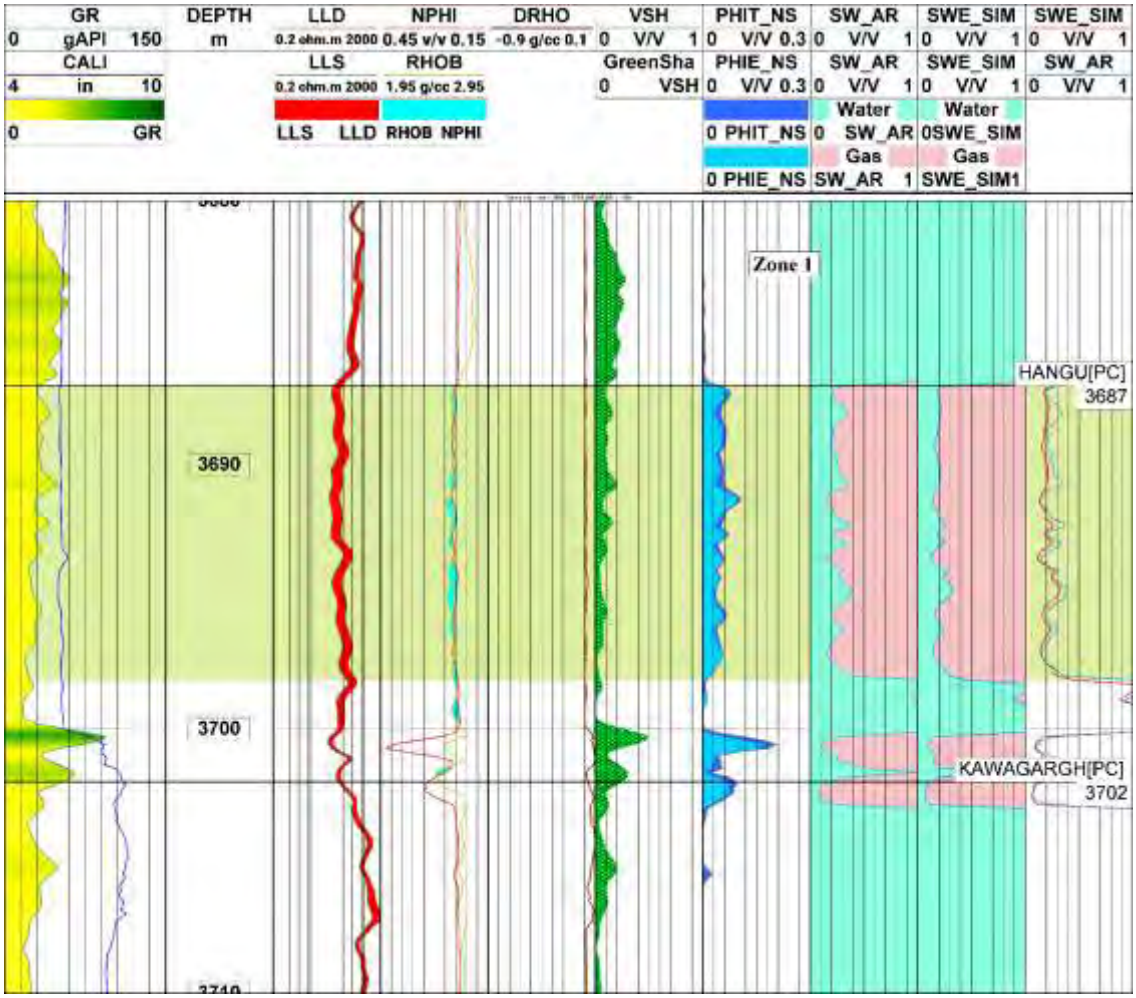

Figure 4.5 Petrophysical zone indicated by light green in Hangu Formation in Manzalai-01

Lumshiwal is the third reservoir to be analyzed. A hydrocarbon bearing zone from depth 3926 m to 3945 (approximately 19 m) has been identified. The results for various petrophysical parameters have been listed in Table 4.2 for lumshiwal.

Table 4.2 The average values of the petrophysical parameters estimated for Lumshiwal Formation in Manzalai-01.

Serial No	Calculation Parameter	Value (%)
1	Gross Thickness	19 m
2	Volume of Shale	17.35
3	Effective Porosity	3.16
4	Water Saturation	42.73
5	Hydrocarbon Saturation	57.27

The petrophysical results are shown in figure 4.6 for Lumshiwal Formation.

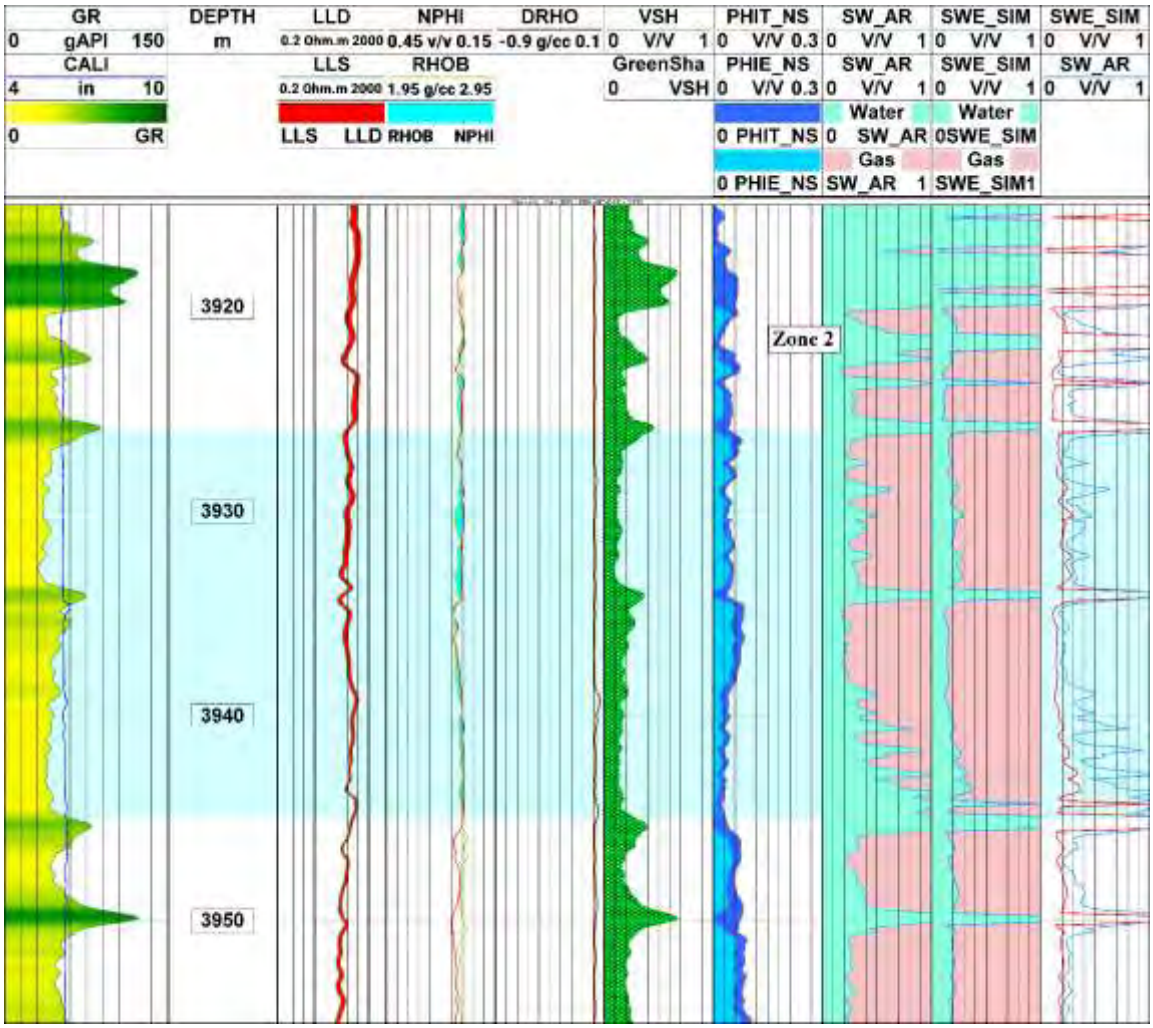

Figure 4.6 Petrophysical zone indicated by sky blue in Lumshiwal Formation in Manzalai-01.

4.6.2 Petrophysics of Manzalai-05

Petrophysical analysis has been conducted on the Lockhart, Hangu, and Lumshiwal formations. Two hydrocarbon bearing zones have been identified on the basis of well log response. Then these are further investigated for quantification. The reservoir zone-01 ranges from depth 3758.602 m to 3764.3932 m and zone-02 ranges from depth 3897.7432 m to 3902.02 m. The petrophysical parameters are computed enlisted in Tables 4.3 and 4.4 for reservoir zones 1 and 2, respectively.

Table 4.3 The average values of the petrophysical parameters estimated for Lockhart Formation (zone-01) in Manzalai-05.

Serial No	Calculation Parameter	Value (%)
1	Gross Thickness	7.0 m
2	Volume of Shale	13.35
3	Effective Porosity	4.23
4	Water Saturation	37.5
5	Hydrocarbon Saturation	62.5

Table 4.4 The average values of the petrophysical parameters estimated for Lockhart Formation (zone-02) in Manzalai-05.

Serial No	Calculation Parameter	Value (%)
1	Gross Thickness	4.5 m
2	Volume of Shale	6.15
3	Effective Porosity	1.18
4	Water Saturation	12.0
5	Hydrocarbon Saturation	88.0

The petrophysical results for Lockhart Formation are shown in figure 4.7.

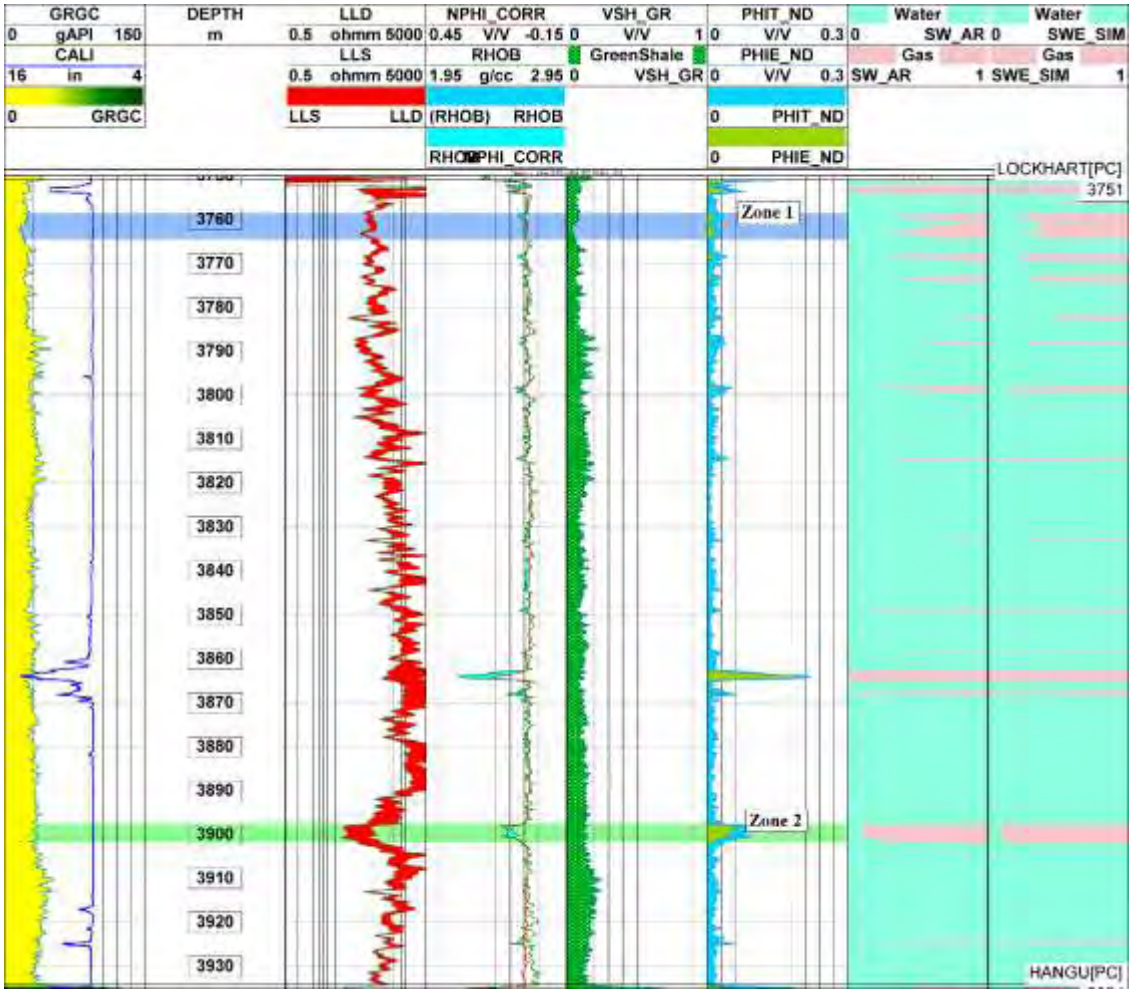

Figure 4.7 Petrophysical zones in blue and green color in Lockhart Formation in Manzalai-05.

The Hangu Formation is the second formation to be analyzed for hydrocarbon bearing reservoir. On the basis of log responses, a hydrocarbon bearing zone from depth 3938.89 m to 3944.9872 m (approximately 6 m) has been identified. The petrophysical parameters computed for this zone are enlisted in Table 4.5.

Table 4.5 The average values of the petrophysical parameters estimated for Hangu Formation in Manzalai-05.

Serial No	Calculation Parameter	Value (%)
1	Gross Thickness	6.0 m
2	Volume of Shale	21.28
3	Effective Porosity	3.8
4	Water Saturation	24.50
5	Hydrocarbon Saturation	75.50

The petrophysical parameters are shown in figure 4.8 for Hangu Formation.

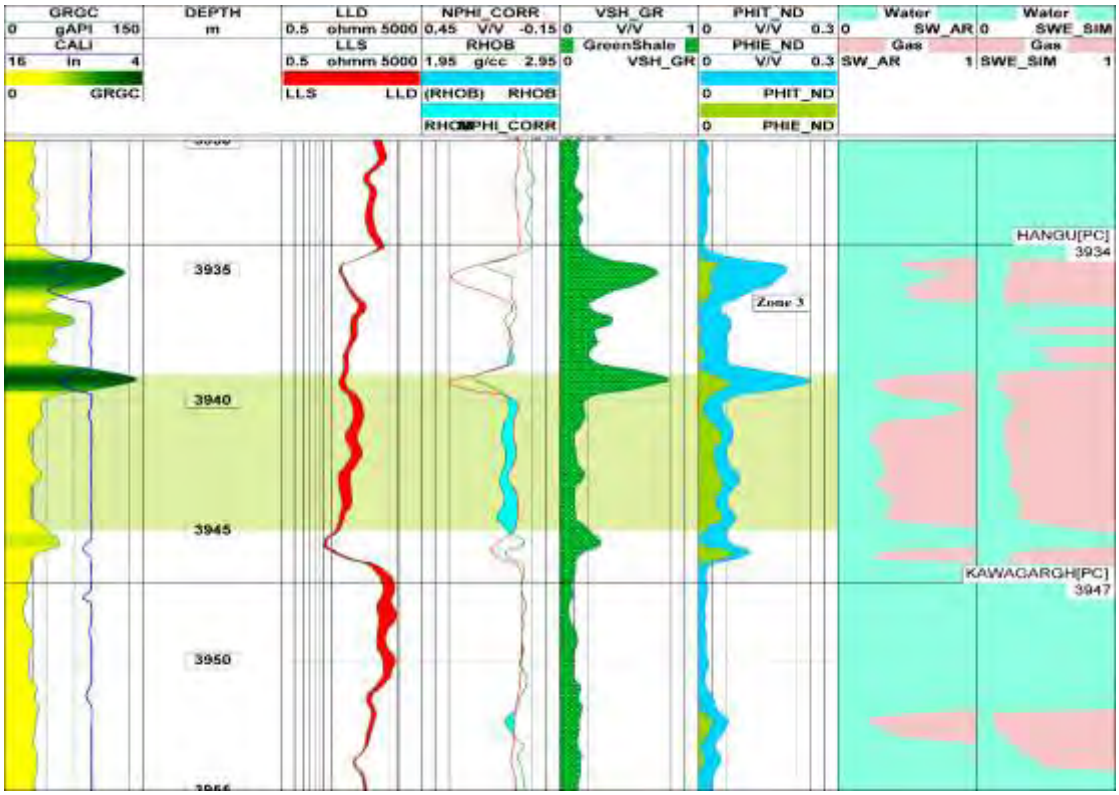

Figure 4.8 Petrophysical zone indicated by light green in Hangu in Manzalai-05

The Lumshiwal Formation shows a hydrocarbon bearing zone at depth ranging from 4085.8 m to 4098.3 m (approximately 12.5 m thickness). The petrophysical results are presented in table 4.6 for Lumshiwal Formation.

Table 4.6 The average values of the petrophysical parameters estimated for Lumshiwal Formation in Manzalai-05

Serial No	Calculation Parameter	Value (%)
1	Gross Thickness	12.5 m
2	Volume of Shale	11.15
3	Effective Porosity	3.19
4	Water Saturation	29.0
5	Hydrocarbon Saturation	71.0

Figure 4.9 depicts the petrophysical zone of lumshiwal.

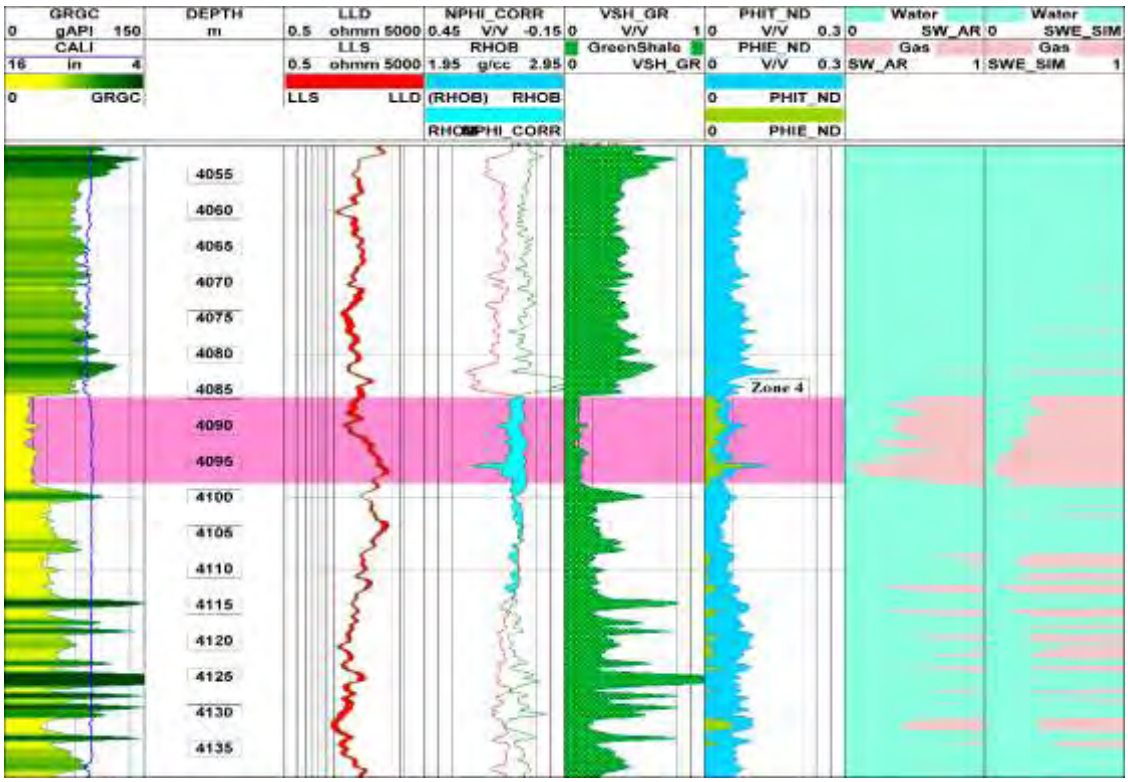

Figure 4.9 Petrophysical Parameters of Lumshiwal in Manzalai-05

4.6.3 Petrophysics of Manzalai-06

The same three reservoirs which are interpreted for Manzalai-01 and Manzalai-05 are analyzed in Manzalai-06 well.

Based on an analysis of petrophysical parameters, it has been observed that the Lockhart formation exhibits an average shale volume reduction of up to 15%. The neutron porosity log indicates almost zero porosity and overlays itself with density log which indicates the lithology to be compact limestone with almost no porosity which makes it non payable reservoir zone. The petrophysical parameters are displayed in figure 4.10.

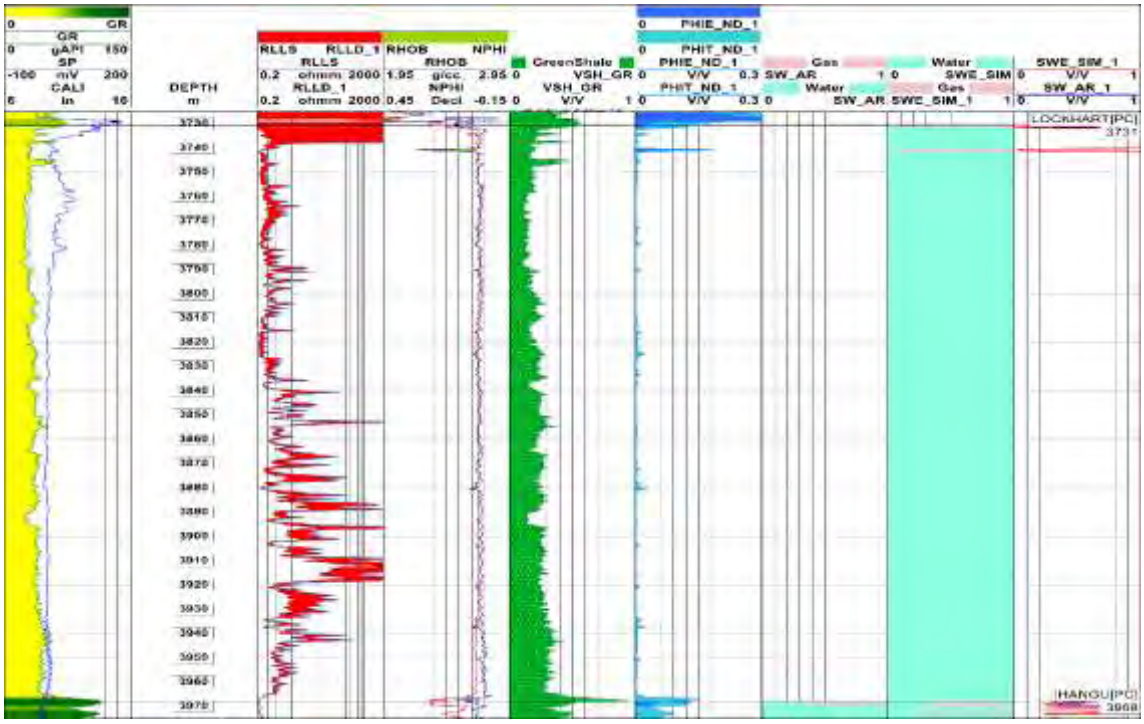

Figure 4.10 Petrophysical Parameters of Lockhart in Manzalai-06

The Hangu Formation shows a hydrocarbon bearing zone from depth ranging 3982.974 m to 4005.072 m (approximately 22 m of thickness). The calculated petrophysical parameters are enlisted in Table 4.7.

Table 4.7 The average values of the petrophysical parameters estimated for Hangu Formation in Manzalai-06.

Serial No	Calculation Parameter	Value (%)
1	Gross Thickness	22.06 m
2	Volume of Shale	5.56
3	Effective Porosity	4.06
4	Water Saturation	15.37
5	Hydrocarbon Saturation	84.63

The petrophysical results for Hangu Formation are shown in figure 4.11.

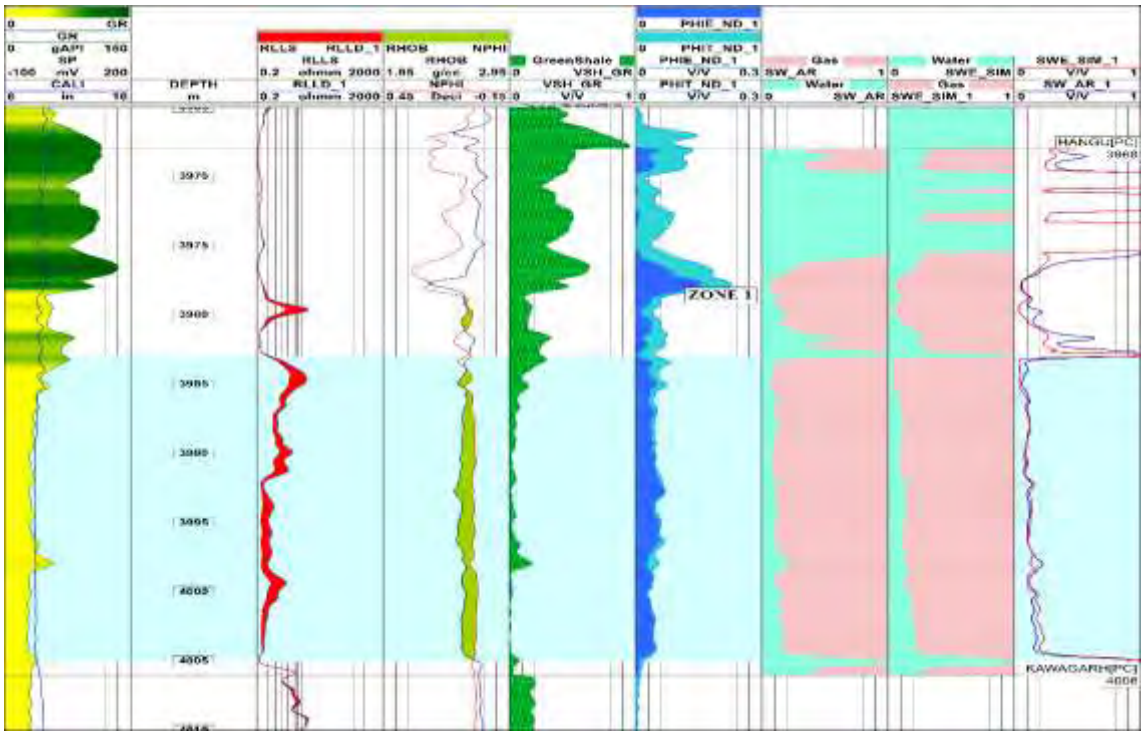

Figure 4.11 Petrophysical Parameters of Hangu in Manzalai-06

The Lumshiwal Formation shows a hydrocarbon bearing zone from depth ranging 4109.466 m to 4120.2864 m (approximately 11 m thickness). The calculated petrophysical parameters are enlisted in Table 4.8.

Table 4.8 The average values of the petrophysical parameters estimated for Lumshiwal Formation in Manzalai-06.

Serial No	Calculation Parameter	Value (%)
1	Gross Thickness	11.0 m
2	Volume of Shale	5.68
3	Effective Porosity	2.51
4	Water Saturation	20.89
5	Hydrocarbon Saturation	79.11

The petrophysical results for Lumshiwal Formation are shown in figure 4.11.

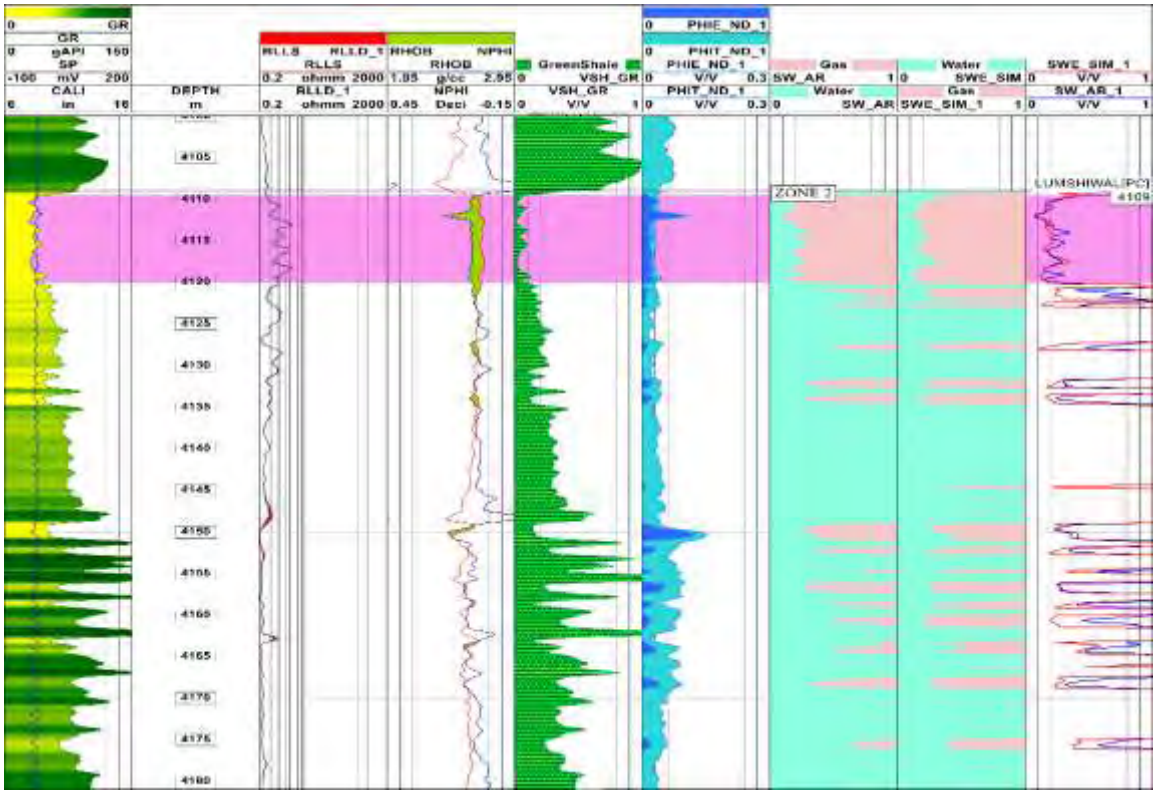

Figure 4.12 Petrophysical Parameters of Lumshiwal in Manzalai-06.

Chapter 05

Electro facies and Rock Physics Modelling

5.1 Introduction

The term "electrofacies" was first established in 1980 by Serra and Abbott (1980). The term "meaning" can be defined as the collection of logical responses that establish the characteristics of a bed and facilitate its differentiation from other beds. Log responses are commonly used as quantitative evaluations of the physical properties of rocks, whereas electro facies are associated with one or more lithofacies. The aim of this study is to determine a relationship between logarithmic reactions and geological features, as discussed by Doveton (1994). The approach experienced a notable surge in popularity throughout the 1990s; however, its usage later waned and became less frequent. Presently, there is a resurgent tendency towards the application of this methodology in the petroleum sector. This technique is utilized to characterize reservoir features, perform investigations on unconventional resources, and estimate reservoir volume (Kumar and Mahendra, 2006; Stinco, 2006).

The recognition of different rock types that constitute a reservoir is a vital aspect of petroleum exploration. The identification of facies was accomplished by employing the manual technique of cross-plotting wire-line recordings and finding correlations between their attributes and core samples. In recent times, notable advancements have been made in the domain of facial recognition owing to the emergence of diverse mathematical techniques that facilitate the automation of this procedure. Principal Component Analysis (PCA), Multivariate Analysis (MA), Nonparametric Regression, Classification Trees, Artificial Intelligence (AI)-based Approaches, and Clustering are all examples of statistical techniques and regression-based procedures used in multivariate data analysis.

5.2 Facies Classification

After the logs were chosen, a unified procedure was implemented to mitigate any discrepancies arising from changes in measurement throughout the complete set of well data. To evaluate differences in wells caused by variable drilling conditions,

a standardized logarithmic scale was applied to all wells. Furthermore, a comprehensive facies clustering study was performed, and the consistency of the logs was reevaluated.

A group of observations of variables that may be correlated are subjected to an orthogonal transformation in the statistical method known as principal component analysis (PCA).

The classification procedure was performed by employing principal component analysis (PCA), clustering methodologies, and self-organizing maps (SOMs). Principal Component Analysis (PCA) entails the process of loading well logs into a matrix X_nxp, where n denotes the number of objects (log curves), and p denotes the number of variables. The third phase entailed the examination of the relationship between these factors and the synthesis of a summary. This was done by considering the axes that were determined to have no association.

The variance of each well log curve is determined by calculating the mean squared variation of all its n values, which can be computed using the following formula:

$$c_{ij} = \frac{1}{n-1}\sum_{m-1}^{n}(x_{im} - x_i)(x_{jm} - x_j) \qquad (5.1)$$

In this context, Cij represents the covariance of variables i and j. xim and xjm denote the values of variables i and j, respectively, in object m. $\bar{x}i$ and $x\bar{j}$ represent the arithmetic means of the variables i and j, respectively.

Both covariance and variance are important measures to utilize when analyzing the differences within a collection. The variables chosen for the principal component analysis (PCA) consist of gamma ray logs and resistivity measurements. Following the introduction of Principal Component Analyses (PCAs), cross-plots were constructed to examine the correlation between PCAs and the integration of various log curves. In addition, the utilization of Principal Component Analysis (PCA) was employed to execute cross-plotting, self-organizing maps, and cluster analysis with the aim of identifying electrofacies.

5.3 Fuzzy Classification

The utilization of unsupervised techniques is a widely adopted strategy in the application of fuzzy classification methodology for conducting cluster analysis and self-organizing maps within the field of electrofacies classification. In the context of fuzzy classification, the assignment of each node to a certain group is determined using a stochastic process, where a designated probability is assigned to each group.

Part 1: A barycenter computation is performed for each group, weighted by the likelihood that each point belongs to that group:

$$\mu_k = \sum_{i=1}^{n} P_{ik}^{\frac{1}{QQ-1}} . x_i \qquad (5.2)$$

The probability that the point i belongs to the group k is denoted here by P_{ik}. A precise estimate of the number of categories is given by the class number parameter. Group k's barycenter is the letter k. QQ is the deciding element.

Part 2: According on the separation between each node and the barycenter of each group, new probabilities are computed:

$$P_{nk} = \sum_{i=1}^{nbclasses} \left(\frac{ecart_{in}}{ecart_{kn}}\right)^{\frac{1}{QQ-1}} \qquad (5.3)$$

Here, p_{nk} is the likelihood that the point n belongs to the group k, where $ecart_{kn} = \|x_n - \mu_k\|^2$ the separation between point n and the group k's barycenter.

Part 3: Convergence test: the algorithm examines whether the new and old probability differ in any way.

- If so, the updated probabilities are input.
- If not, the output of the model is the updated probabilities.

Output: The algorithm creates the probability. The highest likelihood determines the class of each point.

5.4 Electrofacies of Manzalai-01

The study on electrofacies was conducted by utilizing well logs from three drilled wells in order to discover correlations and detect electrofacies. The electrofacies investigation reveals the presence of five distinct facies, namely gas sands, Shaly

sand, shale, limestone (packstone), and limestone (wackestone). The categorization outlined above is based on the analysis of eight separate well logs, including gamma ray, resistivity, Caliper, bulk density, photoelectric factor, spontaneous potential, and acoustic logs. Please refer to Figure 5.1 and 5.2 provided thereafter for a graphical representation.

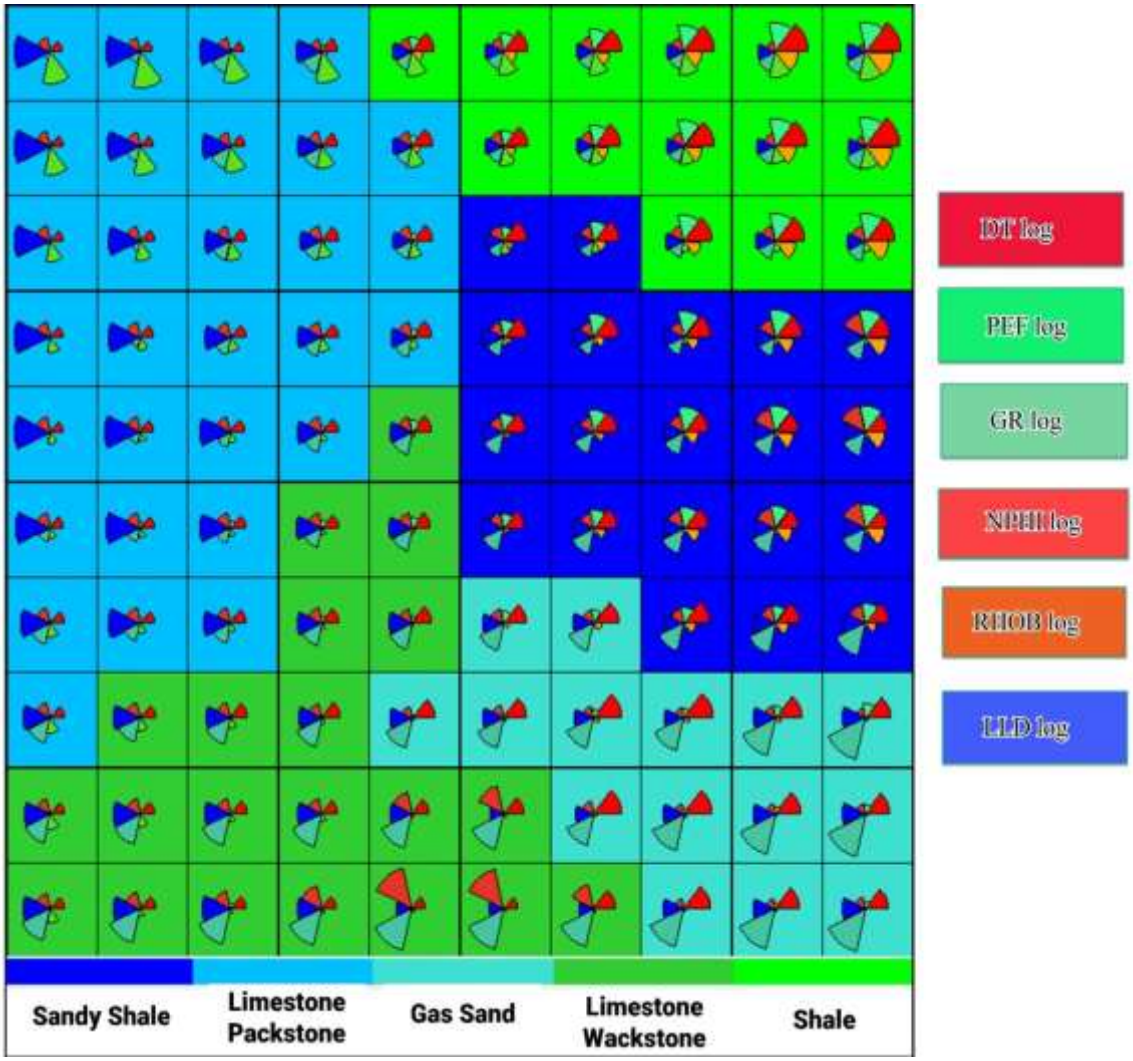

Figure 5.1 Ipsom Electrofacies classification based on well logs.

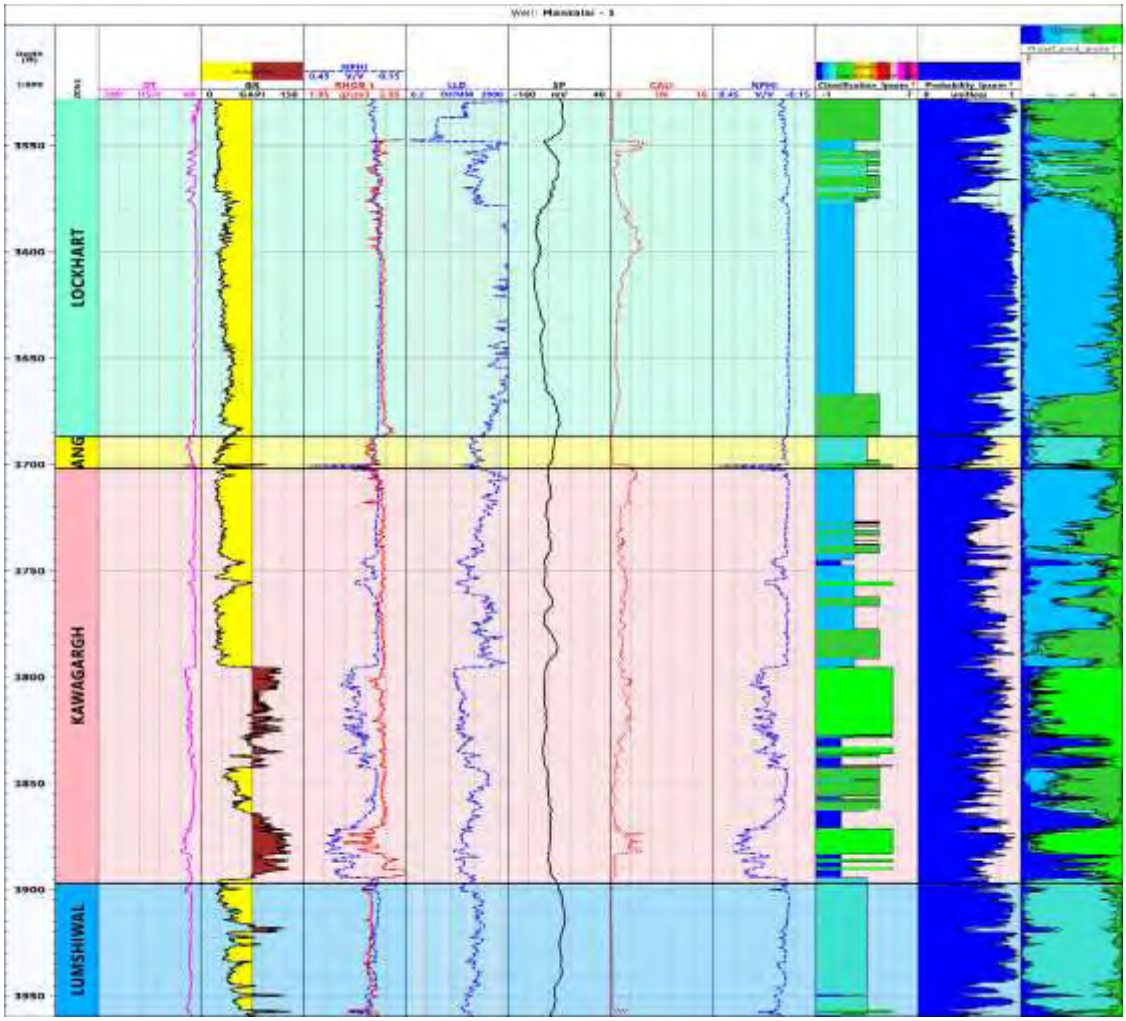

Figure 5.2 Facies Analysis of Formations in Manzalai-01

5.5 Introduction to Rock physics

The discipline of Rock Physics attempts to create a correlation between the elastic properties and reservoir attributes (Bosch, Mukerji & Gonzalez, 2010). The existing correlation investigates the relationship between various parameters of the geological reservoir, including porosity, clay content, sorting, lithology, and saturation, and seismic properties, which encompass acoustic impedance, Vp/Vs ratio (indicating the ratio of P-wave velocity to S-wave velocity), bulk density, and elastic modules. Rock-physics models are employed to interpret the measured sound and seismic velocities in relation to reservoir parameters or to extrapolate predictions beyond the available data range, with the aim of investigating potential scenarios such as variations in fluid or lithology. Moreover, these methods are employed for the purpose of forecasting the

seismic response to the postulated reservoir, together with the characteristics and circumstances of high stress (Avseth et al., 2010).

The primary objective of rock physics is to get a comprehensive comprehension of the correlations between seismic data and the characteristics of rocks. In order to comprehensively understand the elastic properties of a uniform medium, it is imperative to take into account three fundamental parameters: the velocity of primary waves (Vp), the velocity of secondary waves (Vs), and the density. The utilization of rock physics to extrapolate data obtained at the well site to the seismic volume is widely acknowledged as a substantial and influential practice. The utilization of rock physics analysis enables the comprehension of the influence of lithology, porosity, and fluid saturation on seismic data, particularly in regions that are geographically distant from the well (Avseth et al., 2005).

The comprehensive determination of seismic wave propagation and reflection amplitudes in an isotropic linear elastic media is contingent exclusively upon the parameters of compressional wave velocity (Vp), shear wave velocity (Vs), and density. The concurrent usage of these parameters leads to the estimation of rock moduli, which encompass the Lamé elastic constants, Young's modulus, bulk modulus, and shear modulus. The initial step in facies modelling workflow for rock physics analysis often involves the comparison of various elastic properties obtained from borehole data in order to distinguish distinct facies clusters. The seismic lithofacies, as described by Avseth et al. (2005) and Buland (2019), are classifications that distinguish themselves based on their sedimentological and rock physics properties.

The aim of rock physics in this study is to predict the compressional sonic, shear sonic and density logs, compare the actual and predict logs at given reservoir conditions and to enhance the comprehension of the correlation between Petro-elastic properties and effectively define the reservoir facies. Through the optimization of this methodology, it is expected that it will contribute to the accurate prediction of lithology and the spatial distribution of fluids across the entirety of the volume. To attain this purpose, a thorough methodology is implemented, which entails the integration of petrophysics and rock physics models. The utilization of petrophysical analysis has been utilized to

discern the reservoir intervals within the targeted formations. The workflow has been presented in figure 5.3.

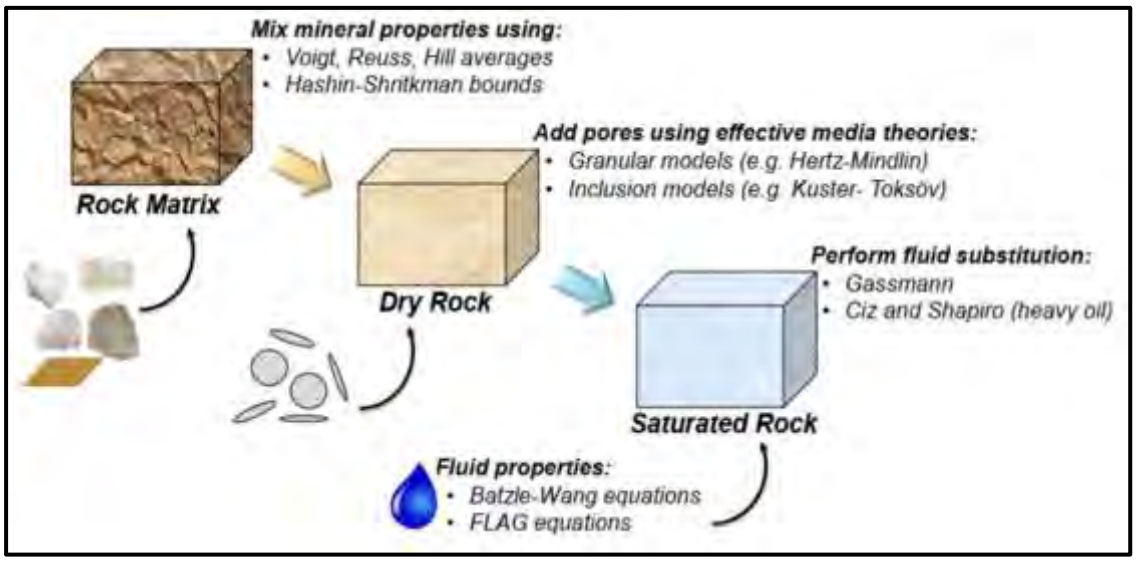

Figure 5.3 Petro elastic Workflow (Xu and Payne, 2009)

5.6 Rock Physics Model

Each Rock Physics model integrates mineral properties, fluid properties, and dry rock properties to produce the elastic responses at a specific saturation level. Subsequently, these responses are incorporated into seismic responses. The rock physics modelling has been performed for manzalai-01. The next sections will discuss them.

5.6.1 Mineral Properties

To ascertain the bulk modulus of the mineral matrix, it is important to possess knowledge pertaining to the mineral composition of the rock. The acquisition of this data can be accomplished by conducting laboratory examinations on core samples. In the absence of empirical laboratory data, it is fair to propose a hypothesis suggesting that lithology predominantly comprises quartz and clay minerals. The quantification of clay content can be achieved by the examination of the volume of shale (Vsh) curve, which is a frequently computed metric derived from wireline log data, particularly the Gamma-ray log. The typical composition of shale consists of around seventy percent clay and thirty percent other minerals, with quartz being the major component. Once the mineral abundances have been determined, the K_{matrix} can be obtained through the application of the Voigt-Reuss-Hill (VRH) averaging method, as first suggested by Hill in 1952.

$$K_{matrix} = \frac{1}{2}\left(\left[V_{SH}K_{SH} + V_{qz}K_{qz}\right] + \left[\frac{V_{SH}}{K_{SH}} + \frac{V_{qz}}{K_{qz}}\right]\right) \quad (5.4)$$

Where V_{SH} and V_{qz} represents shale volume and quartz volume respect

The density of mineral matrix can be estimated using arithmetic averaging of individual mineral components.

$$\rho_{matrix} = V_{SH}\rho_{SH} + V_{qz}\rho_{qz} \quad (5.5)$$

Where ρ_{SH} and ρ_{qz} represents density of shale and density of quartz. The values are used for Hangu and Lumshiwal Formations which are in sand shales layering. The other reservoir lockhart is composed of dominantly by calcite mineral but for the purpose of rock physics modelling the former are selected as Lockhart is non producer in Manzalai-01 well.

5.6.2 Fluid Properties

The calculation of the bulk modulus and density of the pore fluid (brine, oil, and gas) is performed by determining the average values of the data pertaining to each respective fluid type. First and foremost, it is crucial to calculate the factors that are linked to each type of fluid, specifically brine, gas, and oil. The brine bulk modulus can be computed from known seismic velocity and density by the below expression.

$$K_{brine} = \rho_{brine}V_{brine}^2 \times 10^{-6} \quad (5.6)$$

The variables K_{brine} (GPa), ρ_{brine} (g/cm3), and V_{brine} (m/s) represent the bulk modulus, density, and P-wave velocity in brine, respectively.

Density and velocity of brine can be computed with the help of Batze and Wang (1992). Density of brine can be computed using the following expression.

$$\rho_{brine} = \rho_w + 0.668S + 0.44S^2 + 10^{-6}S[300P - 2400PS + T(80 + 3T - 3300S - 13P + 47PS)] \quad (5.7)$$

The variables P (MPa) and T (℃) represent the pressure and temperature, respectively, at in-situ circumstances. These values were computed in order to determine the water resistivity as part of the petrophysical investigation, S represents the salinity of water computed using well header information utilizing

the type of drilling mud values, ρ_w represents density of water taken as 1.0 g/cm^3. The velocity of P-waves in brine, denoted as V_{brine} (m/s), is provided as

$$V_{brine} = V_w + S(1170 - 9.6T + 0.055T^2 - 8.5 \times 10^{-5}T^3 + 2.6P - 0.0029TP - 0.0476P^2) + S^{1.5}(780 - 10P + 0.16P^2) - 1820S^2 \quad (5.8)$$

Where V_w represents water's P-wave velocity.

The bulk modulus and density of gas in a reservoir are influenced by various factors, including pressure, temperature, and the specific composition of the gas. The hydrocarbon gas demonstrates the capacity to exist as a combination of several gases, with each gas possessing its own distinct specific gravity (G). The term "specific gravity" pertains to the proportion between the density of a gas and the density of air at a temperature of 15.60°C and under standard atmospheric pressure. The estimation of gas density can be derived from the experiment conducted by Batzle and Wang in 1992.

$$\rho_{gas} = \frac{28.8GP}{ZR(T+273.15)} \quad (5.9)$$

In the equation provided, G represents the specific gravity of gas in terms of the American Petroleum Institute (API) scale. R denotes the gas constant, which has a value of 8.314. Lastly, Z represents the compressibility factor, as defined by the given equation.

$$Z = \left[0.03 + 0.00527\left(3.5 - T_{pr}\right)^3\right]P_{pr} + \left(0.642T_{pr} - 0.007T_{pr}^4 - 0.52\right) + E \quad (5.10)$$

and

$$E = 0.109(3.85 - T_{pr})^2 \exp\{-\left[0.45 + 8\left(0.56 - \frac{1}{T_{pr}}\right)^2\right]\frac{P_{pr}^{1.2}}{T_{pr}}\} \quad (5.11)$$

Where T_{pr} and P_{pr} represents pseudo-reduced temperature and pressure which are given in the below formulation.

$$T_{pr} = \frac{T+273.15}{94.72+170.75G} \quad (5.12)$$

and

$$P_{pr} = \frac{P}{4.892 - 0.4048G} \quad (5.13)$$

The estimation of the bulk modulus of a gas can be achieved through the utilization of the Batze and Wang equation but here its value is taken as 0.1 GPa.

The pore spaces of the geological formation contain a mixture of brine and hydrocarbon compounds, such as oil and/or gas. The determination of the bulk modulus and density of the mixed pore fluid phase can be accomplished by employing the technique of inverse bulk modulus averaging, which is popularly known as Wood's equation. In a similar manner, the density can be ascertained by utilizing arithmetic averaging of the densities of the several fluid phases, so ensuring a preservation of mass. The fluid phase is distinguished by its bulk modulus (K_{fl}) and density (ρ_{fl}).

$$\frac{1}{K_{fl}} = \frac{S_w}{K_{brine}} + \frac{(1 - S_w)}{K_{gas}} \quad (5.14)$$

and

$$\rho_{fl} = S_w \rho_{brine} + (1 - S_w)\rho_{gas} \quad (5.15)$$

Where S_w represents water saturation and (1-S_w) represents hydrocarbon saturation which are taken from the petrophysical computed logs.

5.6.3 Dry Rock Properties

The K-T model, which was proposed by K and T in 1974, is employed to ascertain the dry rock qualities of a certain rock specimen. It is postulated that the configuration of the pores can be classified as ellipsoidal, with the aspect ratio serving as a defining characteristic. According to Toksöz et al. (1976), there is a negative correlation between the porosity of an object and its velocity. Keys and Xu (2002) utilized a simplified approach in their research to determine the effective modulus of arid rock. This assumption entails the constancy of the Poisson's ratio of the dry rock with respect to porosity.

$$K_{dry} = K_m(1 - \phi)^P \quad (5.16)$$

$$G = G_m(1 - \phi)^q \quad (5.17)$$

In this context, the symbols K_d and μ_d denote the bulk and shear moduli of dry rock, respectively, while considering the presence of porosity represented by the symbol ϖ. The symbols μ_m and K_m represent the effective shear and bulk moduli, respectively, of the mineral that comprises a rock.

$$K_{sat} = K_{dry} + \frac{(1-\frac{K_{dry}}{K_m})^2}{\frac{\varphi}{K_f}+\frac{(1-\varphi)}{K_m}-\frac{K_{dry}}{K_m^2}} \tag{5.18}$$

Additionally, the K-T approach is utilized to assess the elastic characteristics of the composite system comprising kerogen and a mixture of fluids (namely, oil, gas, and water), assuming that the fluids are already enclosed within the kerogen matrix. The quantification of stiffness can be accomplished by employing a certain mathematical correlation.

$$\frac{K_{ke}}{K_k} = \frac{1+\left[\frac{4\mu_k\left(K_f-K_k\right)}{\left(3K_f+4\mu_k\right)K_k}\right]S}{1-\left[\frac{3\left(K_f-K_k\right)}{\left(3K_f+4\mu_k\right)K_k}\right]S} \tag{5.19}$$

$$\frac{\mu_{ke}}{\mu_k} = \frac{(1-S)(pK_f+8\mu_k)}{9K_k+8\mu_k+S(6K_k+12\mu_k)} \tag{5.20}$$

In this context, the variables ϖ_f and ϖ_k represent the volume of fluid and kerogen, respectively. The variables μ_k and K_k denote the shear and bulk moduli of kerogen, whereas μ_{ke} and K_{ke} represent the effective shear and bulk moduli of the fluid.

5.6.4 Gassmann's equation

In Gassmann's fundamental work in 1951, the determination of the modulus of saturated rock is achieved through a comparative analysis with the moduli of dry rock, minerals, and known pore fluids. The equations proposed by Gassmann are valid solely under the condition that there is no presence of stiffness in the fluid filling the pores. The expression of the saturated moduli of rock is as follows:

$$K_{sat} = K_{dry} + \frac{(1-\frac{K_{dry}}{K_m})^2}{\frac{\varphi}{K_f}+\frac{(1-\varphi)}{K_m}-\frac{K_{dry}}{K_m^2}} \tag{5.21}$$

$$\mu_{sat} = \mu_{dry} \tag{5.22}$$

$$K_{dry} = \frac{K_{sat}\left(\frac{\phi K_{matrix}}{K_{fluid}} + 1 - \phi\right) - K_{matrix}}{\frac{\phi K_{matrix}}{K_{fluid}} + \frac{K_{sat}}{K_{matrix}} - 1 - \phi} \quad (5.23)$$

The symbols K_d, K, K_f, and K_m are used in this context to represent the bulk modulus of dry rock, rock saturated with pore fluid, pore fluid, and mineral, respectively. Similarly, μ_d and μ are used to indicate the shear modulus of dry and saturated rock, respectively, while ω reflects the porosity of the rock.

5.7 Rock Physics Modelling for Manzalai-01

A lithology log is typically established prior to the development of a Rock Physics Model (RPM). The categorization of lithofacies is established based on the variables of Vsh (volume of shale) and density log. Multiple thresholds are employed for parameter classification, resulting in the emergence of five distinct lithofacies: gas sand, sandy shale, shale wackstone, and packstone. The sand formation that is of particular interest is the one that contains hydrocarbons, mostly due to its low shale volume (Vsh) and low bulk density. The fundamental input parameters required for the formulation of a rock physics model pertaining to the Hangu and Lumshiwal formations. The development of sandstone is characterized by many factors, such as the volume fractions, densities, and elastic moduli of the matrix. These factors encompass different facies, including gas sand, sandy shale, shale, and minor limestone. Additionally, fluid saturation is another significant aspect influencing sandstone formation. In the present context, the utilization of Manzalai_01 serves as a main source for the derivation of a rock physics model. The model is utilized to predict the P- and S-wave velocities in both wells, with the intention of conducting a comparison with the wireline log data that has been documented.

The provided diagram depicts a comparative analysis of the simulated elastic parameters, specifically Vp, Vs, and Rho, in relation to the equivalent well data obtained from Manzalai-01. The lithofacies classification of the Lockhart, Hangu, Kawagarh, Lumshiwal, and Chichali Formations is illustrated in Track 4. The green curve illustrates the values of Vp, Vs, and Rho derived from a developed rock physics model, exhibiting a significant correlation with the recorded values of well log data

shown by the black curve for Hangu and Lumshiwal. The finding demonstrates a significant concurrence between the projected and observed values of Petro elastic characteristics for the regions of Hangu and Lumshiwal. The determination of correlation is commonly based on two factors: the correlation coefficient (CC) and the normalized root mean square (NMRS) value, which spans a range of -1 to 1.

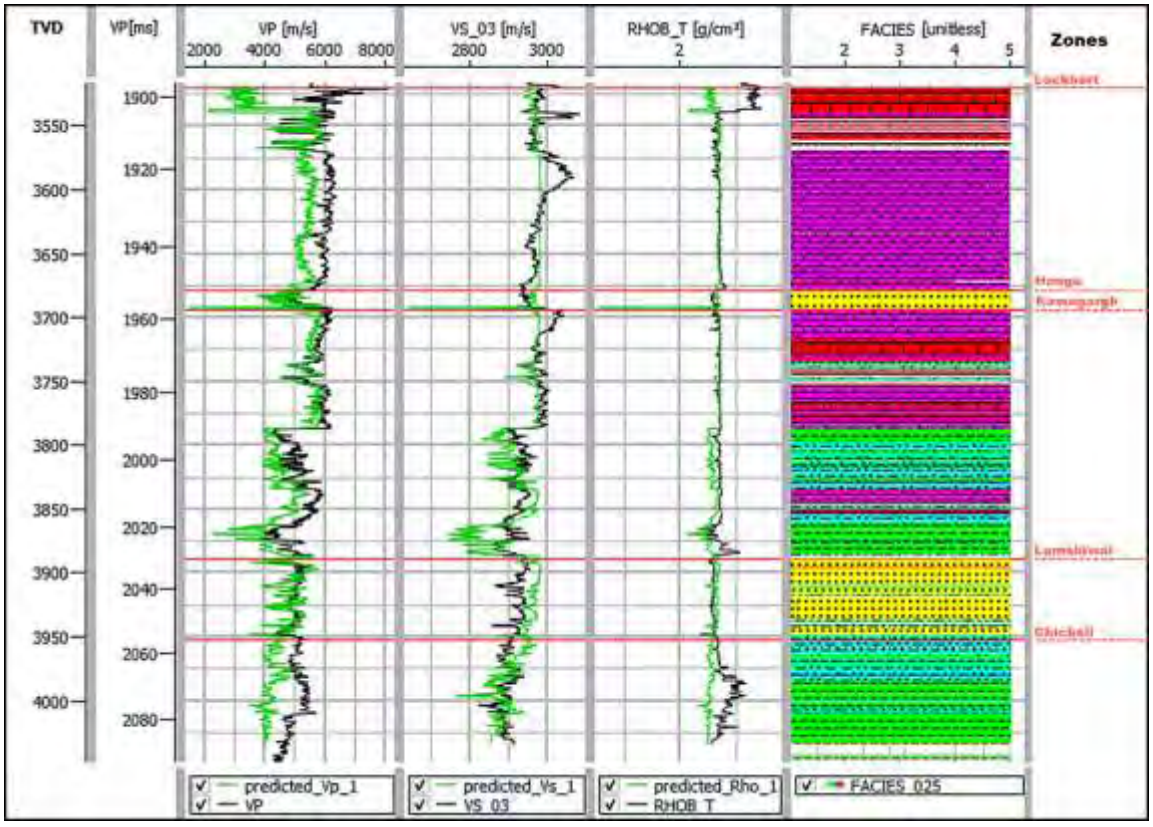

Figure 5.4 Results of actual well logging data (black color) and modeled well logging data (Vp, Vs, and Rho in green color) for Manzalai-01.

By employing a built rock physics model, we have successfully classified our lithofacies using the collected data. Figure 5.4 illustrates the diverse cross plots of Petro-elastic characteristics pertaining to the Manzalai-01 well, effectively demarcating individual facies.

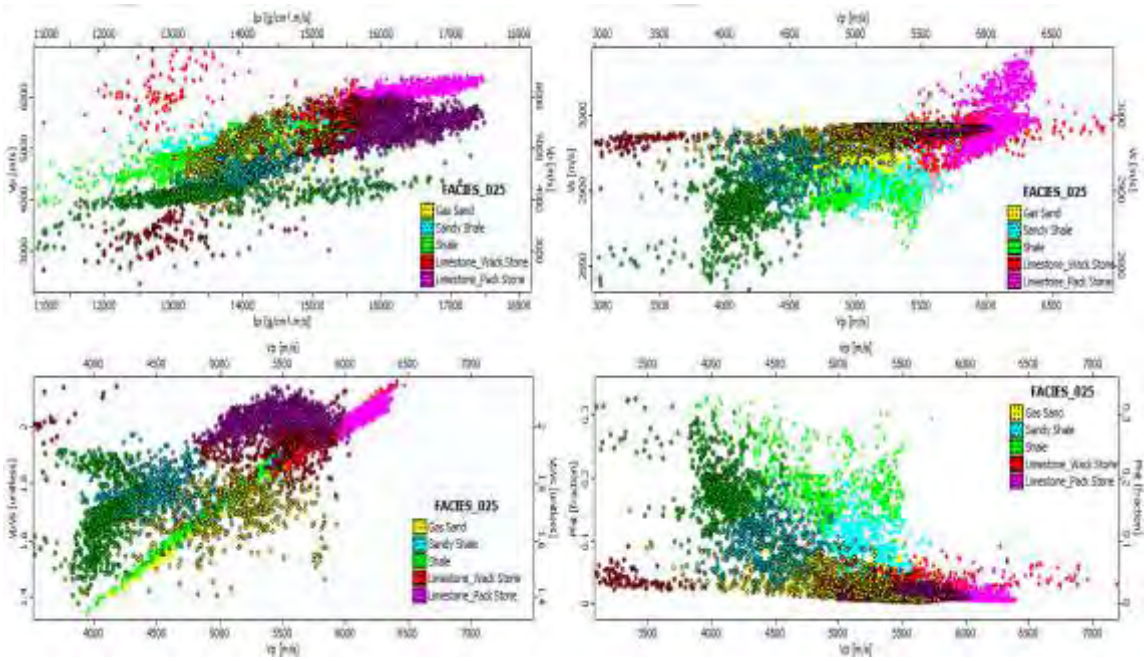

Figure 5.5 Rock physics model estimates the Petro-elastic characteristics that distinguish each facie. (Ip vs V_p), (Vp vs Vs), (VpVs vs Vp) and (Phit vs V_P) respectively a), b), c) and d).

5.7.1 Crossplot Analysis for Hangu Formation

After performing Rock Physics Modelling, different cross plots have been generated for Hangu Formation for the comparison of actual and predicted elastic properties. These cross plots indicate that Hangu Formation is mostly dominated by Gas sands which is evident from petrophysical modelling and rock physics model confirms that, and minor amount of calcite dominated limestone facie indicating calcareous sands. The cross plots are shown in Figure 5.6.

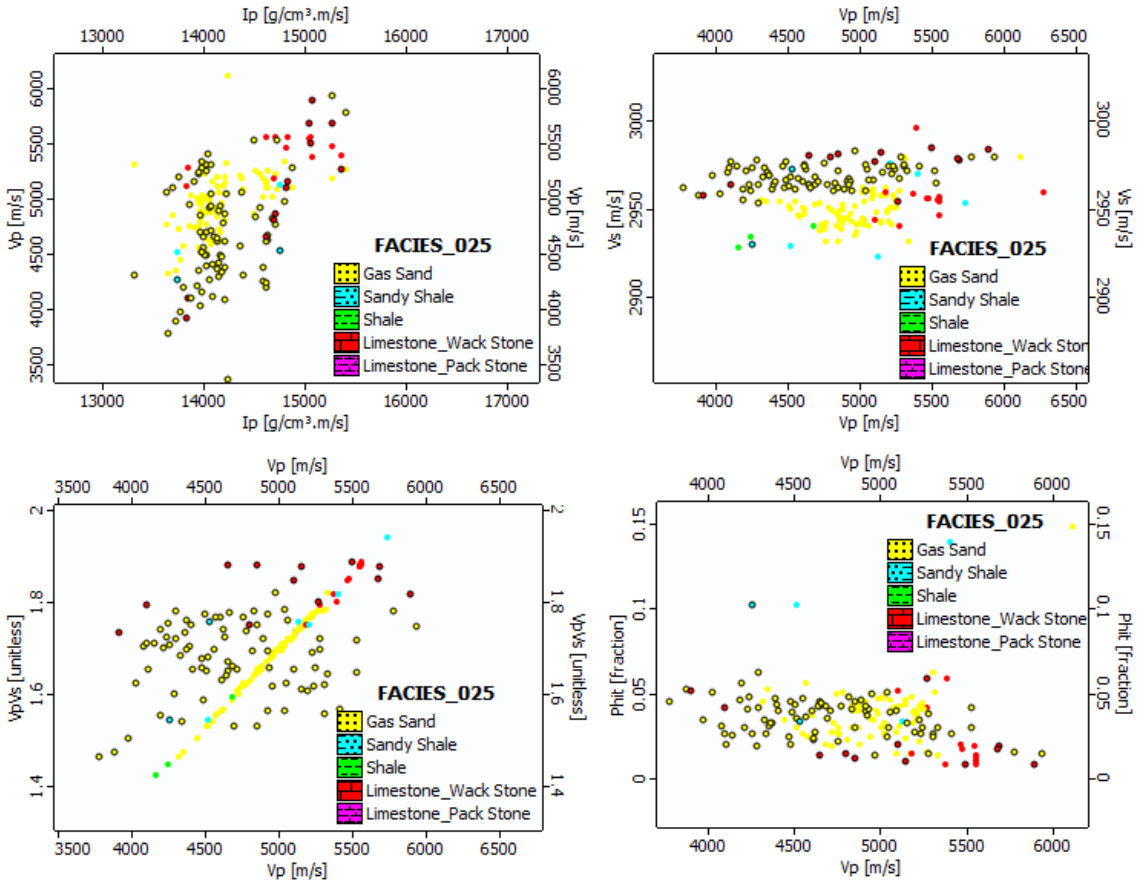

Figure 5.6 Rock physics model estimates the Petro-elastic characteristics that distinguish each facie. (Ip vs V_p), (Vp vs Vs), (VpVs vs Vp) and (Phit vs V_P) respectively a), b), c) and d).

5.7.2 Crossplot Analysis for Lumshiwal Formation

Following the implementation of Rock Physics Modelling, a variety of cross plots have been developed to facilitate the comparison between the elastic properties of the Lumshiwal Formation as predicted by the model and their actual values. The cross plots shown in this study demonstrate that the Lumshiwal Formation is primarily characterized by the presence of gas sands. This observation is supported by petrophysical modeling, which further validates the dominance of gas sands. Additionally, sandy shales and shales are also present within the formation. The cross plots are depicted in Figure 5.7.

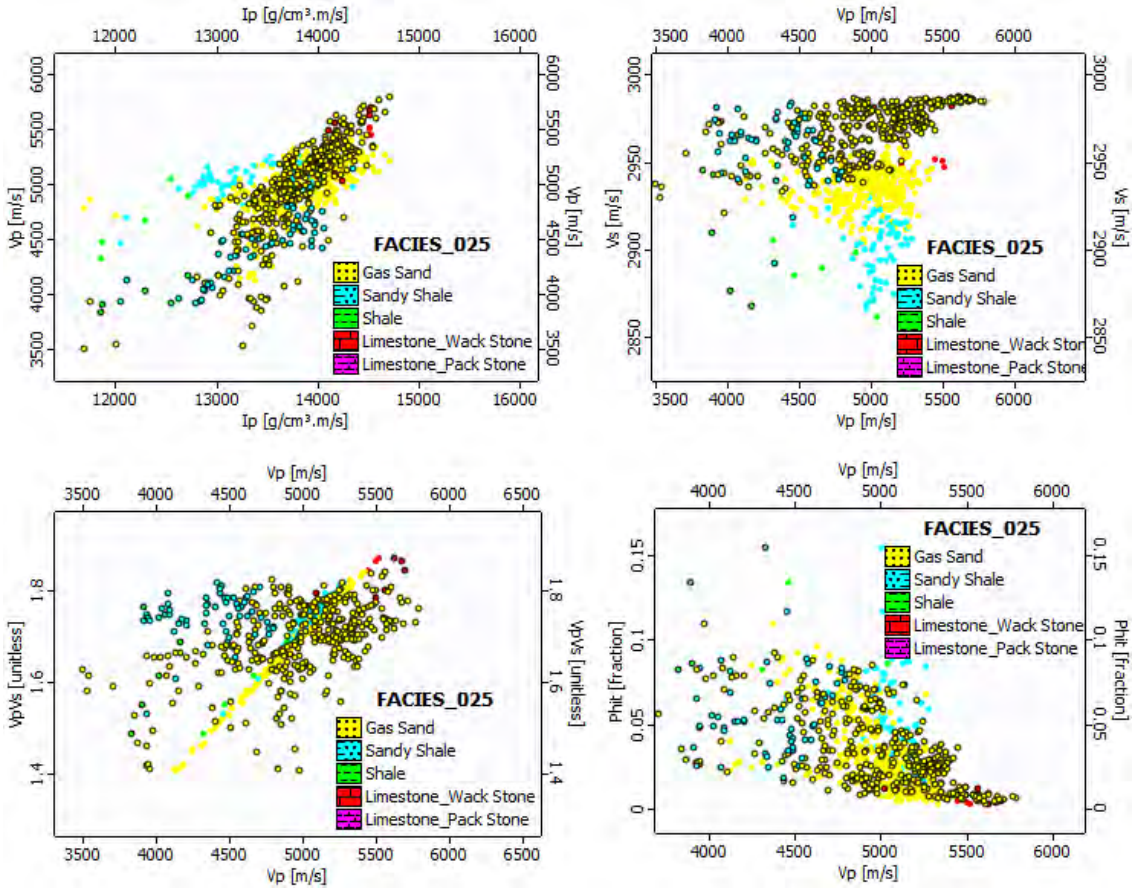

Figure 5.7 Rock physics model estimates the Petro-elastic characteristics that distinguish each facie. (Ip vs V_p), (Vp vs Vs), (VpVs vs Vp) and (Phit vs V_P) respectively a), b), c) and d).

Chapter 06

Seismic Inversion Analysis

6.1 Introduction

The development of precise three-dimensional models depicting petrophysical parameters is crucial for the effective characterization of reservoirs. It is imperative to position these models within a geological framework. The use of structural seismic analysis as a fundamental approach in the development of the reservoir model is a widely adopted convention. Nevertheless, the utilization of this method for obtaining with three dimensions generated petrophysical characteristics is not extensively utilized in current practice. The occurrence of this phenomenon can be described as multiple contributing factors, encompassing restricted availability of an all-encompassing 3D dataset, difficulties in establishing a quantitative relationship between seismic data and reservoir characteristics, insufficient vertical resolution for the creation of accurate property models, and various additional factors (Rowbotham et al., 2003). The resolution of the current problem could potentially be achieved by employing 3D seismic technology, which offers impedance volumes computed through seismic methods that can be directly correlated with reservoir properties. Addressing the lack of vertical resolution in classification applications has proven to be a significant difficulty. Gunning and Glinsky (2003) assert that the application of stochastic seismic inversion with improved vertical resolution is a methodology utilized for the creation of accurate three-dimensional models of reservoir features.

Geostatistical approaches are commonly utilized in the estimate of several geophysical properties through the analysis of seismic and well-log data. In order to create a surface for each site based on the observed locations, geostatistical methods use sample points, which refer to the well's petrophysical properties (Haas and Dubrule, 1994). The topic of geostatistics utilizes two main techniques, deterministic and geostatistical interpolation, as outlined by Russell et al. (1999). Deterministic interpolation methods depend on the application of mathematical functions, while geostatistics integrates both mathematical and statistical methodologies (Hampson et al., 2001). There is an extensive range of strategies available for determining reservoir

parameters by employing interpolation techniques. Geostochastic inversion (GeoSI), a method that makes it easier to transform bandlimited seismic data into high-frequency seismic data, is one of the methods that is most frequently used in this context. The utilization of lowering the sample interval to 1 ms in GeoSl is employed with the aim of enhancing reservoir models via inversion outcomes, while simultaneously mitigating mistakes (Rowbotham et al., 2003).

Substantial progress has been achieved in the geostatistical inversion process since the mid-1990s. The introduction of data integration and the calibration of reservoir models utilizing seismic data and pre-existing rock physics knowledge are notable developments in this field. The stochastic realizations of impedance undergo a sequence of statistical techniques, including collocated co-kriging (Doyen et al., 1989), Bayesian classification, and linear regression functions, to integrate seismic conditioned reservoir properties into reservoir modeling (Coulon et al., 2005). The early advancement in this subject is demonstrated by Torres-Verdin and Sen's (2004) study, which focuses on the co-simulation of lithofacies and impedance. Saussus and Sams (2012) have proven the reliability of employing seismic data to condition reservoir parameters inside a three-dimensional model that integrates the facies concept. The challenge arises when attempting to verify the consistency of elastic characteristics with a saturation height function, particularly in cases where saturation is not incorporated into the inversion model (Sams et al., 2011). Within a theoretical framework, the concurrent implementation of all limitations results in improved integration and the formulation of reservoir models that exhibit more comprehensiveness, resilience, and coherence.

Recent scholarly research has mostly concentrated on the development of stochastic algorithms that go beyond acoustic inversion and cover simultaneous elastic inversion. Considerable focus has also been directed towards the application of position stochastic inversion within a more robust Bayesian framework. The current situation involves the clarification of a seismic inverse problem and the measurement of the corresponding degree of uncertainty by employing a posterior distribution function.

Reservoir models that are created exclusively using log data possess notable vertical resolution but exhibit constrained areal (horizontal) resolution. The reason for this phenomenon is that the log data demonstrates a significant level of detail in the vertical dimension while lacking the same level of detail in the spatial dimension. The reason for this might be linked to the coexistence of both qualities inside the log data. The areal resolution of seismic data, particularly the bin size utilized in 3D surveys, demonstrates a significant degree of precision. Nevertheless, the vertical resolution of this data is rather insufficient, as it relies on the seismic frequency content and the reservoir's velocity.

The application of stochastic seismic inversion offers a unique framework that enables the integration of the benefits provided by seismic and well-log data (Marion et al., 2000). Seismic data are of paramount importance in the production of stochastic impedance volumes that exhibit a high level of areal resolution. Conversely, log data employed in the inversion approach contribute to the attainment of improved vertical resolution for this particular technique. The created 3D volumes demonstrate remarkable quality and are well-suited for sophisticated property development applications. The average stochastic inversion approach typically has a vertical resolution that spans around 1 to 2 meters. Petrophysical reservoir characteristics models are commonly developed utilizing this scale. The combination of impedance data and well-log data can be utilized to develop reservoir property models, such as porosity (Rowbotham et al., 2003b). Haas and Dubrule (1994) were the pioneers in implementing geostatistics for seismic inversion, specifically employing sequential Gaussian simulation as the primary methodology.

Pseudo-logs are produced by employing seismic survey traces and well-log data, which encompass variables such as density and acoustic properties, for each individual trace. A synthetic seismogram is produced by utilizing the pseudo-impedance log, which is then compared to the actual seismic trace acquired at the relevant point. The inversion solution applies to a computational model that generates a synthetic seismogram that closely resembles the observed seismic trace at a specific time. The determination of the vertical resolution of the simulated log data is dependent upon the dimensions of the cells in the vertical direction, as opposed to the frequency of the seismic data. The GeoSl software generates a volumetric

representation that integrates log data and seismic data, demonstrating a horizontal resolution comparable to seismic data and a vertical resolution.

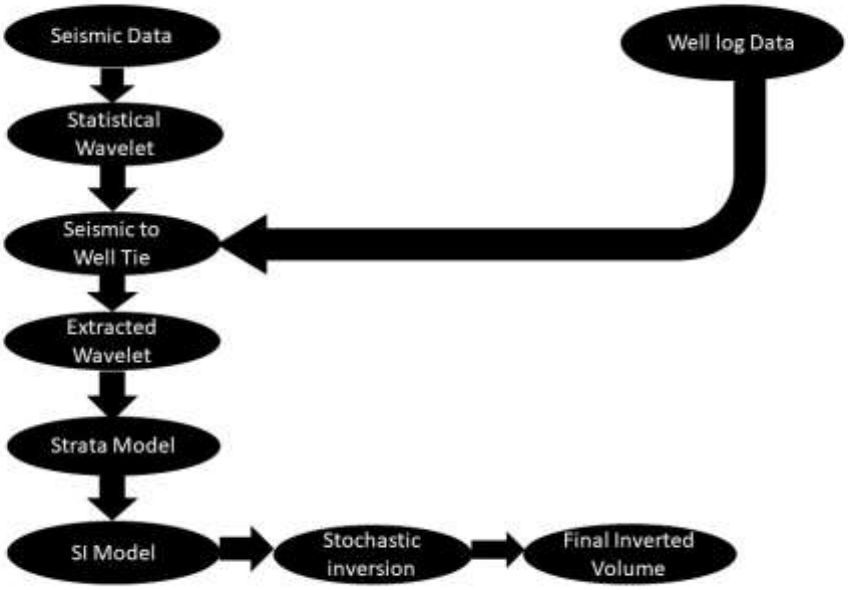

Figure 6.1 Generalized Workflow of Stochastic Inversion

6.2 Wavelet Extraction and Seismic to Well Tie

The wavelet seen in Figure 6.2 needs to be appropriately scaled to align with the stratum model. The wavelets exhibited zero phase characteristics in the context of post-stack data, and distinct wavelets were extracted from seismic data for each individual case. Subsequently, the wavelets underwent a process of scaling to facilitate their utilization within the stratum (GeoSI previous) model.

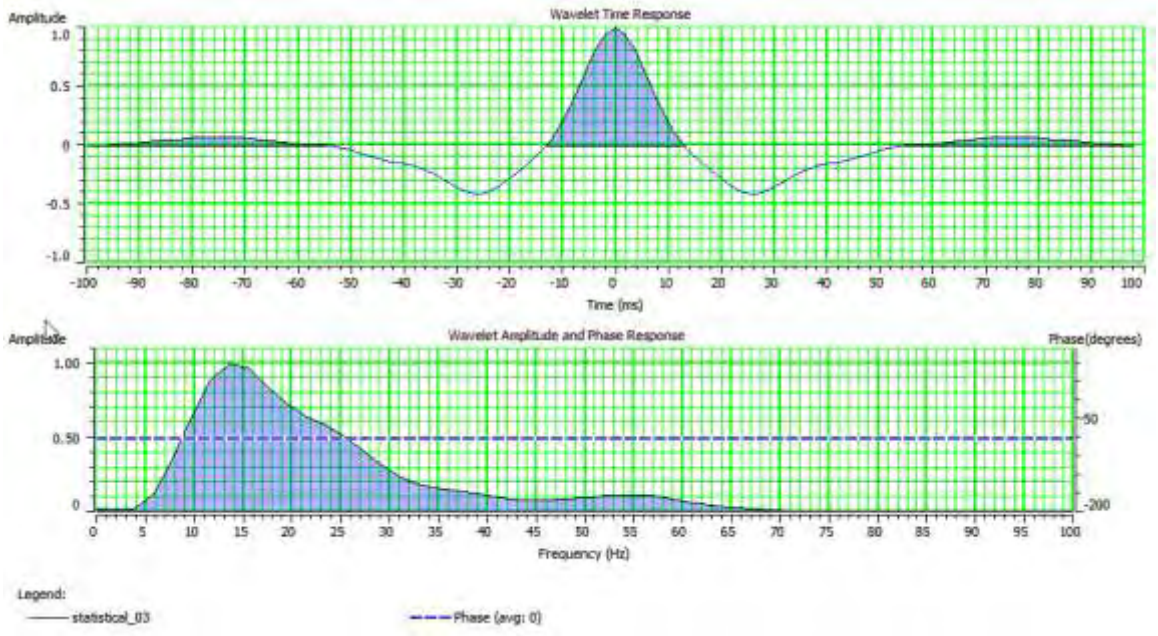

Figure 6.2 Extracted Wavelet and its Spectrum.

The inversion process was exclusively applied to the designated time range of 2010-2350 ms, within which the relevant horizons of interest are situated, as depicted in Figure 6.3. The findings of the inversion process reveal the presence of distinct layers exhibiting varying levels of acoustic impedance. The findings of the stochastic inversion demonstrate a significant lateral variation in acoustic impedance, which can be effectively utilized for the depiction of shelling out sequence.

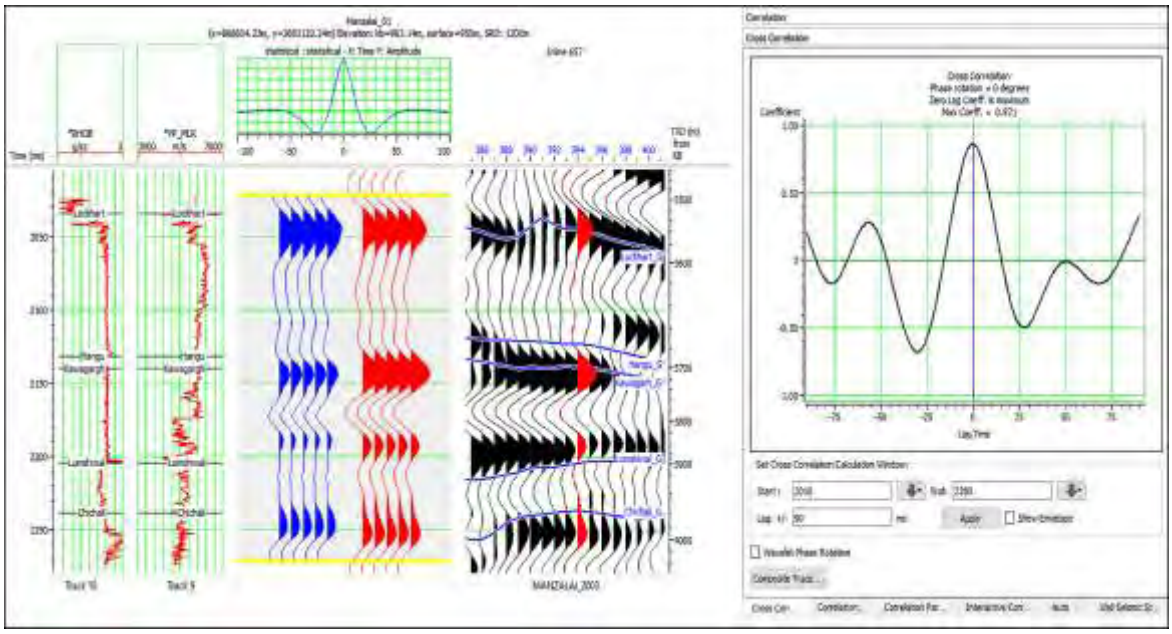

Figure 6.3 Initial model analysis for post stack inversion at well Manzalai-01

6.3 Low-Frequency Model

In the same manner, many inversion methodologies, like GeoSI, commence the procedure by creating a correlation between a borehole and seismic data. The highest degree of correlation was achieved through the well-to-seismic link conducted as part of the Petroleum Systems and Seismic Interpretation (PSSI) project. The Low-Frequency Model (LFM), alternatively referred to as the Strata Model in GeoSI, is developed by a preceding inversion process, resulting in the subsequent formation of a more recent model. The task was performed with a focus on preserving the structural tendencies. Hence, the inclusion of latent factor models (LFMs) as previous models is crucial for ensuring efficacy. The low Frequency Model has been presented in figure 6.4.

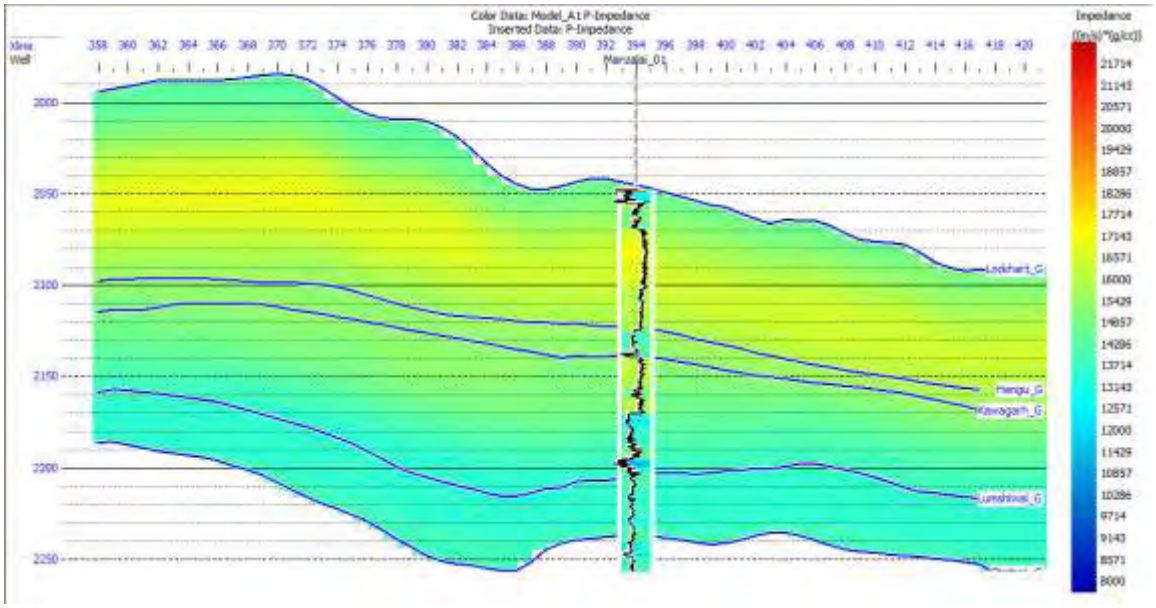

Figure 6.4 Low Frequency Model Generated Using Mnazalai-01

6.4 Prior Model (SI Model)

In the scenario of conventional inversion, the initial model, commonly referred to as LFM, is typically generated through the integration of well logs throughout the entirety of the seismic volume. However, the utilization of GeoSl necessitates the utilization of a pre-existing model that integrates distinct attributes and considers supplementary constraints provided by seismic data. Using regular domain samples with a period of 1 millisecond at first, a high-resolution stratigraphic grid was created that corresponded to petrophysical characteristics. The stratigraphic geo-cellular grid

is composed of four separate levels of finely detailed Lockhart Limestone, Hangu Sandstone, Kawagarh Limestone, Lumshiwal Sandstone, and Chichali Shales. These layers are identified as the target Formations. To address the fluctuations in thickness and deposition patterns, a constant layer thickness of 0.1ms was employed to achieve a significant level of precision. Figure 6.5 depicts the parameters utilized in deriving the aforementioned model.

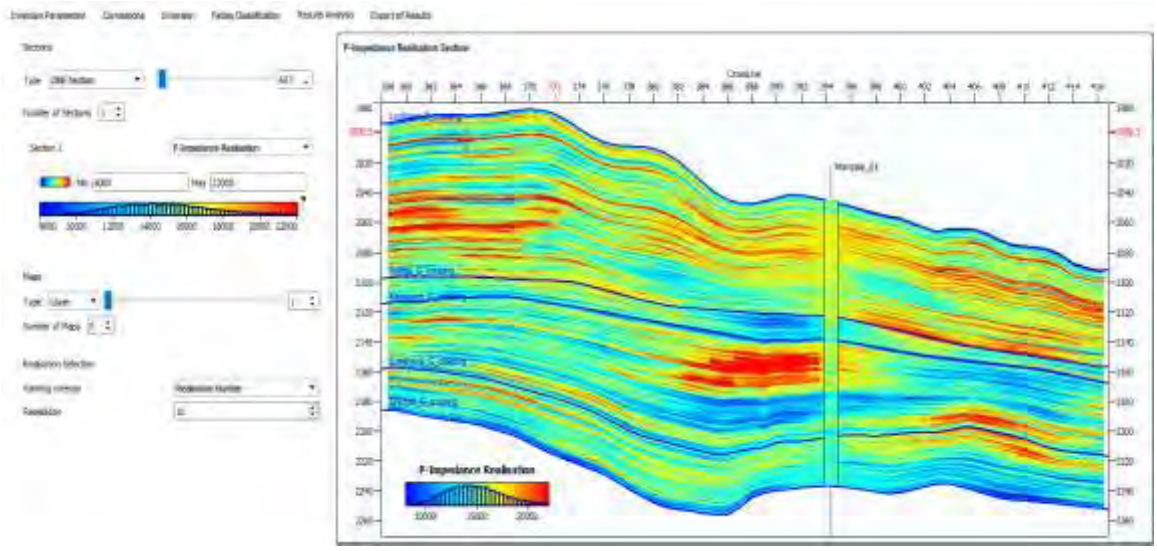

Figure 6.5 Impedance Section generated by SI Model

6.5 Variogram

The variogram is a useful tool for evaluating spatial consistencies or variations in geographical variances, irrespective of the data's sparsity or richness, as exemplified by seismic data. The computation of spatial variations within stratigraphic grids involves the use of variograms, which apply a statistical methodology and utilize Kriging/Co-kriging processes. The "regionalized variables" that are the subject of the variograms mentioned in this context have a posterior distribution based on location. These variables exhibit properties that fall along the spectrum between full randomness and determinism.

The presence or absence of a specific element or arrangement in a sample is dependent on its spatial positioning on the surface where it was deposited, as denoted by the grid (Saussus and Sams, 2012). The assessment of a theoretical variogram necessitates the examination of three fundamental factors, namely range, nugget, and sill. The range is defined as the collection of potential outcomes that are limited by the

lowest and highest values. The variogram measurements will eventually reach a state of equilibrium and demonstrate a "plateau" phenomenon. This phenomenon is widely recognized and referred to as the range. Liu et al. (2018) state that data points that fall within the specified "range" will be declared significant and included in the calculations. On the contrary, any data points that fall beyond this range will be disregarded.

The value attributed to the "Sill" parameter in the variogram denotes the point at which the observed variations in the graph reach a plateau and cease to increase further. The lack of a geographic link between the sill and the reference point renders the offset irrelevant. The data points in this specific circumstance are not utilized in the computation of the unknown value. The term "nugget" denotes a deviation from the uninterrupted flow of its source. Despite the ideal assumption of a zero value, sampling error and the intrinsic variability at a tiny scale cause a non-zero result (Bosch et al., 2012).

6.5.1 Lateral and Vertical Variograms

The utilization of variogram models in geostatistical inversion, commonly referred to as GeoSI, encompasses the integration of both vertical and horizontal modelling elements. The vertical variograms were generated using high-quality log data, and the calculation of horizontal ranges was performed by integrating seismic data, taking into account the impact of structural and stratigraphic differences. Figure 6.6 illustrates the vertical variograms that were developed for the layer that displays variances for all four layers.

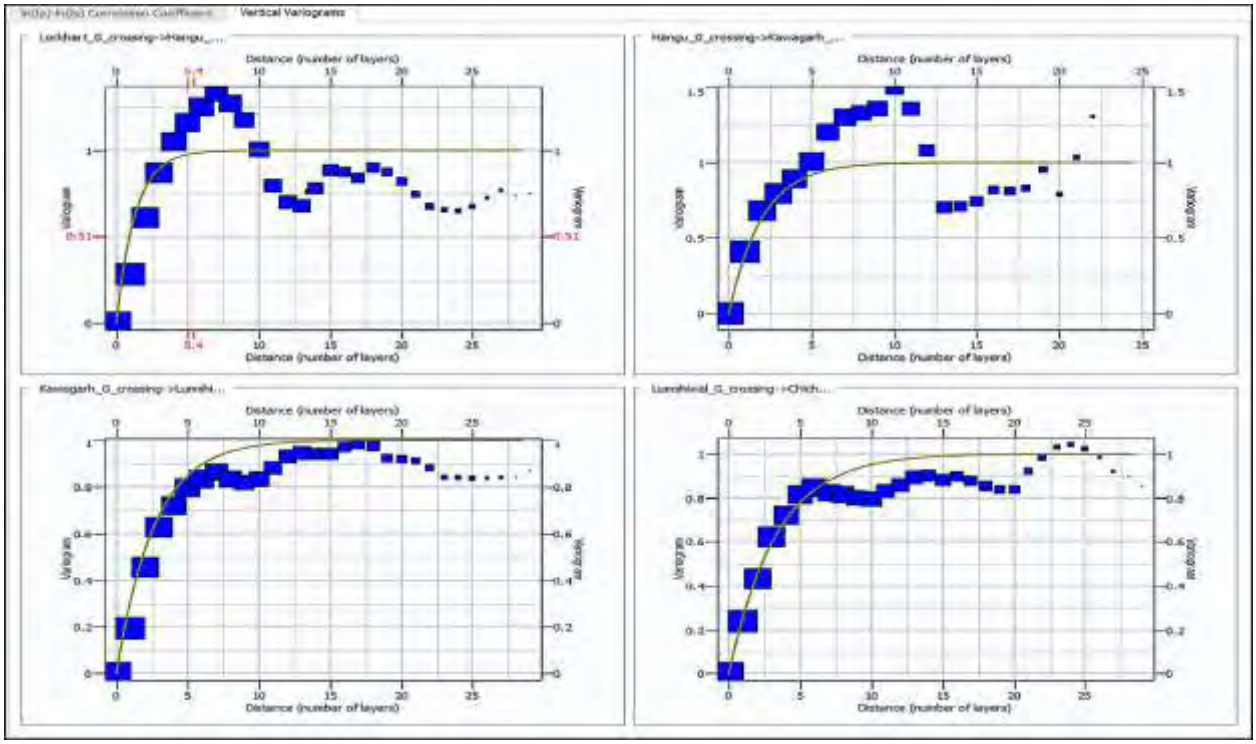

Figure 6.6 Variogram Correlation section for all four layers

6.6 Facies Classification

During this stage, the Litho-SI approach employed a straightforward equation to determine the reservoir facies for the modelled wells. One of the most straightforward methods for facies identification involves the utilization of a gamma-ray log. Consequently, a threshold of 30 API was employed to differentiate between reservoir facies with an API of 30 and non-reservoir facies with an API greater than 30 (Supplementary F). The process of facies categorization was applied to the reservoir section spanning from layer 1 to layer 150. Utilizing the available well data, an estimation of the gas bearing, shale, and limestone may be made, indicating a notable Net to Gross value inside the reservoir segment. The connection analysis was conducted subsequent to the classification of the inverted model in order to generate the volume realizations of the geo-bodies.

6.7 Inverted Impedance Section

The utilization of the layered strata model, scaled wavelet, and facies classification algorithms enabled the implementation of 100 realizations. To provide a thorough examination, it is important to create a collection of 100 unique distribution scenarios for the various facies, including shaly sand, hydrocarbon bearing and limestone and

shale. Furthermore, it is crucial to construct volumetric representations for the geological formations and conduct connectivity analysis. The performance of a variogram analysis is essential in effectively capturing the spatial variation in all directions when employing stochastic inversion, which is grounded in geostatistical approaches. The inversion variogram analysis revealed a significant correlation between the data cloud that exhibited a high degree of similarity and a continuous pattern, as illustrated in Figure 6.7.

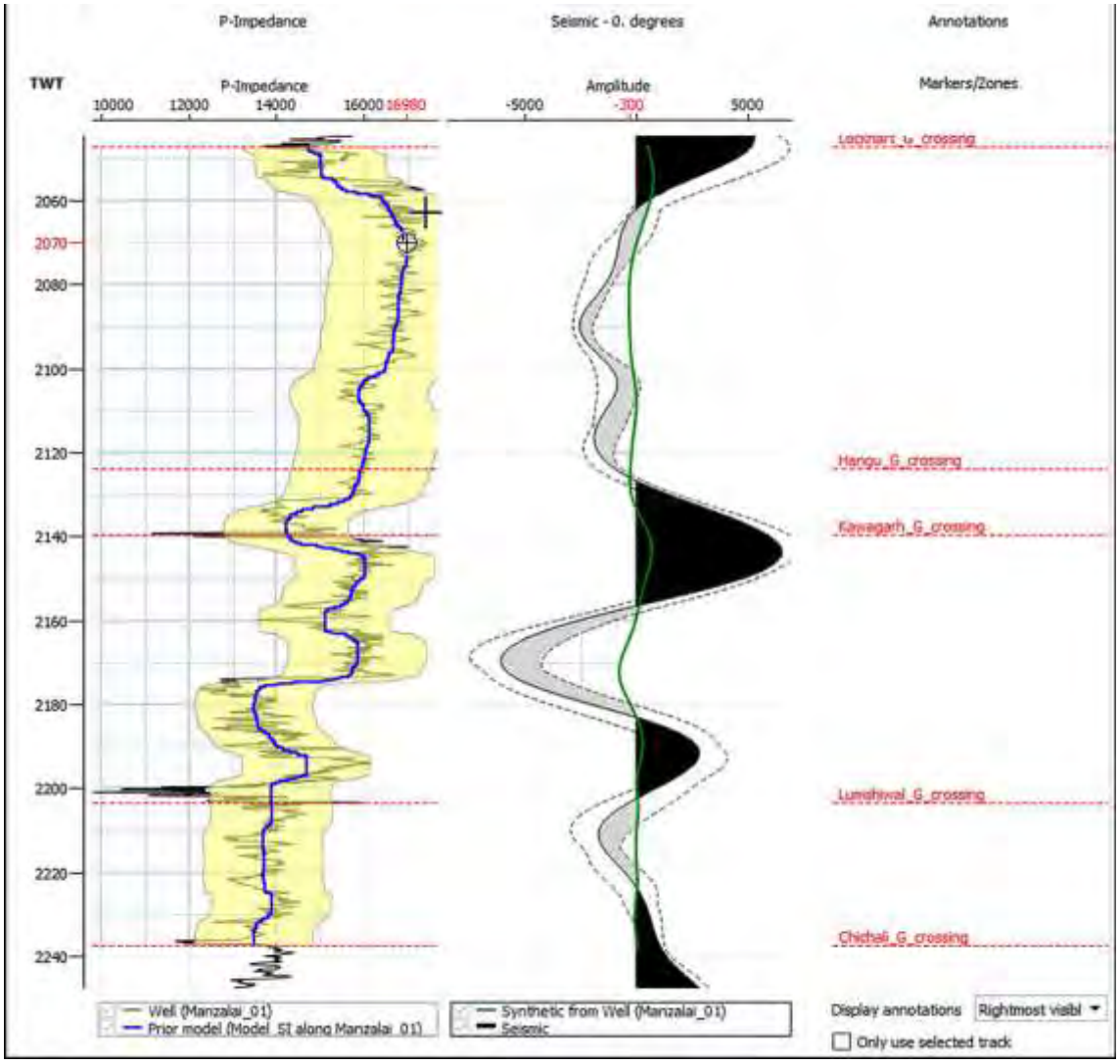

Figure 6.7 Demonstrates the relationship between the well log and the seismic data.

6.8 Facies Slice from Inverted Section

Slices are taken from the inverted section in order to comprehend the geographical distribution of the reservoir zones identified by petrophysical investigation. For them, impedance is the criterion. While non-reservoir zones have high impedances,

hydrocarbon zones have lower impedances. Figures 6.7, 6.8, and 6.9 show the extracted slices for Lockhart, Hangu, and Lumshiwal, respectively.

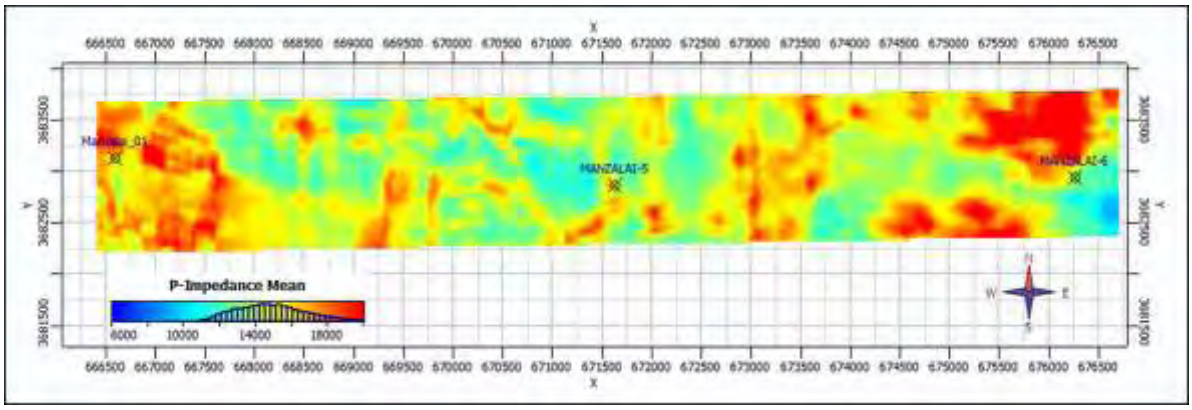

Figure 6.8 Impedance Slice generated for lockhart showing lower impedance with blue color and higher impedance by red color

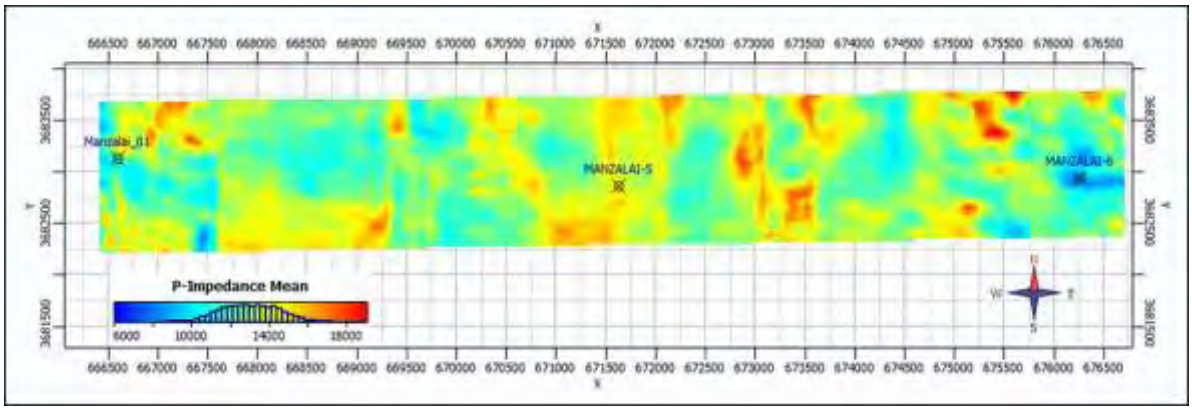

Figure 6.9 Impedance Slice generated for Hangu showing lower impedance with blue color and higher impedance by red color.

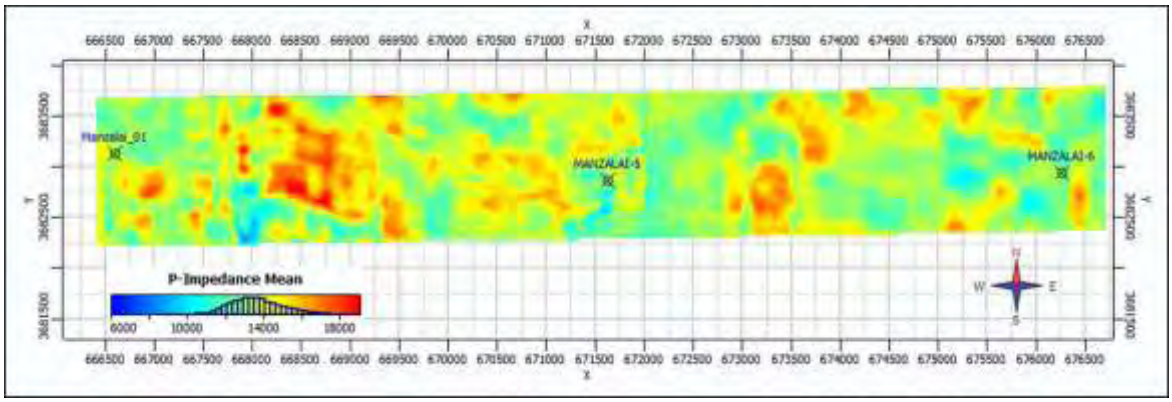

Figure 6.10 Impedance Slice generated for Lumshiwal showing lower impedance with blue color and higher impedance by red color.

DISCUSSIONS

The primary objective of this work is to analyze and describe the properties of the reservoir intervals found within the Hangu, Lockhart and Lumshiwal Formations, specifically in the Manzalai Gas Field located in the Upper Indus Basin of Pakistan. The study is divided into several stages, beginning with the seismic structural interpretation and identification of horizons in the subsurface. Following this, petrophysical analysis is conducted to ascertain the presence of hydrocarbon indicators in the well. Based on these findings, the reservoir characterization is established to more accurately quantify the properties of the reservoir. The spatial distribution is conducted by employing inversion techniques to effectively map the quantitative features of the reservoir. Two distinct inversion approaches are utilized for this purpose.

The research area demonstrates considerable potential for an abundance of resources, as indicated by the notable discoveries of gas and oil in adjacent areas (Amjad et al., 2019, Siddique et al., 2016, Khan et al., 2019). Several studies have been carried out in the research area, although there is a lack of quantitative analysis on reservoir characteristics. The majority of the case scenarios have prioritized the examination of regional cross sections that make advantage of the accessible surface geology (Gardezi et al., 2021, Najaman et al., 2010, Ghani et al., 2018). The focus of this work concerns the quantification and spatial distribution analysis of zones containing hydrocarbons. The first stage of the investigation entailed the determination of subsurface geology within the designated study area, which highlighted the existence of inclined horizons. The area under investigation displayed heterogeneity in the depth of its structure, characterized by a shallower configuration in the northwestern region and a deeper configuration in the southeastern part. The aforementioned finding has been confirmed by the time contour maps.

Once the spatial arrangement of the underlying geological formations has been ascertained, the subsequent task involves the identification and subsequent quantification of the zones that contain hydrocarbon deposits. In order to fulfil the objective, the reservoirs known as Hangu, Lumshiwal, and Lockhart were assessed in the wells Manzalai-01, Manzalai-05, and Manzalai-06. In the case of a hydrocarbon-

bearing zone, one can expect to observe a decrease in gamma ray readings, an increase in resistivity values, a decrease in bulk density, and a decrease in neutron porosity (resulting in a crossover between neutron and density measurements). Refer to Figure 4.7. The Lockhart Formation in the Manzalai-05 well exhibits two zones with hydrocarbon presence, characterized by satisfactory hydrocarbon saturation. However, the effective porosity in these zones is significantly low, indicating a tight reservoir. Conversely, Figures 4.4 and 4.10 illustrate that the Lockhart Formation in the Manzalai-01 and Manzalai-06 wells lacks porosity, rendering it non-reservoir in other wells. The Hangu Formation demonstrates the presence of hydrocarbon-rich zones in all three wells, with a high degree of hydrocarbon saturation. However, the effective porosity, as depicted in Figures 4.5, 4.8, and 4.11, is notably low, indicating that the reservoir is characterized as tight. The Lumshiwal Formation consistently exhibits the occurrence of hydrocarbon in all three wells. However, the reservoir is characterized by a low effective porosity, as depicted in Figures 4.6, 4.9, and 4.12. Based on the petrophysical investigation, the research area exhibits a favorable reservoir potential.

Once the reservoir at the well location has been identified, the subsequent stage involves utilizing the petrophysical parameters to derive the distribution of facies in the given wells. In order to achieve this objective, the application of an unsupervised machine learning technique known as Fuzzy Classification has been employed. The results of the study reveal the presence of five distinct facies, namely Gas sands, shale sand, shale, limestone-packstone, and limestone-wackstone. These facies were identified based on various well log measurements including gamma ray, spontaneous potential, deep resistivity, neutron porosity, sonic, and photoelectric factor. Figures 5.1 and Figure 5.2 illustrate the distribution of these facies. While packstone indicates the presence of higher shales as it is mud plus grain dominated and wackstone for lower shales as it is grain dominated has been designated to the carbonates (Lockhart and Kawagarh). shaly sand and shales are designated to clastics (Hangu and Lumshiwal) while gas sands for hydrocarbon bearing zones. The facies classification indicates that gas sand is the dominant facies in the Hangu and Lumshiwal Formation.

Ali et al. (2021) asserts that a petrophysical analysis of the zone of interest can provide insights into differentiating between reservoir and non-reservoir intervals.

Nevertheless, several factors, including the absence of log data, unfavorable drilling circumstances, the presence of mud cake and washouts, variations in temperature, and salt levels, frequently contribute to the deterioration of log data quality. Consequently, this degradation can lead to erroneous petrophysical interpretation. To mitigate these constraints, rock physics modelling is employed for Manzalai-01 to forecast the compressional velocity, shear velocity, and density log. These predictions are subsequently compared with the actual logs to enhance the characterization of facies distribution throughout the reservoir. The cross plots depicted in Figures 5.6 and 5.7 illustrate a distinct differentiation between the observed and projected elastic logs, thereby highlighting the influence of the borehole environment on the observed logs and their exclusion in the predicted log.

The last stage involves acquiring knowledge about the spatial distribution of low impedance zones inside the reservoir. In order to achieve this objective, a geo stochastic inversion technique was employed. The findings from the stochastic inversion analysis indicate the existence of a hydrocarbon-rich zone in the Hangu and Lumshiwal areas. This zone is characterized by a comparatively low impedance compared to the surrounding well locations, as depicted in figures 6.9 and 6.10. The Lockhart impedance slice depicted in Figure 6.8 has a lower impedance value at the well location Manzalai-05, whereas significantly higher impedances are observed at Well Locations Manzalai-01 and Manzalai-06, which aligns with the findings of petrophysical analysis.

CONCLUSIONS

- Time contour maps are generated for Lockhart, Hangu and Lumshiwal Formations which shows that the mentioned horizons are dipping from Northwest to Southeast.
- Based on petrophysical examination, major prospective zones within the Hangu, Lumshiwal, and Lockhart areas have been discerned.
- Based on the analysis of well log response, five unique facies have been found and labelled as gas sands, shales, shaly sand, limestone-wackstone, and limestone-packstone.
- The results obtained from rock physics modelling indicate that the predicted compressional velocity, shear velocity, and density have been successfully mitigated, hence eliminating the adverse consequences caused by the presence of a poor-quality borehole.
- The results of the inversion analysis reveal the existence of relatively low impedance zones in the Lumshiwal and Hangu formations across the whole research region. However, low impedance is only observed in the Lockhart formation at the Manzalai-05 well and its surrounding areas.

REFERENCES

- Ahmad N, Khan MR (2012) Evaluation of a Distinct SubPlay for Enhanced Exploration in an Emerging Petroleum Province, Bannu-Kohat Sub-Basin, Pakistan, AAPG International Conference and Exhibition, Search and Discovery Article: 10391.
- Amjad, M. R., Hameed, M. S., Mujtaba, M., & Munir, M. N. (2019). Petrophysical and Geochemical Analysis of Chichali Formation for the Source Rock Evaluation: A Case Study of Chanda-01 Well, Upper Indus Basin, Pakistan. *International Journal of Economic and Environmental Geology*, 32-39.
- Angeleri, G. P., and Carpi, R. 1982. Porosity prediction from seismic data; Geophys
- Ashcroft, W. 2011. A Petroleum Geologist's Guide to Seismic Reflection, Wiley–Blackwell.
- Avseth, P., Mukerji, T., and Mavko, G. 2005. Quantitative seismic interpretation: Applying rock physics tools to reduce interpretation risk, Cambridge University Press, https://doi.org/10.1017/CBO9780511600074
- Avseth, P., Mukerji, T., Mavko, G., & Dvorkin, J. (2010). Rock-physics diagnostics of depositional texture, diagenetic alterations, and reservoir heterogeneity in high-porosity siliciclastic sediments and rocks—A review of selected models and suggested work flows. *Geophysics*, *75*(5), 75A31-75A47.
- Bacon, M., Simm, R., and Redshaw, T. 2007. 3-D seismic interpretation, Cambridge University Press, https://doi.org/10.1017/CBO9780511802416.
- Bardon, C., & Pied, B. (1969, May). Formation water saturation in shaly sands. In *SPWLA Annual Logging Symposium* (pp. SPWLA-1969). SPWLA.
- Batzle, M. L., and Wang, Z., 1992, Seismic properties of pore fluids: Geophysics, 64, 1396-1408.
- Bosch, M., Carvajal, C., Rodrigues, J., Torres, A., Aldana, M., and Sierra, J. 2009. Petrophysical seismic inversion conditioned to well-log data: Methods and application to a gas reservoir; Geophysics 74 O1–O15, https://doi.org/10.1190/1.3043796.

- Bosch, M., Mukerji, T., & Gonzalez, E. F. (2010). Seismic inversion for reservoir properties combining statistical rock physics and geostatistics: A review. *Geophysics*, *75*(5), 75A165-75A176.
- Castagna, J. P. (1993). Petrophysical imaging using AVO. *The Leading Edge*, *12*(3), 172-178.
- Chen, Q., and Sidney, S. 1997. Seismic attribute technology for reservoir forecasting and monitoring; Lead Edge 16 445–448, https://doi.org/10.1190/1.1437657
- Chopra, S., and Marfurt, K. J. 2007. Seismic attributes for prospect identification and reservoir characterization: Geophysics. Dev. Ser. 11465
- Coulon, T., Bornard, R., Allo, F., & Freudenreich, Y. (2005). Petrophysical Seismic Inversion SEG Technical Program Expanded Abstracts 2005 (pp. 1355–1358). Society of Exploration Geophysicists.
- Dobrin and Savit.,1988, Geophysical Exploration, Hafner Publishing Co.
- Dobrin and Savit.,1988, Geophysical Exploration, Hafner Publishing Co.
- Doveton, J. H. (1994). *Geologic log analysis using computer methods*. American Association of Petroleum Geologists.
- Doyen, P. M., De Buyl, M. H., & Guidish, T. M. (1989). Porosity from seismic data, a geostatistical approach. Exploration Geophysics, 20(2), 245.
- Fatmi AN (1973) Lithostratigraphic units of the KohatPotwar Province, Indus Basin, Pakistan, Geological Survey of Pakistan 10: 80.
- Gakkhar, R. A., Bechte, A., & Gratzer, R. (2011). Source-rock potential and origin of hydrocarbons in the Cretaceous and Jurassic sediments of the Punjab Platform (Indus Basin, Pakistan). *Pakistan Journal of Hydrocarbon Research*, *21*, 1-17.
- Gardezi, S. A. H., Ahmad, S., Ikram, N., & Rehman, G. (2017). Geological constraints on the Western Kohat foreland basin, Khyber Pakhtunkhwa, Pakistan: Implication from 2D and 3D structural modelling. *Arab J Earth Sci*, *4*(2), 95-116
- Gassmann, F., 1951, Über die elastizität poröser medien: Vierteljahrss-chrift der Naturforschenden Gesellschaft in Zurich, 96, 1-23. The English translation

of this paper is available at http://sepwww.stanford.edu/sep/berryman/PS/gassmann.pdf.

- Gee ER (1945) The age of the Saline Series of the Punjab and of Kohat, National Academy of Sciences , Proc. Sec B. 14(6): 269-310.
- Ghaffari M, Rashidnejad-Omran N, Dabiri R, Santos JF, Mata J, Buchs D, McDonald I, Appel P, GarbeSchönberg D (2015) Interaction between felsic and mafic magmas in the Salmas intrusive complex, Northwestern Iran: Constraints from petrography and geochemistry, Journal of Asian Earth Sciences 111: 440-458. doi: http://dx.doi.org/10.1016/j.jseaes.2015.06.019
- Ghani H, Zeilinger G, Sobel ER, Heidarzadeh G (2018) Structural variation within the Himalayan fold and thrust belt: A case study from the Kohat-Potwar Fold Thrust Belt of Pakistan, Journal of Structural Geology, 116: 34-46
- Ghani H, Zeilinger G, Sobel ER, Heidarzadeh G (2018) Structural variation within the Himalayan fold and thrust belt: A case study from the Kohat-Potwar Fold Thrust Belt of Pakistan, Journal of Structural Geology, 116: 34-46
- Grana, D. and Dvorkin, J. 2011. The link between seismic inversion, rock physics, and geostatistical simulations in seismic reservoir characterization studies; Lead Edge 30 54–61, https://doi.org/10.1190/1.3535433.
- Gunning, J. A. M. E. S., & Glinsky, M. I. C. H. A. E. L. (2003). Bayesian seismic inversion delivers integrated sub-surface models. In 65th EAGE Conference & Exhibition (pp. cp-6). EAGE Publications BV.
- Haas, A., & Dubrule, O. (1994). Geostatistical inversion-a sequential method of stochastic reservoir modelling constrained by seismic data. *First break*, *12*(11).
- Hampson, D., Schuelka, J. S., & Quirein, J. A. (2001). Use of multi attribute transforms to predict log properties from seismic data. Geophysics, 66, 220–236. https://doi.org/10.1190/1. 1444899
- Hearts, J. R., Nelson, P. H., and Paillet, F. L. 2002. Well Logging for Physical Properties: A Handbook for Geophysicists, Geologists and Engineers, 2nd edn, John Wiley & Sons, Chichester.

- Hearts, J. R., Nelson, P. H., and Paillet, F. L. 2002. Well Logging for Physical Properties: A Handbook for Geophysicists, Geologists and Engineers, 2nd edn, John Wiley & Sons, Chichester.
- Hill, R., 1952. The elastic behavior of crystalline aggregate. Proc. Phys. Soc., London 65, 349–354.
- Kazmi AH, Abbasi IA (2008) Stratigraphy & Historical Geology of Pakistan, National Centre of Excellence in Geology, University of Peshawar, Peshawar, Pakistan: 524.
- Kazmi AH, Jan M Q (1997) Geology & tectonics of Pakistan, Graphic Publishers, 5C, 6/10, Nazimabad, Karachi, Pakistan.
- Keys, R. G., & Xu, S. (2002). An approximation for the Xu-White velocity model. *Geophysics*, *67*(5), 1406-1414.
- Khan MA, Ahmed A, Raza HA, Kemal, A (1986) Geology of Petroleum in Kohat-Potwar Depression, Pakistan, American Association of Petroleum Geologists Bulletin 70(4): 396-414.
- Khan MA, Ahmed A, Raza HA, Kemal, A (1986) Geology of Petroleum in Kohat-Potwar Depression, Pakistan, American Association of Petroleum Geologists Bulletin 70(4): 396-414.
- Khan, N., & Rehman, K. (2019). Petrophysical evaluation and fluid substitution modeling for reservoir depiction of Jurassic Datta Formation in the Chanda oil field, Khyber Pakhtunkhwa, northwest Pakistan. *Journal of Petroleum Exploration and Production Technology*, *9*, 159-176.
- King, D. E. 1990. Incorporating geological data in well log interpretation; In: Geological Applications of Wireline Logs, pp. 45–55, https://doi.org/10.1144/gsl.sp.1990.048.01.06
- Kumar, B., & Kishore, M. (2006, October). Electrofacies classification—A critical approach. In *Proceedings of the 6th International Conference and Exposition on Petroleum Geophysics, Kolkata, India* (pp. 822-825).
- Kumar, M., Dasgupta, R., Singha, D. K., & Singh, N. P. (2018). Petrophysical evaluation of well log data and rock physics modeling for characterization of Eocene reservoir in Chandmari oil field of Assam-Arakan basin, India. Journal of Petroleum Exploration and Production Technology, 8, 323-340.

- Kumar, M., Dasgupta, R., Singha, D. K., & Singh, N. P. (2018). Petrophysical evaluation of well log data and rock physics modeling for characterization of Eocene reservoir in Chandmari oil field of Assam-Arakan basin, India. Journal of Petroleum Exploration and Production Technology, 8, 323-340.
- Kuster, G. T., & Toksöz, M. N. (1974). Velocity and attenuation of seismic waves in two-phase media: Part I. Theoretical formulations. *Geophysics*, *39*(5), 587-606.
- Landa, J. L., Horne, R. N., Kamal, M. M., and Jenkins, C. D. 2000. Reservoir characterization constrained to well-test data: A field example SPE Reserv. Eval. Eng. 3 325–334, https://doi.org/10.2118/65429-PA.
- Lindseth, R. O. 1979. Synthetic sonic logs – a process for stratigraphic interpretation; Geophysics 44-3, https://doi.org/10.1190/1.1440922.
- McDougall JW, Khan SH (1990) Strike Slip faulting in a foreland fold thrust belt: The Kalabagh fault and western Salt Range Pakistan, Tectonics 9: 1061-1075
- Meissner CR, Hussain M, Rashid MA, Sethi UB (1975) Geology of the Parachinar quadrangle, Pakistan, United States Geological Survey Professional Paper 76-F.
- Meissner CR, Master JM, Rashid MA, Hussain M (1974) Stratigraphy of the Kohat Quadrangle, Pakistan, United States Geological Survey Professional Paper 716- D: 30.
- Mollai H, Dabiri R, Torshizian HA, Pe-Piper G, Wang W (2019) Cadomian crust of Eastern Iran: evidence from the Tapeh Tagh granitic gneisses, International Geology Review 1-21.
- Najman Y, et al., (2010) Timing of India-Asia collision: geological, biostratigraphic, and palaeomagnetic constraints, Journal of Geophysical Research 115: B12416.
- Pivnik DA, Khan MJ (1996) Transition from foreland to piggyback basin deposition, Plio-Pleistocene Upper Siwalik Group, Shinghar Range, Northwest Pakistan, Sedimentology 43: 631-646.

- Poupon, A., & Leveaux, J. A. C. Q. U. E. S. (1971, May). Evaluation of water saturation in shaly formations. In SPWLA 12th Annual logging symposium. OnePetro
- Rider, M. H. (1986). The geological interpretation of well logs.
- Rider, M., & Kennedy, M. (2011). The geological interpretation of well logs: Scotland. *Rider-French Consulting Limited*, 432.
- Rowbotham, P. S., Marion, D., Lamy, P., Insalaco, E., Swaby, P. A., & Boisseau, Y. (2003). Multidisciplinary stochastic impedance inversion: integrating geological understanding and capturing reservoir uncertainty. Petroleum Geoscience, 9(4), 287- 294.
- Russell, B. (1999). Comparison of post-stack seismic inversion methods SEG Technical Program Expanded Abstracts (p. 10). Society of Exploration Geophysicists.
- Saddique, B., Ali, N., Jan, U. I., Hanif, M., Shah, S. A., Saleem, I., ... & Arafat, M. Y. (2016). Petrophysical analysis of the reservoir intervals in Kahi-01 well, Kohat Sub-Basin, Pakistan. *Journal of Himalayan Earth Science*, *49*(1).
- Saddique, B., Ali, N., Jan, U. I., Hanif, M., Shah, S. A., Saleem, I., ... & Arafat, M. Y. (2016). Petrophysical analysis of the reservoir intervals in Kahi-01 well, Kohat Sub-Basin, Pakistan. *Journal of Himalayan Earth Science*, *49*(1).
- Sameeni SJ, Haneef M, Rehman O, Lipps JH (2009) Paleogene biostratigraphy of Kohat area, Northern Pakistan, Geol. Bull. Punjab Univ. 44: 27-42.
- Sams, M., Millar, I., Satriawan, W., Saussus, D., & Bhattacharyya, S. (2011). Integration of geology and geophysics through geostatistical inversion: a case study. First Break. https://doi.org/10. 3997/1365-2397.2011023
- Saussus, D., & Sams, M. (2012). Facies as the key to using seismic inversion for modelling reservoir properties. *First Break*, *30*(7).
- Serra, O., & Abbott, H. T. (1980). The contribution of logging data to sedimentology and stratigraphic, SPE 9270. In *55th Annual Fall Technical Conference and Exhibition, Dallas, Texas, 19p*.

- Shah SMI (2009) Stratigraphy of Pakistan. Geological Survey Memoir 22: 381.
- Shakir, U., Ali, A., Amjad, M. R., & Hussain, M. (2021). Improved gas sand facies classification and enhanced reservoir description based on calibrated rock physics modelling: A case study. *Open Geosciences*, *13*(1), 1476-1493.
- Shanley, K. W., Cluff, R. M., & Robinson, J. W. (2004). Factors controlling prolific gas production from low-permeability sandstone reservoirs: Implications for resource assessment, prospect development, and risk analysis. *AAPG bulletin*, *88*(8), 1083-1121.
- Sheriff R. E., Telford W. M., and Geldart L. P., 1990, Applied geophysics, Cambridge University Press.
- Silva, M. Da., Rauch-Davies, M., and Cuervo, A. 2004. Data conditioning for a combined inversion and AVO reservoir characterisation study, 66th EAGE Conf.
- Silva, M. Da., Rauch-Davies, M., and Cuervo, A. 2004. Data conditioning for a combined inversion and AVO reservoir characterisation study, 66th EAGE Conf.
- Simm, R., and Bacon, M. 2014. Seismic Amplitude: An interpreter's handbook, Cambridge University Press.
- SM, I. S. (1977). Stratigraphy of Pakistan. *Mem. Geol. Surv. Pakistan*, *12*, 1-138.
- Stinco, L. P. (2006, June). Core and log data integration; the key for determining electrofacies. In *SPWLA 47th annual logging symposium* (Vol. 7). Society of Petrophysicists and Well-Log Analysts.
- Telford, W. M., Geldart, L. P., & Sheriff, R. E. (1990). *Applied geophysics*. Cambridge university press.
- Telford, W.M., Geldart, L.P., Sheriff, R.E., and Keys, D.A., 1999, Applied Geophysics, Cambridge University Press, London
- Tiab, D., & Donaldson, E. C. (2015). Petrophysics: theory and practice of measuring reservoir rock and fluid transport properties. Gulf professional publishing.

- Toksoz, M. N., Cheng, C. H., & Timur, A. (1976). Velocities of seismic waves in porous rocks. *Geophysics*, *41*(4), 621-645.
- Torres-Verdin, C., & Sen, M. K. (2004). Integrated Approach for the Petrophysical Interpretation of Post-and Pre-Stack 3-D Seismic Data, Well-Log Data, Core Data. US: University of Texas.
- Veeken, P. C. H. 2007. Seismic Stratigraphy, Basin Analysis and Reservoir Characterisation, Elsevier, Amsterdam.
- Veeken, P. C. H., and Da Silva, M. 2004. Seismic inversion methods and some of their constraints; First Break 22 47–70.
- Veeken, P. C. H., and Rauch-Davies, M. 2006. AVO attribute analysis and seismic reservoir characterization; First Break 24 41–52, https://doi.org/10.3997/1365-2397.2006004.
- Walls, J., Dvorkin, J., and Carr, M. 2004. Well logs and rock physics in seismic reservoir characterization; Offshore Technol. Conf., https://doi.org/10.4043/16921-MS.
- Wang, Y. 2017. Seismic Inversion: Theory and Applications, Wiley Blackwell.
- Wells NA (1984) Marine and Continental Sedimentation in the early Cenozoic Kohat basin and adjacent northwestern Indo-Pakistan, Ph.D. Dissertation, University of Michigan
- Wyllie, M. R. J., Gardner, G. H. F., & Gregory, A. R. (1963). ADDENDUM TO –STUDIES OF ELASTIC WAVE ATTENUATION IN POROUS MEDIA" BY MRJ WYLLIE, GHF GARDNER, AND AR GREGORY (GEOPHYSICS, OCTOBER, 1962, PP. 569–589). *Geophysics*, *28*(6), 1074-1074.
- Xu S. and Payne M.A (2009). Modeling elastic properties in carbonate rocks. The Leading Edge 28, 66-74.
- Yao, F., and Gan, L. 2000. Application and restriction of seismic inversion; Pet. Explor. Dev. 27 53–56.
- Yazdi A, Sharifi Teshnizi E (2021) Effects of contamination with gasoline on engineering properties of fine-grained silty soils with an emphasis on the

duration of exposure, Springer, SN Applied Sciences 3:704. doi: https://doi.org/10.1007/s42452-021-04637-x.